

**Synergistic SNARE Modulators of Neurotransmission:
Complexins and SNAP-29**

Dissertation

for the award of the degree

“Doctor rerum naturalium” (Dr.rer.nat.)

of the Georg-August-Universität Göttingen

within the doctoral program Sensory and Motor Neuroscience

of the Georg-August-University School of Science (GAUSS)

submitted by

Nandhini Sivakumar

From Anantapur, India

Göttingen 2015

Thesis Committee

Dr. JeongSeop Rhee
Dept. of Molecular Neurobiology, Max-Planck-Institute of Experimental Medicine

Prof. Dr. Thomas Dresbach
Dept. of Anatomy and Embryology, University of Göttingen

Prof. Dr. Tobias Moser
Dept. of Otorhynolaryngology, University Medical Centre Göttingen

Reviewers

Reviewer 1: Dr. JeongSeop Rhee
Dept. of Molecular Neurobiology, Max-Planck-Institute of Experimental Medicine

Reviewer 2: Prof. Dr. Thomas Dresbach
Dept. of Anatomy and Embryology, University of Göttingen

Reviewer 3: Prof. Dr. Tobias Moser
Dept. of Otorhynolaryngology, University Medical Centre Göttingen

Further members of the Examination Board

Prof. Dr. Erwin Neher
(Professor Emeritus at the Max-Planck-Institute for Biophysical Chemistry)

Dr. Dr. Oliver Schlüter
(Molecular Neurobiology, European Neuroscience Institute)

Camin Dean Ph.D.
(Trans-synaptic Signaling, European Neuroscience Institute)

Date of the oral examination: 7th May 2015

Declaration

I hereby declare that I have written this dissertation independently, with no other sources or aids than those cited.

Nandhini Sivakumar
Göttingen, 12.03.2015

TABLE OF CONTENTS

I.	Table of Contents	5
II.	Acknowledgements	9
III.	List of Abbreviations	13
IV.	List of tables	15
V.	List of figures	16
VI.	Abstract	19
1.	Introduction	21
1.1.	Neuronal Communication	21
1.2.	Physiology of synaptic neurotransmitter release	21
1.2.1.	Action potential evoked transmitter release	21
1.2.2.	Spontaneous synaptic transmitter release	23
1.3.	Core molecular machinery of synaptic vesicle release	24
1.3.1.	Synaptic vesicles	24
1.3.2.	Formation of the SNARE core complex	25
1.4.	Molecular regulators of vesicle docking and priming	26
1.4.1.	Docking factors	27
1.4.2.	Priming of synaptic vesicles - The RRP	28
1.4.2.1.	Priming proteins - Munc13 and CAPS	30
1.5.	Ca ²⁺ -mediated vesicle fusion – role of cognate SNAREs	31
1.5.1.	Synaptobrevin-2	31
1.5.2.	Syntaxin-1	32
1.5.3.	SNAP-25 and its paralogs	33
1.6.	1 st Aim of the study - Biochemical and functional study of SNAP-29	36
1.7.	Ca ²⁺ -mediated vesicle fusion - role of Complexin	37
1.7.1.	Complexin structure and homology	37
1.7.2.	Complexin - SNARE interactions	38
1.7.3.	Complexin structure - function discrepancy	40
1.7.3.1.	Complexins as facilitators of release	40
1.7.3.2.	Complexins as fusion clamps in various models	41
1.7.4.	Complexin – Synaptotagmin interactions	43
1.8.	SNARE disassembly and synaptic vesicle recycling	44
1.9.	2 nd Aim of the study - To study Complexin structural domains in transmitter release	46
2.	Materials and Methods	47
2.1.	Materials	47
2.1.1.	Buffers	47
2.1.2.	Gel solutions	49
2.1.3.	Reagents	50
2.1.4.	Cell culture media	51
2.1.5.	Reagents for electrophysiology	52
2.1.6.	Antibiotics, media supplements and solutions	53
2.1.7.	Antibodies for Western Blotting and Immunocytochemistry	54
2.1.8.	Primer Sequences, PCR reaction mixes and programs	55
2.2.	Methods	59
2.2.1.	Transformation of plasmid DNA into competent bacteria	59
2.2.2.	Plasmid DNA “Maxi” purification	59

2.2.2.1.	Determination of yield of purified DNA	60
2.2.3.	Recombinant protein purification	60
2.2.3.1.	Equilibration of beads	60
2.2.3.2.	IPTG induction	60
2.2.3.3.	Preparation of protein extract and binding of protein to beads	61
2.2.3.4.	Wash and protein elution	61
2.2.3.5.	Protein precipitation	61
2.2.4.	Genotyping of DNA samples from tissues	61
2.2.4.1.	Equilibration of nexttec™ cleanplate96	61
2.2.4.2.	Lysis	62
2.2.4.3.	Purification of genomic DNA	62
2.2.5.	Polymerase chain reaction	62
2.2.6.	Agarose gel electrophoresis	62
2.2.6.1.	Genotyping results from PCR and electrophoresis	62
2.2.7.	SDS-Polyacrylamide Gel Electrophoresis	64
2.2.7.1.	Preparation of SDS-Polyacrylamide Gels	64
2.2.7.2.	Preparation of samples	65
2.2.7.3.	Electrophoresis of gels	65
2.2.8.	Coomassie staining of gels	65
2.2.9.	Western Blotting	65
2.2.9.1.	Protein transfer from gel to nitrocellulose membrane	65
2.2.9.2.	Ponceau S staining of proteins	66
2.2.9.3.	Immunoblotting for ECL analysis	66
2.2.9.4.	Immunoblotting for Odyssey® analysis	66
2.2.10	Growth and maintenance of HEK293FT cell lines	67
2.2.10.1.	Thawing cells	67
2.2.10.2.	Subculturing cells	67
2.2.10.3.	Freezing cells	68
2.2.11.	Lentivirus production	68
2.2.11.1.	Coating dishes	68
2.2.11.2.	Transfection into HEK293FT cells	68
2.2.11.3.	Harvesting lentivirus	69
2.2.11.4.	Lentiviral infections in neurons	69
2.2.12.	Mouse strains	69
2.2.13.	Autaptic neuron culture	70
2.2.13.1.	Preparation of glass coverslips	70
2.2.13.2.	Preparation of plates	70
2.2.13.3.	Stamping the agarose coated coverslips	70
2.2.13.4.	Culturing cortical astrocytes in T-75 cm ² flasks	71
2.2.13.5.	Preparation of astrocyte microislands	71
2.2.13.6.	Preparation of neurons for autaptic culture	71
2.2.14.	Electrophysiology of autaptic neurons	72
2.2.15.	Collagen-PDL coating of 24-well and 6 cm dishes	72
2.2.16.	Continental neuron culture	72
2.2.17.	Immunochemistry on continental neuron cultures	73
2.2.18.	Harvesting proteins from continental neuron cultures	73

2.2.19.	Bradford's assay	74
3.	Results	75
3.1.	SNAP29	75
3.1.1.	Insights into the role of SNAP29 at neuronal synapses	75
3.1.1.1.	Protein composition in the Nex-Cre SNAP29 KO mice	75
3.1.1.2.	Normal glutamatergic synaptic transmission in the Nex-Cre SNAP29 KO mice	76
3.1.1.3.	Protein composition in the brain of constitutive SNAP29 KO mice	80
3.1.1.4.	Immunocytochemical analysis of SNAP29 in hippocampal neurons	81
3.1.1.5.	Normal glutamatergic synaptic transmission in Constitutive SNAP29 KO mice	83
3.1.1.6.	Normal GABAergic synaptic transmission in Constitutive SNAP-29 KO mice	86
3.2.	Complexins	89
3.2.1.	Wild-type mammalian Complexins facilitate glutamatergic synaptic transmission	89
3.2.1.1.	Endogenous Complexin-1 is essential for Ca ²⁺ -triggered release of vesicles but not for vesicle priming	89
3.2.1.2.	Loss of Complexins does not dramatically affect spontaneous vesicle fusion	92
3.2.1.3.	Role of endogenous Complexin-1 in synchronous and asynchronous vesicle release	93
3.2.1.4.	Lentiviral expression of wild-type Complexins can restore efficient transmitter release in Cplx-TKO neurons	96
3.2.2.	Mutation of the SNARE-binding domain and Farnesylation domain in Complexins impedes glutamatergic synaptic transmission	100
3.2.2.1.	Rescue efficacies of Complexin1 wild type (Cplx1-WT) and Complexin1 SNARE binding domain mutant (Cplx1-K69A/Y70A) proteins in Cplx TKO neurons	101
3.2.2.2.	Rescue efficacies of Complexin2 wild type (Cplx2-WT) and Complexin2 SNARE binding domain mutant (Cplx2-K69A/Y70A) proteins in Cplx TKO neurons	105
3.2.2.3.	Rescue efficacies of Complexin3 wild type (Cplx3-WT), Complexin3 SNARE binding domain mutant (Cplx3-K79A/Y80A) and Complexin3 Farnesylation domain mutant (Cplx3-C155S) proteins in Cplx TKO neurons	109
3.2.2.4.	Rescue efficacies of Complexin4 wild type (Cplx4-WT), Complexin4 SNARE binding domain mutant (Cplx4-K80A/Y81A) and Complexin4 Farnesylation domain mutant (Cplx4-C157S) proteins in Cplx TKO neurons	114
3.2.3.	Lentiviral expression and quantification of wild type and mutant Complexin proteins in Cplx-TKO neurons	120
3.2.3.1.	Cplx1 protein estimation	122

3.2.3.2.	Cplx2 protein estimation_____	123
3.2.3.3.	Cplx3 protein estimation_____	125
3.2.3.4.	Cplx4 protein estimation_____	127
4.	Discussion_____	130
4.1.	SNAP-29_____	130
4.1.1.	SNAP-29 - localization and interactions with presynaptic SNAREs_____	130
4.1.2.	SNAP-29 - no key role in synaptic vesicle exocytosis_____	132
4.1.3.	SNAP-29 - clinical implications due to loss of function_____	135
4.2.	Complexins_____	136
4.2.1.	Mammalian Complexins improve the release efficacy of vesicles via binding to the neuronal SNARE complex_____	136
4.2.2.	Mammalian Complexins act on a fusion-competent vesicle pool in glutamatergic autapses_____	140
4.2.3.	Mammalian Complexins do not 'clamp' vesicle fusion at glutamatergic synapses_____	141
4.2.4.	Mode of Complexin function - Synaptotagmin interaction in transmitter release_____	142
5.	Summary and Perspectives_____	145
5.1	SNAP-29_____	146
5.2	Complexins_____	146
6.	Appendix_____	148
7.	Bibliography_____	150
8.	Curriculum vitae_____	164

Acknowledgements

I feel immensely gifted and lucky to have received this wonderful opportunity to pursue my doctoral studies in Germany, one of the finest places for Science, in the world. I am happy that I could take up the opportunity to work on my doctoral research in Neuroscience at the Max-Planck-Institute of Experimental Medicine. Foremost, I express my deepest gratitude to Prof. Dr. Nils Brose, who offered me a full funded PhD position in his department, during my interview for the Sensory and Motor Neuroscience doctoral program. Nils has been compassionate, supportive, and confident of my capacity throughout the course of my PhD. I am immensely grateful to my primary supervisor, Dr. JeongSeop Rhee, who also approved of my candidacy and gave me an opportunity to work in his lab on electrophysiology. Although I started as an amateur in electrophysiology, JeongSeop's excellent supervision and proficient experimental design has helped me accomplish the objectives in my research. I am extremely thankful to my second supervisor Dr. Kerstin Reim, who has offered me exceptional guidance in biochemistry. Kerstin taught me the basics of biochemistry when I joined the lab, and advised me on all my biochemistry experiments. This has helped me develop and hone my skills in the best possible way. I am indeed very happy that I have received outstanding guidance from my supervisors.

I express my sincere gratitude to my collaborators, Dr. Sandra Goebbels and PhD student Georg Wieser of the Department of Neurogenetics (MPI-EM), for generating the SNAP-29 mice and entrusting me with the project. Georg's help is worth appreciating, as he has always been ready to share information and clarify my doubts.

I thank my thesis committee members Prof. Dr. Thomas Dresbach and Prof. Dr. Tobias Moser for their presence at all my thesis committee meetings, and providing critical feedback on my research work.

I immensely thank the GGNB Office and team of people - Kirsten Pöhlker, Rike Göbel and Susanne Kracke, who have been helping me with paperwork and formalities for administrative purposes ever since I applied for my PhD with the GGNB. I would like to acknowledge the secretaries of the Department of Molecular Neurobiology at the MPI-EM - Christine Bogatz and Birgit Glaeser and the secretary of the MPIEM's directors and public relations officer, Svea Viola Dettmer. Christine and Birgit have been offering me help and advice on various issues both on the personal and professional scale. Svea graciously offered me a comfortable office space during my dissertation preparation. I am ever grateful for all of their continuing support. I would like to acknowledge Anja Guenther, Ines Beulshausen, Sabine Bolte, Thea Hellmann, and Dagmar Michels-Hitzing for

excellent technical assistance. I thank Dr. Hiroshi Kawabe, who generously offered to share his protocols and knowledge. I express my sincere thanks to Dr. Fritz Benseler, head of the AGCT lab MPIEM, Christiane Harenberg, Dayana Schwerdtfeger, Ivonne Thanhäuser, and Maik Schlieper for immense help with genotyping. I would also like to thank Astrid Ohle and Cornelia Casper of the MPIEM Tierhaus (animal house) facility, who have been primary caretakers of the Complexin and SNAP-29 mice I have sacrificed to perform my doctoral research. I am grateful to members of the IT department at the MPIEM, Beate Beschke, Lothar Demel, Hans-Joachim Horn, and Rolf Merker, for their support with computer related issues. I am indeed happy to have worked with my nice colleagues Mimi, Cordelia, Ben, Dennis, Silvia, Noa, Ramya, Albrecht, Liam, and Jennifer, who have helped me at the lab on different occasions and been friendly all the time. Carolina, Farrah and Sünke, who are also my colleagues, have become close friends to me in the short time I have known them, and have given me a lot of support. I hope that we can share a long-lasting happy bond.!

My best friend Subashri (subbi), and her sincere prayers for me have always been with me. Our sweet friendship continues forever more!

I am forever indebted to my family and overwhelmed that they love me so much. My Kamala paati (grandma) and my late granddad - Mr. Rajagopal gave me, my second name 'Vidya', which in Sanskrit means 'Education', foreseeing that I will scale the heights of education. My daddy and amma (mom) - Mr. Sivakumar and Mrs. Padmavathy Sivakumar - are the best parents ever in the world. They have given me all the love and freedom to pursue the highest of my ambitions. Daddy's words - "Hard work and sincere efforts will never go waste" have been my best motivation. My ambition to do my PhD was indeed a dream that was made for me about 9 years ago, by Mr. Karan Vij. Today, I see my success and inspiration has blossomed from his jubilant nature. Karan's "Be Positive" ideology forever lingers in me. Karan's parents - Mrs. Romi Vij and Mr. Kamal Pradeep Vij - mummy and papa, as I have forever known them, have always encouraged me, loved and cared for me, and most of all, blessed me immensely!

- And now, I make you proud, my dear family! Om

*Somewhere over the rainbow, skies are blue,
And the dreams that you dare to dream really do come true.*

-Lyman Frank Baum

Dedicated to Karan and our family.

List of Abbreviations

a.a.	amino acid
Ach	Acetylcholine
AMPA	α -Amino-3-hydroxy-5-methyl-4-isoxazolepropionic acid
AP	Action potential
ATP	Adenosine tri-phosphate
BotN	Botulinum Neurotoxin
β -PE	β -Phorbol ester
bp	basepairs
BSA	Bovine serum albumin
CAAX	C is Cysteine, A is aliphatic amino acid, X is amino acid, X is Methionine
CaM	Calmodulin
CAPS	Ca ²⁺ -dependent activator proteins for secretion
CD	Circular Dichroism
cDNA	complementary Deoxy-ribonucleic-acid
CEDNIK	Cerebral dysgenesis–neuropathy–ichthyosis–keratoderma syndrome
<i>C. elegans</i>	<i>Caenorhabditis elegans</i>
CNQX	6-cyano-7-nitroquinoxaline-2,3-dione
Cplx	Complexin
cpx	<i>Caenorhabditis elegans</i> Complexin
C-terminal	Carboxy-terminal
DAG	Diacylglycerol
dmCplx	Drosophila Complexin
DMEM	Dulbecco's Modified Eagle Medium
DKO	Double knockout
DMSO	Dimethyl sulfoxide
E18	Embryonic day 18
ECL	Enhanced Chemiluminescence
EGFP	Enhanced Green Fluorescent Protein
EPSC	Excitatory post-synaptic current
GABA	γ -Aminobutyric acid
GABAergic	γ -Aminobutyric acidergic
GluR	Glutamate Receptor
GPI	Glycerophosphatidylinositol
GS32	Golgi SNARE 32
GST	Glutathione S-transferase
GTP γ S	guanosine 5'-O-[gamma-thio] triphosphate
HEK293	Human Embryonic Kidney 293 cells
His	Histidine
Hz	Hertz
IPSC	Inhibitory post-synaptic current
IPTG	Isopropyl- β -thiogalactopyranoside
kDa	Kilodalton
miRNA	Micro ribonucleic acid
mOsm	milliosmole
mEPSC	miniature Excitatory post-synaptic current
mIPSC	miniature Inhibitory post-synaptic current
μ g	Micrograms
nA	Nanoamperes
nC	Nanocoulomb
ng	Nanograms
NMDA	<i>N</i> -Methyl-D-aspartic acid

NMR	Nuclear Magnetic Resonance
NPF	asparagine-proline-phenylalanine
NRK	Normal rat kidney epithelial cells
NSF	N-ethylmaleimide sensitive fusion protein
N-terminal	Amino-terminal
ORF	Open Reading Frame
P0	Postnatal day 0
pA	picoamperes
pmol	picomoles
PBS	Phosphate Buffered Saline
PC12	Pheochromocytoma 12
PDZ	Post synaptic density protein (PSD95), Drosophila disc large tumor suppressor (Dlg1), and zonula occludens-1 protein (zo-1)
PI-PLC	Phosphatidylinositol-specific phospholipase C
PSC	post-synaptic current
RIM	Rab3 interacting molecule
RRP	Readily releasable pool
s	Seconds
SAP	Synapse Associated Protein
SCG	Superior Cervical Ganglion
SNAP-29	Synaptosomal Associated Protein of 29 kDa
SDS	Sodium dodecyl sulphate
SFV	Semliki Forest Virus
shRNA	Small Hairpin ribonucleic acid
siRNA	Small interfering ribonucleic acid
SNAP	Soluble NSF attachment protein
SNARE	SNAP Receptor
Syt-1	Synaptotagmin-1
TBE	Tris-Borate-EDTA Buffer
TBS	Tris Buffered Saline
TEMED	N,N,N',N'-Tetramethylethylene diamine
TKO	Triple knockout
TMR	Transmembrane Region
t-SNARE	target SNARE
TTX	Tetrodotoxin
UV	Ultraviolet
VAMP	Vesicle associated membrane protein
VGLUT	Vesicular glutamate transporter
VIAAT	Vesicular inhibitory amino acid transporter
v-SNARE	Vesicle SNARE
WT	Wild type

List of Tables

Table 1	Primary Antibodies
Table 2	Secondary Antibodies
Table 3	Primer Sequences for Cplx1
Table 4	PCR reaction for Cplx1 WT
Table 5	PCR reaction for Cplx1 KO
Table 6	PCR program for Cplx1
Table 7	Primer sequences for Nex-Cre SNAP29
Table 8	PCR reaction mix for Nex-Cre SNAP29 KO
Table 8.1	PCR program for Nex-Cre SNAP29 KO
Table 9	PCR reaction mix for Nex-Cre SNAP29 KO
Table 9.1	PCR program for Nex-Cre SNAP29 KO
Table 10	Primer sequences for Constitutive SNAP29 KO
Table 11	PCR reaction mix for Constitutive SNAP29 KO
Table 11.1	PCR program for Constitutive SNAP-29 KO
Table 12	Synaptic parameters measured from excitatory autaptic hippocampal neurons of WT and Nex-Cre SNAP29 KO mice
Table 13	Synaptic parameters measured from excitatory autaptic hippocampal neurons of WT and Constitutive SNAP29 KO mice
Table 14	Synaptic parameters measured from inhibitory autaptic striatal neurons of WT and constitutive SNAP29 KO mice
Table 15	Synaptic parameters measured from excitatory Cplx TKO neurons expressing EGFP and Cplx1, Cplx2, Cplx3, Cplx4 WT lentiviral proteins
Table 16	Synaptic parameters measured from excitatory Cplx TKO neurons expressing Cplx1-WT and Cplx1-K69A/Y70A lentiviral proteins
Table 17	Synaptic parameters measured from excitatory Cplx TKO neurons expressing Cplx2-WT and Cplx2-K69A/Y70A lentiviral proteins
Table 18	Synaptic parameters measured from excitatory Cplx TKO neurons expressing EGFP, Cplx3-WT, Cplx3-K79A/Y80A, and Cplx3-C155S lentiviral proteins
Table 19	Synaptic parameters measured from excitatory Cplx TKO neurons expressing EGFP, Cplx4-WT, Cplx4-K80A/Y81A, and Cplx4-C157S lentiviral proteins
Table 20	Estimation of endogenous and lentiviral Cplx1 proteins
Table 21	Estimation of endogenous and lentiviral Cplx2 proteins
Table 22	Estimation of lentiviral Cplx3-WT protein
Table 23	Estimation of lentiviral Cplx4 proteins

List of Figures

- Figure 1 (A. and B.) Excitatory and Inhibitory post-synaptic currents
- Figure 2 Spontaneous miniature release - mEPSCs and mIPSCs
- Figure 3 Schematic representation of synaptic vesicle exocytosis
- Figure 4 Protein interactions at the active zone governing synaptic vesicle exocytosis
- Figure 5 Readily releasable pool of synaptic vesicles
- Figure 6 (A. and B.) Short-term synaptic plasticity - EPSC Depression and EPSC facilitation
- Figure 7 Domain structure of the Complexin protein family
- Figure 8 Amino acid sequence homology between mouse, worm and fly Cplx-1
- Figure 9 Interaction of the Complexin-SNARE complex
- Figure 10 (A. and B.) Genotyping results for Cplx1 WT and Cplx1 KO PCR
- Figure 11 (A. and B.) Genotyping results for SNAP29 conditional and constitutive deletion
- Figure 12 Biochemical analysis of the protein composition in the Nex-Cre SNAP29 KO neurons
- Figure 13 (A. B. C.) Normal excitatory synaptic transmission in hippocampal neurons of Nex-Cre SNAP29 KO
- Figure 14 (D. and E.) Normal short-term plasticity in hippocampal neurons of Nex-Cre SNAP29 KO
- Figure 15 (F. G. H. I.) Normal mEPSC release in excitatory hippocampal neurons of Nex-Cre SNAP29 KO
- Figure 16 Protein composition in SNAP29 constitutive KO mouse brain
- Figure 17 (A. and B.) Immunocytochemical analysis of SNAP29 in neurons
- Figure 18 (A. B. C.) Normal excitatory synaptic transmission in hippocampal neurons of Constitutive SNAP29 KO
- Figure 19 (D. and E.) Normal short-term plasticity in hippocampal neurons of Constitutive SNAP29 KO
- Figure 20 (F. G. H. I.) Normal mEPSC release in excitatory hippocampal neurons of Constitutive SNAP29 KO
- Figure 21 (A. B. C.) Normal inhibitory synaptic transmission in striatal neurons of Constitutive SNAP29 KO
- Figure 22 (D. and E.) Normal short-term plasticity in striatal neurons of Constitutive SNAP29 KO
- Figure 23 (F. and G.) Normal miniature release in inhibitory striatal neurons of Constitutive SNAP29 KO
- Figure 24 (A. B. C.) Evoked synaptic transmission in autaptic hippocampal neurons of Cplx CTRL and Cplx TKO mice
- Figure 24 (D. and E.) Short-term plasticity in autaptic hippocampal neurons of Cplx CTRL and Cplx TKO mice
- Figure 24 (F. and G.) Spontaneous neurotransmitter release (mEPSC) in autaptic hippocampal neurons of Cplx CTRL and Cplx TKO mice
- Figure 25 (A. and B.) Asynchronous neurotransmitter release in autaptic hippocampal neurons of Cplx CTRL and Cplx TKO

- Figure 25 (C.) Representation of synchronous and asynchronous neurotransmitter release under the effect of exogenously applied EGTA-AM in autaptic hippocampal neurons of Cplx CTRL and Cplx TKO
- Figure 25 (D. and E.) Synchronous and asynchronous neurotransmitter release under the effect of exogenously applied buffer EGTA-AM in autaptic hippocampal neurons of Cplx CTRL and Cplx TKO mice
- Figure 26 (A. and B.) Evoked EPSC amplitudes and synchronous release in autaptic hippocampal Cplx TKO neurons expressing Cplx wild type proteins
- Figure 26 (C. and D.) RRP size and vesicular release probability in autaptic hippocampal Cplx TKO neurons expressing Cplx wild type proteins
- Figure 26 (E. and F.) Short-term plasticity in autaptic hippocampal Cplx TKO neurons expressing Cplx wild type proteins
- Figure 26 (G. and H.) Spontaneous neurotransmitter release (mEPSC) in autaptic hippocampal Cplx TKO neurons expressing EGFP and Cplx wild type proteins
- Figure 27 (A. and B.) Evoked EPSC amplitudes and synchronous release in autaptic hippocampal Cplx TKO neurons expressing Cplx1-WT and Cplx1-K69A/Y70A proteins
- Figure 27 (C. and D.) RRP size and vesicular release probability in autaptic hippocampal Cplx TKO neurons expressing Cplx1-WT and Cplx1-K69A/Y70A proteins
- Figure 27 (E. and F.) Short-term plasticity in autaptic hippocampal Cplx TKO neurons expressing Cplx1-WT and Cplx1-K69A/Y70A proteins
- Figure 27 (G. and H.) Spontaneous neurotransmitter release (mEPSC) in autaptic hippocampal Cplx TKO neurons expressing Cplx1-WT and Cplx1-K69A/Y70A proteins
- Figure 28 (A. and B.) Evoked EPSC amplitudes and synchronous release in autaptic hippocampal Cplx TKO neurons expressing Cplx2-WT and Cplx2-K69A/Y70A proteins
- Figure 28 (C. and D.) RRP size and vesicular release probability in autaptic hippocampal Cplx TKO neurons expressing Cplx2-WT and Cplx2-K69A/Y70A proteins
- Figure 28 (E. and F.) Short-term plasticity in autaptic hippocampal Cplx TKO neurons expressing Cplx2-WT and Cplx2-K69A/Y70A proteins
- Figure 28 (G. and H.) Spontaneous neurotransmitter release (mEPSC) in autaptic hippocampal Cplx TKO neurons expressing Cplx2-WT and Cplx2-K69A/Y70A proteins
- Figure 29 (A. and B.) Evoked EPSC amplitudes and synchronous release in autaptic hippocampal Cplx TKO neurons expressing EGFP, Cplx3-WT, Cplx3-K79A/Y80A and Cplx3-C155S proteins
- Figure 29 (C. and D.) RRP size and vesicular release probability in autaptic hippocampal Cplx TKO neurons expressing EGFP, Cplx3-WT, Cplx3-K79A/Y80A and Cplx3-C155S proteins
- Figure 29 (E. and F.) Short-term plasticity in autaptic hippocampal Cplx TKO neurons expressing EGFP, Cplx3-WT, Cplx3-K79A/Y80A and Cplx3-C155S proteins
- Figure 29 (G. and H.) Spontaneous neurotransmitter release (mEPSC) in autaptic hippocampal Cplx TKO neurons expressing EGFP, Cplx3-WT, Cplx3-K79A/Y80A and Cplx3-C155S proteins
- Figure 30 (A.) Evoked EPSC amplitudes in autaptic hippocampal Cplx TKO neurons expressing EGFP, Cplx4-WT, Cplx4-K80A/Y81A and Cplx4-C157S proteins

Figure 30 (B.)	Synchronous release in autaptic hippocampal Cplx TKO neurons expressing EGFP, Cplx4-WT, Cplx4-K80A/Y81A and Cplx4-C157S proteins
Figure 30 (C. and D.)	RRP size and vesicular release probability in Cplx TKO neurons expressing EGFP, EGFP, Cplx4-WT, Cplx4-K80A/Y81A and Cplx4-C157S proteins
Figure 30 (E. and F.)	Short-term plasticity in autaptic hippocampal Cplx TKO neurons expressing EGFP, Cplx4-WT, Cplx4-K80A/Y81A and Cplx4-C157S proteins
Figure 30 (G. and H.)	Spontaneous neurotransmitter release (mEPSC) in autaptic hippocampal Cplx TKO neurons expressing EGFP, Cplx4-WT, Cplx4-K80A/Y81A and Cplx4-C157S
Figure 31 (A. B. C.)	Recombinant His ₆ -tagged Cplx proteins
Figure 32 (A. and B.)	Quantification of endogenous and lentiviral Cplx1 protein expression
Figure 33 (A. and B.)	Quantification of endogenous and lentiviral Cplx2 protein expression
Figure 34 (A.)	Estimation of endogenous Cplx3 protein expression
Figure 34 (B. and C.)	Quantification of lentiviral Cplx3-WT protein expression
Figure 35 (A. and B.)	Quantification of lentiviral Cplx4 protein expression
Figure 36	Complexin and the molecular pathway of synaptic vesicle release.

Abstract

Neurotransmitter release is a synergistic multistep process occurring at synapses in the brain. Synaptic vesicles containing neurotransmitters tether to the presynaptic active zones, upon which, they are docked and primed to fusion competence by a number of proteins. When an action potential arrives at the terminal, a concomitant rise in the intracellular Ca^{2+} concentration causes the vesicles to fuse to the presynaptic membrane and release their contents into the synaptic cleft. This process of neuronal excitation-secretion is tightly coupled and mediated by cascades of protein-protein interactions. The native SNAREs Syntaxin-1, SNAP-25 and Synaptobrevin-2 form a core complex that effectively facilitates the vesicle docking-priming-fusion process. Two proteins namely Complexins and SNAP-29 that have been shown to interact with the native SNAREs or their paralogs are detailed in the present study.

The SNAP-29 protein belongs to the SNAP-25 family and is believed to be a golgi interacting SNARE. It shares only 17% sequence identity with SNAP-25 due to substantial variations in its structure. SNAP-29 was previously shown to interact with multiple Syntaxins localized on various subcellular organelles and was claimed to negatively modulate synaptic transmission in neurons by preventing SNARE disassembly. In the present study, it is proved that conditional loss of SNAP-29 from the forebrain glutamatergic neurons as well as constitutive loss of SNAP-29 in mice did not cause any deficits in transmitter release at glutamatergic or GABAergic synapses. Although constitutive knockout of SNAP-29 in animals caused perinatal lethality, the normal functioning of glutamatergic and GABAergic synapses in the brain could not account for such a dramatic effect. Rather, the lethality seen in these mice was likely due to perturbations in other secretory pathways.

The Complexin family comprises of four proteins - Cplx1, Cplx2 are expressed in the brain, while Cplx3 and Cplx4 are prominently expressed in the retina. Previously, it was shown that loss of Cplx1, 2 and 3 in hippocampal neurons (TKO) caused profound deficits in the vesicular release probability and synchronicity of transmitter release. In the present study, this claim was confirmed and also shown that the reintroduction of each of the four wild type Complexins in the TKO via lentiviruses could facilitate synchronous neurotransmission, to variable extents. The strong binding of Cplx1 and Cplx2 to the SNARE complex corroborated their higher efficacy to mediate synchronous transmitter release. In case of Cplx3 and Cplx4, although hardly any binding to the SNARE complex was detectable, they could facilitate transmitter release only if their SNARE binding domain was intact and when targeted to membranes due to their C-terminal

CAAX farnesylation. These results prove that all mammalian Complexins are indeed facilitators of synchronous synaptic transmission, and exert their function via SNARE complex binding and additional farnesylation for Cplx3 and Cplx4.

1. Introduction

1.1. Neuronal Communication

The intricate architecture of the mammalian brain highlights the complexity of evolution. The brain is the prime functional organ of the nervous system comprising numerous neurons organized in composite networks across the various brain regions. Neurons are the discrete cellular elements of the nervous system and responsible for varied yet precise signaling. The morphology of a typical neuron includes a cell body or soma - for metabolic activities, axons - for conveying electrical impulses over long distances, and dendrites - for receiving and transmitting signals. Neuronal communication occurs via transmission of both chemical and electrical signals at specialized contact zones called synapses. Synapse formation occurs when the axonal growth cone of one neuron contacts a certain site on another neuron. The nascent synaptic contact so established between two neurons comprises an axonal presynaptic compartment that is separated from the postsynaptic region of the target neuron by a few nanometers of space called - the synaptic cleft.

Intrinsically, many proteins are recruited to the presynaptic and postsynaptic sites for the formation, maturation and maintenance of the synapse for efficient neurotransmitter release. Key proteins such as Neuroligins, Neurexins, and other adhesion proteins trigger synaptic development (reviewed by Brose, 2009; Krueger et al., 2012; Brose 2013). Multi-domain scaffolding proteins aid in local trafficking of various types of receptors on the postsynaptic membrane (Kim and Sheng, 2004). The PDZ proteins PSD-95 and SAP-102 are essential for trafficking of glutamate sensing AMPA receptors and NMDA receptors at mature synapses and during synapse development respectively (Elias et al., 2006; Elias et al., 2008). Large clusters of the scaffolding protein Gephyrin anchor receptors for neurotransmitters glycine and GABA_A on the postsynaptic membrane (Kirsch et al., 1993; Craig et al., 1996), while GluR6a mediates surface expression of the ionotropic kainate receptors, independent of PDZ domain interactions (Jaskolski et al., 2004).

1.2. Physiology of synaptic neurotransmitter release

1.2.1. Action potential evoked transmitter release

Synaptic networks closely resemble electrical circuits and neurons are subject to polarization effects due to substantial changes in transmembrane voltages. At chemical synapses, the

neurotransmitters are released from the synaptic vesicles at the presynaptic terminal into the synaptic cleft and, they bind to receptors on the postsynaptic membrane. This process is coupled to an action potential mediated opening or closure of ion channels and consequent flow of post-synaptic current. An action potential (AP) is an event of short duration that occurs when the electrical membrane potential of a neuron rapidly changes. When the action potential arrives at a presynaptic site, it causes the opening of voltage gated Ca^{2+} -channels, and Ca^{2+} -influx, which triggers the fusion of transmitter filled synaptic vesicles.

Electrophysiology-based studies on neurons best describe the postsynaptic currents elicited at excitatory and inhibitory synapses - EPSCs and IPSCs. At excitatory synapses, the neurotransmitter glutamate is released into the synaptic cleft, and it binds the ionotropic AMPA/Kainate receptors on the postsynaptic membrane allowing permeation of mainly Na^+ ions through ligand-gated ion channels into the post-synaptic cell. This ion influx results in depolarization of the post-synaptic membrane, which is about -70 mV at rest. However, at inhibitory synapses, the binding of GABA to the GABA_A receptors or glycine to glycinergic receptors causes receptor activation and increased permeability of Cl^- ions into the cell that hyperpolarizes the membrane. Application of competitive receptor antagonists, such as CNQX and bicuculine, completely and reversibly blocks the EPSCs and IPSCs, respectively (Schneeggenburger et al., 1992; Wilcox et al., 1994).

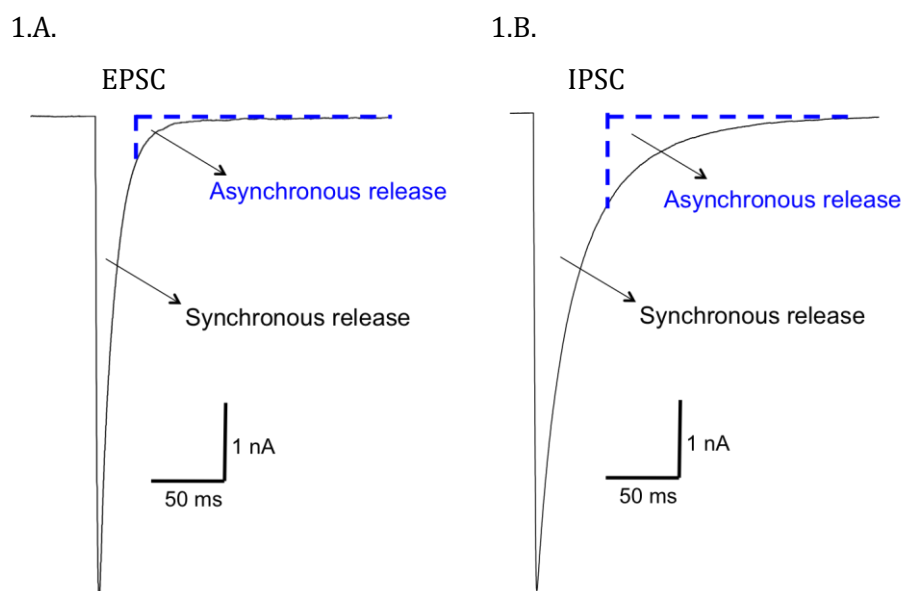


Figure 1 (A) Excitatory post-synaptic current (EPSC) and (B) Inhibitory post-synaptic current (IPSC). The EPSCs decay with a lower time constant compared with IPSCs. The post-synaptic current is represented by the two distinct kinetics phases - a fast synchronous phase and a slow asynchronous phase of release.

The post-synaptic currents at central synapses are biphasic in nature, due to two kinetically distinct components of transmitter release - a fast synchronous component that decays rapidly with a time constant of 5-10 ms and a slow asynchronous component with an exponential decay of 100-200 ms (Goda and Stevens, 1994). The synchronous component of the postsynaptic response is tightly coupled to arrival of an action potential and researchers believe that a low affinity primary Ca^{2+} sensor promotes synchronous release when intraterminal Ca^{2+} concentration is enhanced within a few hundred microseconds after the stimulus. On the other hand, a high affinity Ca^{2+} sensor is believed to sustain the asynchronous phase of release that occurs during the clearance of residual Ca^{2+} from the terminal (Goda and Stevens, 1994; Sabatini and Regehr, 1996).

1.2.2. Spontaneous synaptic transmitter release

Rate of secretion of acetylcholine in the absence of impulse propagation was first studied using Tetrodotoxin (TTX) that blocks electrical excitation by preventing Na^+ entry through depolarized membrane (Katz and Miledi, 1967). Spontaneous miniature end-plate potentials of normal frequency and amplitude were first recorded from paralyzed Sartorius muscles of frogs by application of TTX (Katz and Miledi, 1967). This technique has been used to study neurotransmitter release at central synapses in the absence of a depolarizing stimulus. Spontaneous transmitter release at synapses can be measured as miniature currents that occur in the absence of an action potential. This form of neurotransmitter release, also known as quantal release, occurs at both excitatory and inhibitory synaptic terminals, due to spontaneous fusion of synaptic vesicles with the presynaptic plasma membrane.

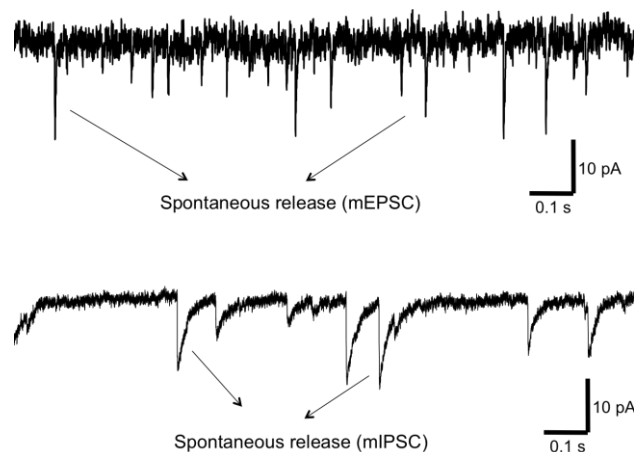


Figure 2. Spontaneous release. Spontaneously occurring miniature quantal release events (mEPSCs and mIPSCs) in the absence of depolarizing stimuli (application of 300 nM Tetrodotoxin blocks action potentials).

1.3. Core molecular machinery of synaptic vesicle release

Neurotransmitter release is a synergistic multistep process transpiring with high temporal and spatial precision at the presynaptic terminal of a neuron. The process of transmitter release is classified into distinctive stages: transmitter uptake by synaptic vesicles, tethering of vesicles to presynaptic membrane, priming vesicles to fusion competence, Ca^{2+} influx causing synaptic vesicle exocytosis, and vesicle recycling.

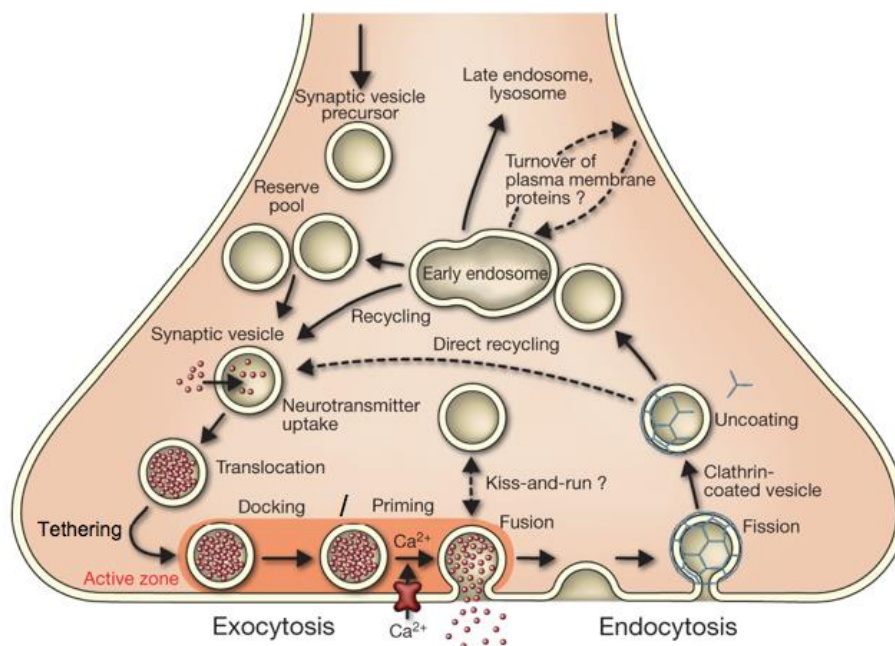


Figure 3. Schematic representation of synaptic vesicle exocytosis. Synaptic vesicles take up neurotransmitters and tether to the active zone on the presynaptic plasma membrane, after which they are morphologically docked and functionally primed to fusion competence by a number of proteins. The vesicles fuse to the presynaptic membrane upon the arrival of an action potential and a concomitant rise in the intracellular Ca^{2+} concentration, and release their neurotransmitter content into the synaptic cleft. The fused vesicles are retrieved via clathrin-mediated endocytosis and are recycled for the next round of exocytosis. (Adapted and modified from Jahn and Fasshauer, 2012).

1.3.1. Synaptic vesicles

Synaptic vesicles are spherical secretory organelles about 40 nm in diameter, found at the presynapse. They take up neurotransmitters with the help of vesicular transporter proteins in a proton-pump driven fashion. Hydrolysis of ATP in the cell causes translocation of protons onto the vesicular lumen, generating a potential/pH gradient that aids the transporter proteins to move the neurotransmitter molecules into the vesicle (reviewed by Bennett and Scheller, 1994).

The proteins that have been identified to aid in transport of neurotransmitters are specific to the type of neurotransmitter and its respective synapse. Vesicular glutamate transporters (VGLUTs) are required for loading synaptic vesicles with glutamate whereas the vesicular inhibitory amino acid transporter (VIAAT) acts as a shared vesicular carrier for the uptake and release of both GABA and glycine (Wojcik et al., 2004; Wojcik et al., 2006).

Synaptic vesicles go through two essential steps mediated by SNAREs and SNARE regulatory proteins in order to release neurotransmitters - 1. Docking to the presynaptic membrane and priming to a release-ready state, and 2. Ca²⁺-mediated vesicle fusion.

1.3.2. Formation of the SNARE core complex

Fusion of synaptic vesicles to the presynaptic plasma membrane requires the concerted action of various structurally and functionally unique presynaptic proteins at distinct steps. Three main proteins namely Synaptobrevin-2, Syntaxins and SNAP-25 are the core components of the membrane fusion apparatus at most brain synapses. They constitute the SNARE (SNAP receptor) complex - a receptor site for interaction of the soluble NSF attachment proteins (SNAP), and have a high degree of vesicle and target membrane specificity. The SNARE complex was first purified from a crude bovine brain detergent extract based on its ability to form the multisubunit 20S particle with recombinant NSF and SNAPs (Söllner et al., 1993a). Syntaxins and SNAP-25 localize to the plasma membrane and are termed t-SNAREs, whereas Synaptobrevin-2 (also known as VAMP) is partially cytoplasmic, but inserted into synaptic vesicles via its C-terminus (Söllner et al., 1993b). Synaptobrevin, Syntaxin and SNAP-25 form a stable ternary complex with a 1:1:1 stoichiometry (Fasshauer et al., 1997). Such association of the SNAREs is thought to represent the minimal fusion machinery, and to drive the vesicle fusion reaction. Indeed, proteoliposomes reconstituted with the cognate SNAREs spontaneously fuse upon SNARE complex assembly (Weber et al., 1998).

In-vivo, it is believed that the close proximity of the synaptic vesicles to the target plasma membrane allows the formation of a thermodynamically stable SNARE complex. Circular dichroism spectroscopy and crystallography have well described the structural nature of the SNARE complex. The α -helical content is enriched as the C-terminal H3 domain of Syntaxin-1A binds to the cytoplasmic domain of Synaptobrevin and the truncated N- and C-terminal fragments of SNAP-25B (Fasshauer et al., 1998a). The crystal structure of the SNARE complex resolved at 2.4 Å showed that the heterotrimeric components are arranged in a parallel orientation comprising of α -helical interactions between Syntaxin, Synaptobrevin and the C-

terminal helices of SNAP-25 (Sutton et al., 1998). The ionic layer 0 at the centre of the assembled SNARE complex is comprised of an arginine (R) residue contributed by Synaptobrevin (R-SNARE), and glutamine (Q) residue contributed by Syntaxin (Qa-SNARE), N-terminal SNAP-25 (Qb-SNARE) and C-terminal SNAP-25 (Qc-SNARE) (Fasshauer et al., 1998b). Researchers believe that the Q-SNAREs partially assemble into a Qabc acceptor scaffold, which initiates stable SNARE binding and nucleates the zipping of the *trans*-SNARE four-helical bundle from its membrane-distal (N-terminus) towards the membrane-proximal (C-terminus) end. This process is tightly coupled to vesicle fusion and the mechanical force exerted during SNARE assembly is believed to be sufficient to overcome the steric repulsions and energy barriers of the associating membranes, thus allowing them to fuse (reviewed by Jahn and Scheller, 2006).

1.4. Molecular regulators of vesicle docking, priming and fusion

The process of synaptic vesicle exocytosis proceeds in distinctive steps, each mediated by multiple proteins.

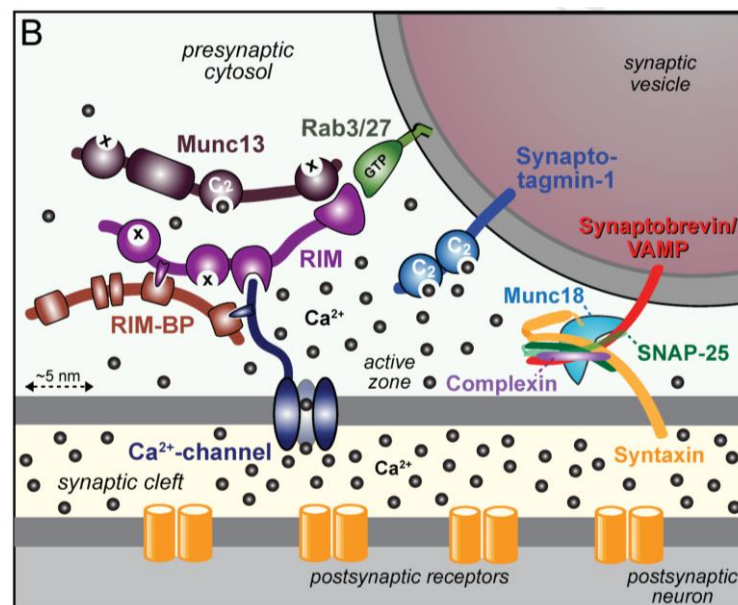


Figure 4. Protein interactions at the active zone governing synaptic vesicle exocytosis. The v-SNARE Synaptobrevin-2 is anchored on the synaptic vesicle membrane, while the t-SNAREs Syntaxin-1 and SNAP-25 are anchored in the presynaptic plasma membrane. Together they form the four-helical bundle. Additional proteins such as Munc18, Munc13s and RIM contribute to vesicle docking and priming to fusion competence. Complexin binds to the preassembled SNARE complex at a late step and helps facilitate Ca²⁺-driven vesicle fusion. (Adapted from Südhof, 2012).

1.4.1. Docking factors

The synaptic vesicles attach at specialized areas on the presynaptic membrane - also known, as active zones in a process termed docking. Some SNARE and SNARE associated proteins have been implicated to play a significant role in docking of vesicles in neurons and neuroendocrine cells. Docking is observable as a morphological recruitment process of vesicles at synapses; hence, it has extensively been studied by analyzing the ultrastructure of presynaptic terminals in either chemically fixed or high-pressure frozen samples using electron tomography - the latter technique being preferable, as it appears to cause minimal sample perturbation and artifacts. Docked vesicles are measured at a distance of roughly 40 nm or closer to the presynaptic membrane.

Munc18-1 is a member of the conserved SM family of proteins involved in membrane fusion reactions, from lower eukaryotes such as *S. cerevisiae* and *C. elegans* to higher mammals. Ultrastructure analysis by solvent fixation of adrenal glands from Munc18-1 null mutant mice revealed a dramatic reduction in the number of secretory large dense core vesicles attached to the plasma membrane of chromaffin cells, implying a deficit in vesicle docking that was rescued by over-expression of Munc18-1 (Voets et al., 2001). Another striking difference observed in the Munc18-1 null mutants compared to control animals was a ~2 fold reduction in the cellular expression levels of the Syntaxin-1AB protein.

Correspondingly, BoNT/C-mediated proteolysis of Syntaxin produced an exact phenocopy of the Munc18-1 mutant docking phenotype in chromaffin cells but not at neuronal synapses confirming that Syntaxin-1-Munc18-1 dimer forms a docking platform for neurosecretory vesicles (de Wit et al., 2006). In *C. elegans*, the protein Unc13 could open the closed conformation of wild-type Syntaxin and prevent the *cis*-interaction of Syntaxin-1 N-terminal Habc domain and the SNARE complex (Hammerlund et al., 2007). The Unc13-deficient mutants exhibited pronounced docking deficit in ACh and GABAergic motor neuronal synapses analyzed by high-pressure freezing, which was eliminated only by over-expression of open Syntaxin and not its wild-type variant (Hammerlund et al., 2007). In mice, deletions of the homologous SNAREs Syntaxin-1, SNAP-25 and Synaptobrevin-2 caused a partial reduction in the number of membrane tethered synaptic vesicles in the respective mutant embryonic hippocampal slices, implying that these proteins are essential for morphological docking of vesicles on the presynaptic active zones (Imig et al., 2014).

1.4.2. Priming of synaptic vesicles - The RRP

Early studies delineated docking and priming to be intrinsically distinct processes essential for vesicle mobilization and fusogenicity, occurring in a sequential fashion. Vesicles in close apposition (<40 nm) to the plasma membrane have typically been considered morphologically docked (Imig et al., 2014). Molecular factors such as phosphoinositides, ATP-dependent NSF activity and protein kinases were thought to be essential in rendering the docked vesicles fusion competent in PC12 and neuroendocrine cells (reviewed by Klenchin and Martin, 2000). Many studies have now proven that SNARE regulatory proteins such as Munc13s, and CAPS are indispensable 'priming factors' that maintain a readily releasable pool (RRP) of vesicles at synapses.

The RRP of vesicles ready for release can be depleted and replenished rapidly at a synapse. Superfusion of dendrites with a hyperkalemic solution caused an initial increase in the quantal release rate followed by an exponential decline - this form of synaptic release was estimated to correspond to the depletion of the vesicle pool and subsequent refilling (Stevens and Tsujimoto, 1995). Later, a hypertonic solution was employed to study the kinetics of the transient exocytotic burst. Tonicity of the solution is a crucial determinant of the quantal release rate as high osmolarity of a solution could prevent the synaptic depolarization induced by the hyperkalemic solution. A hypertonic solution such as 500 mOsm Sucrose effectively depletes all the readily releasable vesicle pool independent of Ca^{2+} influx at the synapse and also clearly delineates the refilling quanta (Rosenmund and Stevens, 1996).

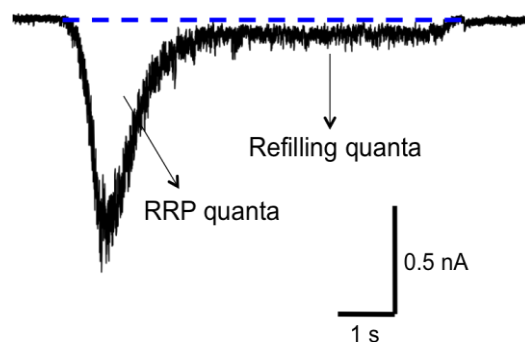


Figure 5. Readily releasable pool (RRP) of synaptic vesicles. The readily releasable quanta at the presynaptic terminal can be completely depleted by application of a hypertonic solution of 500 mM Sucrose. The charge of the transient component depicts all the vesicles that are released and the sustained component indicates the refilling quanta.

However, another method for depletion of the RRP is to stimulate the synapse at high frequencies. High-frequency stimulation of synapses depletes the RRP, which causes a depression of the PSC amplitudes (Dobrunz and Stevens, 1997). A synapse is considered to be plastic when the synaptic strength dynamically varies on distinctive time scales due to prolonged activity. Short-term synaptic plasticity refers to variations in synaptic output over a time span of a few milliseconds to a few minutes.

Depression of a synapse refers to the progressive decline in the amplitudes of evoked responses elicited by repetitive high-frequency stimuli (Zucker, 1989). A fast-depressing synapse is typically thought to indicate a high vesicular release probability. Presynaptic Ca^{2+} influx was found to have a positive effect on the release probability of a synapse - a high external Ca^{2+} concentration accelerated vesicle depletion and consequent depression synaptic currents (Dittman and Regehr, 1998). However, synaptic depression may also occur due to reduced quantal size as well as the quantal content (Scheuss et al., 2002). It was also shown that cross-linking of surface GluR2-AMPA receptors increased paired pulse depression, which was thought to occur as a result of presynaptic glutamate release and consequent desensitization of the agonist bound AMPA receptors (Heine et al., 2008). Contrary to depression, high frequency stimulation may also result in prominent enhancement of synaptic responses. Synaptic facilitation is clearly observable with pairs of stimuli, wherein the amplitude of the latter post-synaptic current is larger compared to the former. Repetitive pairs of stimulations can also cause buildup and decay of synaptic facilitation within a few milliseconds at synapses with a low initial release probability (reviewed by Zucker and Regehr, 2002).

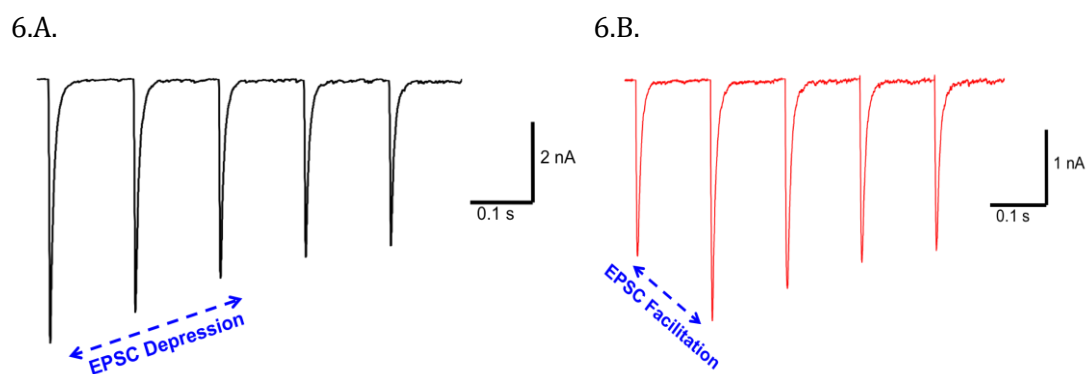


Figure 6. Short-term synaptic plasticity. **(A)** Depression of EPSC amplitudes observed under stimulation at high frequency of 10 Hz, indicative of high vesicular release probability. **(B)** Initial facilitation of the EPSC amplitudes (2^{nd} EPSC > 1^{st} EPSC) a high frequency stimulation of 10 Hz, typically observed in neurons with low vesicular release probability.

Another form of synaptic enhancement that persists on a time scale of a few seconds is augmentation. It occurs owing to slow clearance of residual Ca^{2+} accumulating in the synaptic terminal after repetitive high frequency stimulation. Initially, augmentation was believed to reflect a transient increase in the overall size of the readily releasable vesicle pool. Patch-clamp studies on solitary hippocampal neurons revealed that a moderate reduction in the relative vesicle pool size, but a huge increase in the size of an action-potential induced synaptic current implying a surge in the average quantity of neurotransmitter released at augmented synapses (Stevens and Wesseling, 1999). Later, it was shown that increased rate of Ca^{2+} -dependent priming (increase in RRP) causes augmentation (Junge et al., 2004).

1.4.2.1. Priming proteins

Munc13

The mammalian Munc13 proteins were first discovered to have a high degree of amino acid sequence homology to the Unc13 family in *C. elegans* (Brose et al., 1995). Three isoforms have been identified in the brain, namely Munc13-1, two splice variants of Munc13-2 - the ubiquitously expressed ubMunc13-2 and the brain-specific bMunc13-2, and Munc13-3, each of which have conserved C1 and C2 (C2B and C2C) domains, Ca^{2+} -Calmodulin binding motifs within an amphipathic helix comprised of basic, hydrophobic residues, and a large MUN domain (Augustin et al., 1999a; Augustin et al., 1999b, Betz et al., 2001; Junge et al., 2004).

Presynaptic expression of both Munc13-1 and Munc13-2 is crucial for glutamatergic synaptic vesicle maturation to fusion competence and release (Varoqueaux et al., 2002). Munc13-1 and Munc13-2 dependent synapses exhibit variability in short-term plasticity - the synapses expressing only Munc13-1 depress rapidly but those devoid of Munc13-1 but expressing Munc13-2 show a marked augmentation that is attributed to increases in intracellular Ca^{2+} concentration and releasable vesicle pool size (Rosenmund et al., 2002).

Munc13s also distinctively bind β -phorbol esters and diacylglycerol at the C1 domain, which is thought to be involved in their regulation by second messengers (Rhee et al., 2002). Inactivation of the DAG/ β -PE binding site in Munc13-1 due to a point mutation H567K, did not affect basal synaptic transmission or the RRP size in neurons (Rhee et al., 2002). However, DAG/ β -PE induced synaptic potentiation of evoked transmitter release was completely abolished (Rhee et al., 2002). Point mutation of the Ca^{2+} -CaM binding motif on Munc13-1 (W464R) and ubMunc13-2 (W383R) abolishes calmodulin binding and impairs Ca^{2+} -dependent short-term plasticity, but

does not affect initial vesicular release probability and Ca^{2+} -independent RRP refilling (Junge et al., 2004). Therefore, CaM binding to Munc13s is essential for maintaining a Ca^{2+} -dependent priming of synaptic vesicles. The MUN domain of Munc13s is an independently folding domain essential for vesicle priming and regulated exocytosis, as well as for opening the Munc18-Syntaxin closed conformation to facilitate docking (Basu et al., 2005; Ma et al., 2011), while the C2B domain of Munc13 is a Ca^{2+} and phospholipid-binding module that controls Munc13 activity (Shin et al., 2010).

CAPS

Ca^{2+} -dependent activator proteins for secretion, also known as CAPSs form a family of proteins with two main isoforms CAPS1 and CAPS2. These proteins share a 79% sequence homology. CAPS1 expression is predominant across all brain regions, whereas CAPS2 expression is strong only in the cerebellum and the adrenal glands (Speidel et al., 2003). CAPS proteins share limited homology with Munc13s due to the presence of the MUN domain in their structure. Therefore, the effects of CAPS proteins on exocytosis of synaptic vesicles and secretory vesicles were studied to great detail in CAPS-1/2 double knockout mice. With respect to synaptic vesicles in the mutant mice, 39% neurons elicited no EPSCs in response to low-frequency stimulations, and showed a parallel reduction in the RRP size, and the frequency of miniature EPSCs (Jockusch et al., 2007). These results clearly indicated a severe deficit in vesicle priming, and reduced transmitter content in vesicles, although the priming deficit could be transiently bypassed by an increase in intracellular Ca^{2+} (Jockusch et al., 2007). Similarly, the RRP size of the large dense core vesicles was dramatically reduced in chromaffin cells from CAPS-1/2 mutant mice (Liu et al., 2008). Also, the sustained component of release, representative of the priming of vesicles during stimulation, was virtually absent when measured in the mutant cells (Liu et al., 2008). Thus, CAPS proteins play a highly significant role in vesicle priming.

In recent electron microscopy based studies of synaptic vesicle localization in hippocampal slices, it has been shown that the number of membrane tethered or docked vesicles are dramatically reduced in the absence of Munc13s or CAPS (Siksou et al., 2009; Imig et al., 2014). Taken together, the ultrastructural and electrophysiological data affirm that docking and priming are morphological and functional manifestations of the same process aided by the same proteins.

1.5. Ca²⁺-mediated vesicle fusion - role of Cognate SNAREs

1.5.1. Synaptobrevin-2

Synaptobrevin-2 is the main vesicle associated SNARE isoform expressed in the forebrain. Deletion of VAMP2 lowers the rate of synaptic quantal transmitter release by ten-fold compared to controls, and completely abolishes the Ca²⁺-triggered evoked release in the mouse brain (Schoch et al., 2001). Sequence insertions to increase the intramolecular distance between the SNARE binding motif and transmembrane region of VAMP2 caused a pronounced and length-dependent reduction of evoked release and the vesicular release probability (Deak et al., 2006), alluding to a more preferential role of VAMP2 in catalyzing Ca²⁺-dependent vesicle fusion via a tight molecular link between its complex forming SNARE motif and TMR (Guzman et al., 2010).

1.5.2. Syntaxin-1

Syntaxin in its open conformation was found essential for vesicle docking in *C. elegans* (Hammerlund et al., 2007). In mice, the closed or open state of Syntaxin, did not dramatically affect synaptic vesicle docking but a perpetual open conformation of Syntaxin due to a point mutation on one of its splice variant Syntaxin-1B, accelerated spontaneous synaptic vesicle fusion, moderately reduced the RRP and significantly enhanced short-term depression leading to fulminant epileptic seizures in the mutant mice (Gerber et al., 2008). However, a hypomorphic mutation of Syntaxin-1B coupled with homozygous deletion of Syntaxin-1A not only caused an overall decrease in the expression levels of Syntaxin alongside the formation of fewer SNARE complexes but also reduced various synaptic parameters such as AP-evoked release, spontaneous release, the size of RRP, and the rate of RRP refilling (Arancillo et al., 2013). These results have led to the conclusion that conformational changes in Syntaxin mediate vesicle docking and differentially regulate vesicle fusogenicity.

1.5.3. SNAP-25 and paralogs

SNAP-25 is known to have additional neuronal homologs namely SNAP-23, SNAP-47 and SNAP-29 in mammals. Targeted genetic ablation of SNAP-25 does not cause morphological abnormalities in the mouse brain; mutant neurons develop normal neurite extensions and immature synapses until 8 days in low-density cultures but subsequently degenerate (Washbourne et al., 2001). All parameters such as AP-evoked, sucrose-evoked and spontaneous release at excitatory synapses were severely impaired in SNAP-25 deletion mutant neurons in

culture associating a critical role for SNAP-25 in mediating neuronal exocytosis (Tafuya et al., 2006; Bronk et al., 2007). Similarly, in SNAP-25 mutant chromaffin cells, secretion triggered by UV flash photolysis of caged Ca²⁺ was impaired but rescued by over-expression of SNAP25 isoforms a and b (Sørensen et al., 2003).

SNAP-23

Although SNAP-25 is expressed only in neuronal and neuroendocrine cells, one of its paralogs SNAP-23 is expressed also in non-neuronal tissues. SNAP-23 was first discovered in a human B lymphocyte cDNA library screen, and shares 79% amino acid sequence identity with SNAP-25. In-vitro fusion assays identified SNAP-23 to bind Syntaxin-1, -2, -3, and -4 as well as VAMP-1 and -2 (Ravichandran et al., 1996). In congruence with its SNARE binding abilities, SFV-mediated dramatic over-expression of SNAP-23 in chromaffin cells expressing endogenous SNAP-25 caused a considerable reduction in the exocytotic burst and overall secretion indicating that overexpressed SNAP-23 likely competes with SNAP-25 for cognate SNARE binding (Sørensen et al., 2003). However, lentiviral mediated expression of SNAP-23 in endogenous SNAP-25 expressing wild-type neurons did not modify evoked release significantly, implying that SNAP-25 is preferentially used by SNAREs for neurotransmission (Delgado-Martinez et al., 2007). With respect to subcellular distribution, endogenous SNAP-23 is enriched at excitatory synapses in dendritic spines, and perisynaptic co-localization of SNAP-23 and NMDA receptors is observable. Likewise, in terms of functional characteristics, shRNA mediated knockdown of SNAP-23 caused a significant reduction in the amplitudes of NMDA-receptor mediated EPSCs suggesting that surface expression of NMDA receptors is diminished in the absence of SNAP-23 (Suh et al., 2010).

SNAP-47

SNAP-47, a member of the SNAP-25 subfamily was first identified from proteomic analysis of synaptic vesicle associated peptides that were purified by subcellular fractionation. Expression of murine SNAP-47 is developmentally regulated in the brain, with maximal expression levels observable already at embryonic day 18. Its expression is also detectable in various other organs such as liver, kidneys, lungs, spleen and testis (Holt et al., 2006). As SNAP-47 was identified as a Qbc-SNARE, reconstitution of proteoliposomes with SNAP-47, Syntaxin-1A and Synaptobrevin-2 caused ternary complex formation preceding liposome fusion (Holt et al., 2006). As *in-vitro* data suggested that SNAP-47 might be functionally important for synaptic transmission, it was corroborated recently in a study where shRNA-mediated knockdown of SNAP-47 prevented the glycine induced increase in surface expression of GluA1 receptor levels in cultured neurons and

impaired LTP in acute hippocampal slices - this deficit could be rescued only in the presence of an shRNA resistant wild-type SNAP-47 with its intact functional SNARE complex-interacting C-terminus (Jurado et al., 2013).

SNAP-29

SNAP-29 is a ubiquitously expressed variant of SNAP-25 that has not been extensively studied in well-controlled model systems up until now. SNAP-29 was primarily discovered using the yeast two-hybrid screen approach to identify novel interaction partners of Syntaxin-3. The yeast two-hybrid cDNA clone sequentially matched a 258 a.a. ORF in the human brain cDNA library, encoding a protein of about 28.9 kDa in size, which shared 17% sequence identity with SNAP-25 (Steegmaier et al., 1998). SNAP-29 corresponds to GS32, a ubiquitous SNARE localized to the Golgi apparatus found in both cytosolic and membrane fractions of homogenized NRK cells (Wong et al., 1999). *In-vitro* binding assays showed promiscuous binding of SNAP-29 to GST-fused Syntaxin-1A, -3, -4, -7, -13 and -17, which are expressed on the plasma membrane, Golgi apparatus and late endosomes (Steegmaier et al., 1998). Similarly, transient over-expression of SNAP-29, Syntaxin-4, and Syntaxin-6 in HeLa cells allowed the formation of binary t-SNARE complexes between SNAP-29 and Syntaxins *in-vivo*, which was augmented by co-expression of VAMPs (Hohenstein et al., 2001).

Members of the SNAP-25 family lack transmembrane domains in their structure but possess coiled coil motifs. The structure of SNAP-29 comprises of an NPF (asparagine-proline-phenylalanine) motif at the N-terminal end, two coiled-coil domains at the N-terminal and C-terminal, each preceded by proline rich regions. However, it lacks a stretch of conserved cysteine residues that are present in the other isoforms and are essential for palmitoylation - a post-translational modification of the protein required for subcellular targeting and membrane association (Steegmaier et al., 1998).

In 2005, Sprecher and colleagues made the remarkable discovery that the neurocutaneous CEDNIK syndrome manifests in humans as a result of homozygous deletion of the pyrimidine nucleotide 'G' at position 220 on the SNAP-29 cDNA. The deletion causes premature termination of translation 28 amino acids downstream of the mutation and results in a severely truncated SNAP-29 protein. Prominent symptoms associated with the disease at the tissue level are reduced conductance from peripheral retina, abnormal lamellar granule maturation and secretion, while at the organ level include macular atrophy, facial dysmorphism, severe psychomotor retardation, palmoplantar keratoderma (Sprecher et al., 2005). Another CEDNIK

mutation was identified as a homozygous purine nucleotide 'A' insertion at position 486 of the SNAP-29 cDNA, which results in premature termination of translation 5 amino acids downstream of the mutation (Fuchs-Telem et al., 2010). The mutated SNAP-29 sequence was cloned into a pEGFP construct, transfected into HeLa cells and compared with non-transfected and wild type SNAP-29 transfected cells using confocal microscopy. A punctate pattern of localization was observable along the perinuclear zone of the cells expressing wild-type SNAP-29 - reminiscent of a distribution pattern with Golgi associated proteins, while expression of the mutated SNAP-29 was diffuse in the nucleus and cytosol (Fuchs-Telem et al., 2010). In the rodent brain, SNAP-29 and Rab3A interact in a GTP γ S dependent manner, co-express in myelinating glia, and regulate the trafficking of myelin proteolipid protein to the plasma membrane (Schardt et al., 2009). In HEK cells, an exclusive perinuclear co-localization of the two proteins is observable (Schardt et al., 2009).

Because of its affinity to Golgi-associated Syntaxins, researchers believed that SNAP-29 might play a modulatory role in synaptic transmission. Whole-cell patch clamp experiments performed on wild-type rat hippocampal neurons subjected to viral over-expression of SNAP-29 showed that the synaptic vesicle turnover was significantly reduced after repetitive stimulations at 0.1 Hz and 1 Hz. Such an inhibitory effect was eliminated and the synaptic vesicle turnover after repetitive firing was increased upon siRNA-mediated knockdown of endogenous SNAP-29 (Pan et al., 2005).

Loss of SNAP-29 has been shown to critically affect phagocytic and secretory pathways in non-cranial organs such as in mast cells, fibroblasts, intestinal epithelium, and oocytes, which is not uncommon for a ubiquitously expressed protein (Rapaport et al., 2010; Sato et al., 2011; Wesolowski et al., 2012). The role of SNAP-29 has been predominantly studied in non-mammalian model systems such as *C. elegans* and *Drosophila*. However, a systematic and well-controlled analysis of the role of SNAP-29 in the mammalian brain has not been performed yet.

1.6. Aim1: Biochemical and functional study of SNAP-29

The first aim of my study was to investigate the role of SNAP-29 in mediating synaptic transmission in mice. Although the physiological effects of the other SNAP-25 paralogs have been extensively studied at central synapses, the precise function of SNAP-29 has remained an enigma due to the lack of adequate tools. Over-expression of SNAP-29 was shown to negatively modulate neurotransmitter release at excitatory neurons by inhibiting SNARE disassembly and reducing synaptic vesicle turnover (Pan et al., 2005). While one could agree on a dominant negative effect that may arise due to abundant SNAP-29 binding to the SNARE complex competitively, the roles of endogenous SNAP-29 and the other SNAP-25 paralogs in these neurons remained unexplained. Therefore, in my study, I aimed to characterize the function of SNAP-29 using mice that carried conditional and constitutive deletions of the SNAP-29 gene.

1.7. Ca²⁺-mediated fusion - role of Complexin

1.7.1. Complexin structure and homology

Complexins (Cplx) are a family of small, cytosolic, highly charged, SNARE-associated proteins found in a number of eukaryotic organisms. In mammals, there are four known members of the Complexin gene family, namely *Cplx1*, *Cplx2*, *Cplx3*, and *Cplx4*, which are differentially expressed across various organs. *Cplx1* and *Cplx2* proteins are 134 amino acid long and expressed predominantly in several regions of the brain (McMahon et al., 1995), whereas *Cplx3* with 158 amino acids is relatively less abundant in the brain but more strongly expressed in the retina, along with *Cplx4* consisting of 160 amino acids (Fig.7.) (Reim et al., 2005). *Cplx2* is detectable in the mammalian adrenal glands (Archer et al., 2002; Cai et al., 2008) and peripheral tissues, suggestive of a ubiquitous role. Complexins are evolutionarily conserved across different species with variable sequence identities. For example, Complexin homologs known as Synaphins, are found in the electromotor nerve cell bodies innervating the cartilaginous fish, *Narke japonica* (Ishizuka et al., 1997). Similarly, *C. elegans* and *Drosophila melanogaster* each have homologs of Complexin with an approximate 39% sequence identity with murine *Cplx1* (Fig.8.) (Hobson et al., 2011).

Database searches to compare vertebrate and invertebrate orthologs of Complexins revealed a highly conserved region covering amino-acid residues 34-77 at the centre of the protein (Pabst et al., 2000). NMR and CD spectroscopic analysis of recombinant rat *Cplx1* confirmed that a substantial part (35-40%) of the protein sequence forms a α -helical structure between amino-acid residues 26 and 83 (flanked by the N- and C-terminus) and stoichiometrically binds to the SNARE complex (Pabst et al., 2000). In *Cplx3* and *Cplx4*, a unique CAAX motif at the C-terminal end was discovered to represent the consensus sequence for farnesylation - a form of posttranslational modification that allows the protein to be targeted to membranes (Fig.7.) (Reim et al., 2005).



Figure 7. **Domain structure of the Complexin protein family.** The Complexin proteins have a general structure with four important domains, shown here in *Cplx1*. The N-terminus of the *Cplx* proteins spans amino acid residues 1 to 26, and is essential for the facilitatory function of

Complexins (Xue et al., 2010). The accessory α -helix spans residues 27 to 47, and has been shown to inhibit vesicle fusion by preventing the complete zippering of the SNARE complex (Xue et al., 2010). The central α -helix is essential for Complexin binding to the SNARE complex, and the loss-of-function of this domain impairs release (Xue et al., 2007). The C-terminus has been shown to have different functions, partly depending on the model system - in Cplx1, for example, the C-terminus stimulates liposome fusion *in-vitro* (Malsam et al., 2009), but is essential for vesicle priming and clamping spontaneous vesicle fusion in cortical neurons (Kaeser-woo et al., 2012). The CAAX motif at the end of the C-terminus is a unique site for post-translational farnesylation present only on Cplx3 and Cplx4 (Reim et al., 2005).

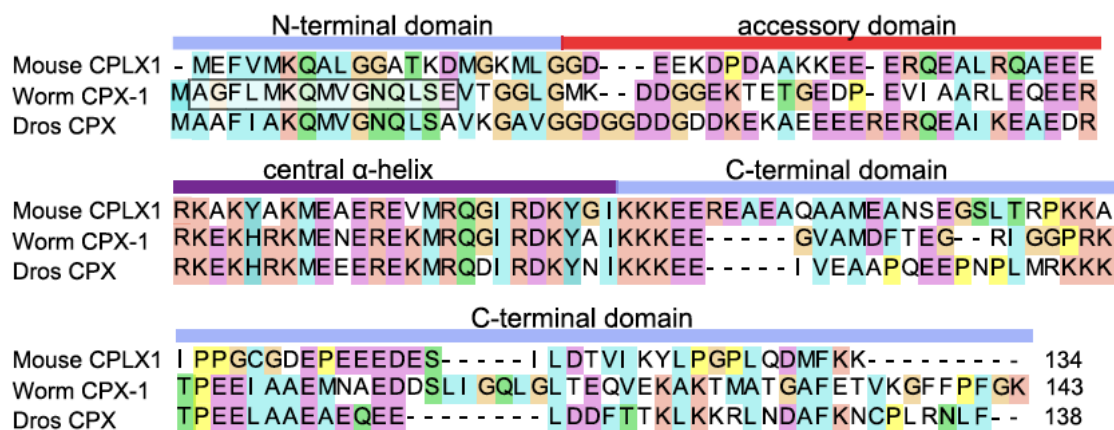


Figure 8. Amino acid sequence homology between mouse, worm and fly Cplx1. The murine Cplx1, *C. elegans* Cplx1 and *Drosophila* Cplx are similar in size. Their overall sequence identity is 39% with maximal sequence conservation in the central α -helical domain (Adapted from Hobson et al., 2011).

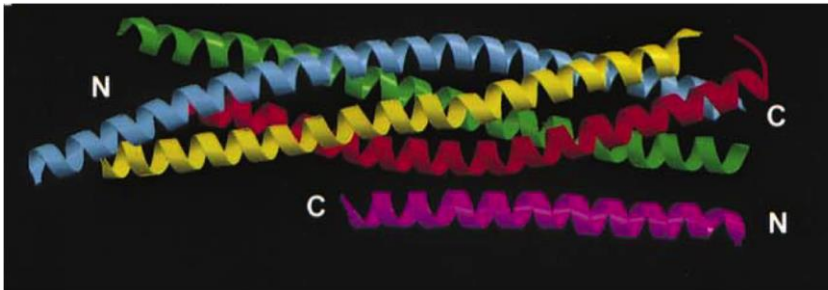
1.7.2. Complexin - SNARE interactions

Mammalian Cplx1 and Cplx2 were first discovered in a syntaxin co-immunoprecipitation of the synaptic SNARE complex from rat brain homogenate, and were shown to bind to the SNARE complex with nanomolar affinity *in-vitro* (McMahon et al., 1995). Biophysical studies attempted to resolve the structure of Complexins and its association with the SNARE complex. Cplx1 and Cplx2 preferentially bound only to preassembled ternary SNARE complex reconstituted on proteoliposomes with a 1:1 stoichiometry via their central α -helical region (Pabst et al., 2000).

Resolution of the three-dimensional crystal structure of the Complexin26-83/SNARE complex in squids and mammals revealed four parallel, highly twisted α -helices formed by the SNARE motifs of Synaptobrevin-2, Syntaxin-1, SNAP-25A, SNAP-25B and a fifth slightly twisted α -helix corresponding to Cplx (Fig.9.) oriented in an anti-parallel fashion within the groove of the 'trans-

SNARE' complex, stabilizing the interface between Synaptobrevin and Syntaxin as well as likely counteracting the repulsive forces of the opposing vesicle- and plasma-membranes (Chen et al., 2002; Bracher et al., 2002).

9.A.



9.B.

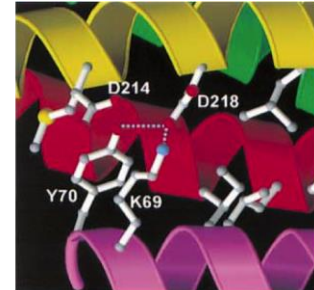


Figure 9. **Interaction of the Complexin-SNARE Complex.** **(A)** Ribbon diagram illustrates the orientation of helices of the SNAREs and Complexin. Colour code is as follows: Yellow - Syntaxin, Red - Synaptobrevin, Blue - SNAP-25 N-terminal SNARE motif, Green - SNAP-25 C-terminal SNARE motif, Pink - Complexin. **(B)** Interaction between lysine (K69) and tyrosine (Y70) residues of Complexin with Aspartate (D218) of Syntaxin is shown. Hydrogen bond is formed between Y70 and D218, whereas a salt bridge is formed between K69 and D218. Oxygen atoms are indicated in red, and nitrogen atoms are indicated in blue (Adapted from Chen et al., 2002).

In support of these findings, a dramatic increase in fluorescence anisotropy indicated that Cplx/SNARE complex binding occurs on a millisecond timescale while EPR and CD spectroscopy inferred no major structural changes to the core SNARE machinery due to the rapid reaction kinetics (Pabst et al., 2002). In summation, the biophysical findings implied that Complexins stabilize the tightly bound 'metastable state' of the SNARE complex in an immediate step likely preceding the actual fusion (reviewed by Marz and Hanson, 2002). Another important tool used in the study of Cplx/SNARE interactions is the single molecule FRET technique. Cplx/SNARE complex binding measured on lipid bilayers showed rapid binding kinetics of full-length Complexins to the SNARE complex (Bowen et al., 2005; Li et al., 2007). In PC12 cells, Complexins demonstrated a high affinity for binding to truncated SNARE complexes mimicking partially assembled intermediates, but Complexin affinity was directly proportional to the extent of SNARE complex assembly (Liu et al., 2006). Mere presence of the core SNARE components in the absence of Complexins aided vesicles to remain in a docked state, however Cplx1 binding to trans-SNARE complex lowered the fusion energy barrier, and with the concerted action of Ca^{2+} , the fusion kinetics was accelerated in a large population of vesicles (Yoon et al., 2008).

1.7.3. Complexin structure - function discrepancy

Complexins are proteins that have often been shown to cause diverse functional phenotypes. Their role in synaptic physiology is highly debated due to their paradoxical effects in different model systems.

1.7.3.1. Complexin as facilitators of synaptic release

In the past decade, successive studies established a significant role for Complexins in facilitating a late-step of neurotransmitter release. Neurons derived from mice carrying constitutive deletions of the major brain isoforms Cplx1 and Cplx2 (Cplx DKO) exhibited a dramatic reduction in synaptic parameters such as peak amplitude of Ca²⁺-evoked EPSCs, vesicular release probability and the apparent Ca²⁺-sensitivity of the synchronous component of EPSCs, quite contrary to littermate control neurons expressing either or both Cplx variants (Reim et al., 2001). Genetic over-expression of full-length Cplx1, Cplx3 and Cplx4 in the Cplx DKO mutant neurons caused a significant rescue of the EPSC amplitudes and release probability, implying a positive role for Complexins in facilitating exocytosis (Reim et al., 2005). However, the existence of Cplx3 at low levels in the brain raised questions on residual effects of Cplx3 in release. Individual deletion of Cplx3 caused no apparent variations in synaptic parameters compared to wild type, and so, a Complexin triple-knock-out (TKO) mouse with constitutive deletions of Cplx1, Cplx2 and Cplx3 was generated (Xue et al., 2008). The Cplx TKO mice exhibited a similar phenotype as observed in Cplx DKO mice including perinatal lethality, and severe deficits in synaptic transmission (Xue et al., 2008).

Although the synaptic deficits were attributed to the complete loss of Complexins, further structural modifications on the Complexin protein structure divulged interesting physiological phenotypes. Point mutations of the arginine (R48), lysine (K69) tyrosines (Y52 and Y70) residues on the central α -helix of Cplx1 were shown to disrupt SNARE complex binding and cause a dramatic reduction in the amplitudes of Ca²⁺-evoked EPSCs implying that SNARE binding of Cplx1 was essential for release (Fig.9.) (Xue et al., 2007; Maximov et al., 2009). Similarly, deletion of the Cplx1 N-terminus (1-15 a.a.) or point mutations of the amino acid residues 3 to 6 was also shown to impair the facilitatory function of Complexin-1 (Xue et al., 2009; Xue et al., 2010). Loss of the Cplx1 N-terminus impaired its ability to facilitate synaptic release, but deletion of the accessory α -helix (27-40 a.a.) reinstated the facilitatory function of the protein (Xue et al., 2007). A recent study has claimed that the inhibitory effect of the accessory α -helix is dependent on the presence of the negative charge of the helix, and that replacing these with positively

charged arginine residues increased the synaptic vesicle fusogenicity (Trimbuch et al., 2014). The C-terminus of Complexins is variable in terms of sequence identity and functionality, although mammalian Complexins have been shown to possess an amphipathic α -helix on the C-terminus (Seiler et al., 2009). The C-terminus of Cplx1 has been shown to stimulate liposome fusion *in-vitro* and its functionality was transferable to Cplx3 (Malsam et al., 2009). However, in cultured cortical neurons the C-terminus of Cplx1 was found to mediate vesicle priming and clamp spontaneous fusion of vesicles (Kaeser-woo et al., 2012). With respect to Cplx3 and Cplx4, the unique CAAX motifs on their C-termini allows for their farnesylation and targeting to membranes. However, the CAAX motif of only Cplx4 was found to be functionally relevant for Ca^{2+} -triggered release from hippocampal neurons (Reim et al., 2005).

1.7.3.2. Complexins as Fusion Clamps in various models

Albeit contradictory, some studies showed that Complexins might also have an inhibitory role in exocytosis. Over-expression of mammalian Cplx2 in adrenal chromaffin cells caused a significant reduction in the charge released during single vesicle fusion events indicating premature termination of release events (Archer et al., 2002). Later, new evidence surfaced in *in-vitro* functional reconstitution assays, and functional studies on *C. elegans*, *Drosophila* as well as in mice, supporting the claim that Complexins act as a 'fusion clamp' of exocytosis.

In-Vitro models

In cell fusion assays with HeLa cells expressing v- and t-SNAREs on their surface along with membrane anchored recombinant Cplx1-GPI, showed that Cplx1 inhibits fusion of the cells due to high local concentration; fusion robustly recovered upon PI-PLC based cleavage of the Cplx1-GPI anchor, and this effect was further enhanced in the presence of the calcium sensor protein - Synaptotagmin-1 (Syt-1), as well as free Ca^{2+} of 200 μM (Giraud et al., 2006). Research on liposome-fusion showed that Complexin-mediated 'hemifusion arrest' could be relieved by Ca^{2+} -Syt-1. Since SNARE-mediated aqueous content mixing is contributed by initial mixing of lipids on outer monolayer of lipids (hemifusion), and is then followed by mixing of the lipids on the inner leaflet (full fusion), the individual effects of Complexins and Synaptotagmin were studied in this process. *Drosophila* Complexin (dmCplx) and mammalian Cplx4 apparently inhibited inner leaflet mixing and caused a 46% reduction of total fusion, which could be restored only upon addition of the calcium binding C_2AB domain of Syt-1 along with 500 μM Ca^{2+} (Schaub et al., 2006). These findings *in-vitro* supported the notion that Complexins may curb release, and further studies examined the role of Complexin homologs in different species and in models of higher

physiological relevance.

Complexins in C. elegans

In *C. elegans*, Complexin homologs *cpx-1* and *cpx-2* were found to have distinctive roles in cholinergic release. The worm mutant ok1552 was generated by deletion of a 1.3 kb exon from *cpx-1*, and it displayed severe aldicarb-induced paralysis due to build-up of non-cleaved acetylcholine (Martin et al., 2011). Synaptic transmission was affected vividly in the ok1552 mutant, as the evoked transmitter release was reduced, coupled with a drastic increase in tonic release. Similarly, deletion or mutation of the SNARE binding region or the C-terminal domain on worm *cpx-1* caused a massive increase (>40%) in spontaneous release (Martin et al., 2011) and a selective reduction of stimulus evoked release by 94% (Hobson et al., 2011), implying an important function of *cpx-1* in synchronizing synaptic release and clamping spontaneous fusion. Although *cpx-1* was found to be highly important for mediating release in *C. elegans*, *cpx-2* had no obvious effects on synaptic transmission (Martin et al., 2011).

Drosophila Complexin

The *Drosophila* genome encodes for only one Complexin isoform. An intragenic 17-kb deletion of the Complexin coding sequence (*dmCplx^{SH1}* null mutant) resulted in an enormous surge in the frequency of miniature excitatory junction potentials at the NMJ, indicating that dmCplx ‘clamps fusion’ at the NMJ of *Drosophila* and its loss leads to increased spontaneous fusion of vesicles (Huntwork and Littleton, 2007). Although spontaneous fusion dramatically increased at the NMJ of the *cpx^{SH1}* mutants, their Ca²⁺-evoked amplitudes were significantly reduced, which was rescued by over-expressing mammalian Cplx1, Cplx2 and Cplx3 (Cho et al., 2010).

Structure-function analysis showed that the dmCplx could execute its fusion-clamp effect via SNARE binding and in the presence of its functional prenylation CAAX motif, as the spontaneous release rate was enhanced if the dmCplx SNARE-interacting domain (K75/Y76) and the prenylation domain (C155) were mutated (Cho et al., 2010). A number of splice variants were predicted from the *Drosophila Cpx* locus, each having a functional consequence on the fusion-clamp function. The mutant *dmCpx⁵⁷²* generated due to deletion in exon 6 of the dmCplx causing premature termination of the C-terminal amino acid sequence showed a marked deficit in clamping spontaneous release (Buhl et al., 2012). Likewise, *dmCpx¹²⁵⁷* generated by a non-sense mutation of the terminal amino acid ‘Q’ on the CAAX motif caused a severe deficit in motor coordination of the mutant flies at elevated temperatures, and this phenotype was also

corroborated by a pronounced inability to clamp spontaneous fusion (Iyer et al., 2013). These studies further emphasized a significant role for CAAX prenylation in mediating the fusion clamp effect of *Drosophila* Complexin.

Murine Complexins

Complexins in mice were found to facilitate synaptic release, based on constitutive in endogenous Complexin knockout models. However, the shRNA-mediated knockdown of Cplx1 and Cplx2, strongly inhibited the protein expression, increased the frequency of miniature excitatory postsynaptic currents and reduced AP-evoked release in cultured cortical neurons (Maximov et al., 2009). Expression of N- and C-terminal deletion mutants of Cplx1 in the Cplx knockdown caused a significant increase in frequency of mEPSCs alluding to requirement of the N- and C-terminal domains for clamping spontaneous release. Mutation of the SNARE binding domain on murine Complexins or prevention of Complexin/SNARE complex binding by substitutions on the Synaptobrevin-2 SNARE motif and subsequent lentiviral expression of the mutant genes in neurons caused a surge in spontaneous release indicating that Complexin-SNARE complex interaction was essential for the apparent 'clamping effect' of murine Complexins (Maximov et al., 2009; Kaeser-Woo et al., 2012). Although Cplx/SNARE complex binding is an integral part of the fusion apparatus (Pabst et al., 2002; Chen et al., 2002), the physiological effects of various Cplx homologs in different model systems have been conflicting.

1.7.4. Complexin-Synaptotagmin interactions

Synaptotagmin was first discovered as a synaptic vesicle protein that acts as a cooperative Ca^{2+} receptor for exocytosis in a phospholipid dependent manner (Brose et al., 1992). Synaptotagmin comprises a transmembrane region and two C2 domains, C2A and C2B, both of which have been shown to bind phospholipids in a Ca^{2+} -dependent manner (Zhang et al., 1998; Fernandez et al., 2001). A loss-of-function study on Synaptotagmin-1 revealed that Syt-1 deficiency selectively impairs Ca^{2+} -dependent synchronous transmitter release in neurons, but does not play a role in maintenance of the synaptic structure or postsynaptic density (Geppert et al., 1994). A single point mutation on the C₂A domain (R233Q) of Syt-1 close to the Ca^{2+} binding sites caused strong reduction in the overall Ca^{2+} -affinity, the EPSC amplitudes, the vesicular release probability as well as the Ca^{2+} -responsiveness of the synaptic vesicles (Fernandez-Chacon et al., 2001). These studies concluded that Synaptotagmin-1 is the primary calcium sensor protein mediating the Ca^{2+} -triggered synchronous fusion of vesicles.

Both Synaptotagmin and Complexins have been shown to individually affect the Ca^{2+} -dependent transmitter release process, and the nature of interaction between Complexins and Synaptotagmin-1 has been explored in a few studies. In-vitro experiments assessing the role of Complexins and Synaptotagmins in stimulating cell-cell fusion found that Complexin-GPI anchor mediated fusion block could be removed by PI-PLC cleavage, but full fusogenicity was accelerated upon addition of $200 \mu\text{M}$ Ca^{2+} and Syt-1 (Giraudo et al., 2006). Similar results were obtained in liposome fusion assays where inhibition of fusion by Complexins was alleviated upon addition of Syt-1 and Ca^{2+} (Schaub et al., 2006).

Some studies have shed light on Complexin and Synaptotagmin acting as competitors while some others have shown that Complexins and Synaptotagmin co-operatively function in vesicle release. In-vitro co-sedimentation assays showed that native Syt-1 bound SNARE complexes at physiological ionic strengths in a Ca^{2+} -dependent manner, and Syt-1 bound to SNARE complexes was quantitatively displaced by full length Complexin (Tang et al., 2006). These results suggested that Complexin and Syt-1 compete for SNARE binding. However, evoked EPSCs generated in Cplx DKO+Syt-1 KO autaptic neurons were dramatically reduced compared with EPSCs in Cplx DKO+Syt-1 WT neurons, implying that Cplxs and Syt-1 are required and cooperatively interact to mediate transmitter release (Xue et al., 2010). A more recent study corroborated this finding by employing size-exclusion chromatography and isothermal titration calorimetry to study Syt-1-Cplx1 interactions and found that the Syt-1 eC_2AB fragment and Cplx1 protein (full length or 26-83 fragment) simultaneously bound SNARE complexes but not each other (Xu et al., 2013).

1.8. SNARE disassembly and synaptic vesicle recycling

In order to maintain fast synaptic neurotransmission during sustained periods of activity, the intracellular machinery has evolved specialized apparatus to support SNARE disassembly and a fast recovery of synaptic vesicles for subsequent fusion. The disassembly of SNARE complex is essential so that the SNARE components can be reused in the subsequent vesicle fusion events. Disassembly of binary and ternary SNARE complexes is driven by concerted action of α -SNAP binding and the NSF ATPase activity (reviewed by Hanson et al., 1997). The tight coupling of synaptic vesicle exocytosis and endocytic membrane retrieval was first described in the frog motor nerve terminals. Stimulation of the frog sartorius muscle nerves at high-frequency caused transient depletion of synaptic vesicles, balanced by parasynaptic cisternal projections, which reappeared in a few minutes as new synaptic vesicles (Heuser and Reese, 1973). Recent studies have shown that different pathways of endocytosis may be adapted depending on the type of activity sustained at the synapse. Two fast pathways have been attributed to cause rapid vesicle

recycling for low frequency stimulations. One allows for vesicles to remain at the active zones for refilling while the other recycles locally - also known as 'kiss and run' (reviewed by Südhof, 2004). At high stimulation frequencies, a slow endosomal-recycling pathway is thought to be involved in vesicle endocytosis. In this scenario, vesicle endocytosis is predominantly mediated by clathrin and dynamin dependent pathways involving endocytic protein scaffolds (reviewed by Haucke et al., 2011).

1.9. Aim2: To study Complexin structural domains in transmitter release

The second objective of my work was to systematically ascertain the functional similarity/variability of the four mammalian Complexin paralogs in the physiological context, by introducing point mutations on the SNARE-binding domains and farnesylation domains of each of the proteins, and assessing their functional characteristics. For this purpose, I used the autaptic Cplx TKO neurons and genetically re-introduced the mutants alongside the wild type variants (via lentiviruses). I studied if the physiological functions of the SNARE binding domains and farnesylation domains are related. This aim was to provide a perspective on the phenotypic alterations contributed by the different Complexins towards neurotransmitter release at central synapses.

2. Materials and Methods

2.1. Materials

2.1.1. Buffers

Buffers	Constituents & Supplier	Final Concentration
10X TBE Diluted to 1X using ddH ₂ O	Tris (Sigma) Boric Acid (Merck) EDTA (Flyka Analytical)	89 mM 89 mM 2 mM
10X PBS Diluted to 1X using ddH ₂ O and pH adjusted to 7.4 with NaOH	NaCl (Merck) KCl (Merck) NaH ₂ PO ₄ ·2H ₂ O (Merck) KH ₂ PO ₄ (Merck)	1.37 M 26.8 mM 80.9 mM 17.6 mM
10X Running Buffer Diluted to 1X using ddH ₂ O	Tris Glycine (Sigma Aldrich) SDS	25 mM 190 mM 1%
10X TBS (Western Blot) Diluted to 1X using ddH ₂ O and pH adjusted to 7.6 with HCl	Tris NaCl	0.2 M 1.37 M
10X TBS (for Lentivirus) Diluted to 1X using ddH ₂ O, pH adjusted to 7.6 with HCl, and stored at 4°C.	Tris NaCl	20 mM 150 mM
Odyssey Blocking Buffer Freshly prepared.	TBS Milk Powder (Reformhaus) Goat Serum (Gibco)	1X 5% 5%
Odyssey Antibody Buffer Freshly prepared.	TBS Milk Powder Goat Serum (Gibco) Tween-20	1X 5% 5% 0.1%
Odyssey Wash Buffer Freshly prepared.	PBS Tween-20	1X 0.1%
Blocking Solution Freshly prepared.	PBS Goat Serum	1X 10%

Permeabilization solution (For ICC)	PBS Triton-X 100 (Roche Diagnostics) Goat Serum	1X 0.2% 10%
Freshly prepared.		
Laemmli Buffer	SDS Tris-HCl EDTA Sucrose (Merck) Bromophenol Blue (Pierce)	10% 0.5 0.1 M 30% 0.2%
1 part of 1.5 M DTT (Biomol) added to 9 parts of laemmli buffer, aliquot and stored at -20°C.		
Transfer Buffer	Trizma Glycine Methanol (Chemie Vertrieb Hannover) ddH ₂ O	25 mM 190 mM 20%
Freshly prepared and stored at 4°C.		
Wash Buffer 1	NaH ₂ PO ₄ (Sodium dihydrogen phosphate) NaCl Imidazole (AppliChem) Urea (Roth) ddH ₂ O	20 mM 500 mM 10 mM 8 M
Freshly prepared.		
Wash Buffer 2	NaH ₂ PO ₄ NaCl Imidazole Urea ddH ₂ O	20 mM 500 mM 20 mM 8 M
Freshly prepared.		
Elution Buffer	NaH ₂ PO ₄ NaCl Imidazole Urea ddH ₂ O	20 mM 500 mM 300 mM 8 M
Freshly prepared.		
ECL Blot Buffer A	TBS Milk Powder Goat Serum (Gibco) Tween-20	1X 5% 5% 0.1%
Freshly prepared.		
ECL Blot Buffer B	TBS Milk Powder Tween-20	1X 5% 0.1%
Freshly prepared.		

ECL Blot Buffer C Freshly prepared.	TBS Tween-20	1X 0.1%
ECL Blot Buffer D Freshly prepared.	TBS	1X
Aprotinin Stored at -20°C.	Aprotinin (Roth) ddH ₂ O	1 mg/ml
Leupeptin Stored at -20°C.	Leupeptin (Pepta Nova) ddH ₂ O	0.5 mg/ml
PMSF Stored at -20°C.	PMSF (Sigma) Isopropanol	17.4 mg/ml
Cell Lysis Buffer Freshly prepared and stored on ice.	PBS Aprotinin Leupeptin PMSF	1X 1:1000 1:1000 1:1000
Tissue Homogenizing Buffer Freshly prepared and stored on ice.	PBS Sucrose Aprotinin Leupeptin PMSF	1X 0.32 M 1:1000 1:1000 1:1000

2.1.2. Gel Solutions

Gels Constituents & Supplier Final Concentration

Agarose Gel	Agarose (AppliChem) TBE Gel Red (Biotium/VWR)	1% 1X 1:20,000
Solution boiled for 3 min, incubated at 50°C for 45 min, poured on to gel cassette, comb gently inserted and allowed to solidify for 45 min.		

Stored at 4°C.	ddH ₂ O	20%
Triton-X 100	Triton-X 100 ddH ₂ O	10%
Stored in the dark at 4°C.		
4% PFA	Paraformaldehyde (Serva) ddH ₂ O	4 gms 60 ml
Heat to 50°C stirring continuously, add few drops of 10 N NaOH to obtain clear solution. Cool down to 4°C and add 4 gms Sucrose. For 100 ml, add 7.74 ml of 1M Na ₂ HPO ₄ and 2.26 ml of 1M NaH ₂ PO ₄ , make up to 100 ml with ddH ₂ O. Aliquot and store at -20°C.		
Coating Solution (For petridishes) Freshly prepared.	PBS (Gibco) Poly-L-Lysine (Sigma Aldrich)	1X 1:12
Stamping Solution (for Astrocytes) Freshly prepared.	17 mM Acetic Acid (Merck) 1 mg/ml Collagen (BD Biosciences) 0.5 mg/ml Poly-D-Lysine (Sigma Aldrich)	3 parts 1 part 1 part
Ethanol Stored at RT.	Ethanol (Sigma Aldrich) ddH ₂ O	70% 30%
Bradford's Reagent Stored in the dark at 4°C.	Dye reagent (Bio-rad) ddH ₂ O	1 part 4 parts
BSA Freshly diluted from -20°C stock.	10 mg/ml BSA (New England Biolabs) ddH ₂ O	1 mg/ml

2.1.4. Cell Culture Media

Media	Constituents & Supplier	Final Concentration
Luria-Bertani Medium (pH 7.5) Autoclaved and stored at RT.	Bacto-Tryptone (Difco) Yeast Extract (Difco) NaCl (Merck) Bacto-Agar (BD) ddH ₂ O	1% 0.5% 1%
Complete Medium (HEK cell culture)	DMEM (Gibco) FBS (Gibco) Pen-Strep (Gibco) L-Glutamine (Gibco) NEAA (Gibco) Geneticin (Calbiochem)	1X 10% 1% 1% 1% 1%

Stored at 4°C.		
OptiMEM Medium (For Lentivirus) Stored at 4°C.	OptiMEM (Gibco) FBS (Gibco)	1X 10%
Changing Medium (For Lentivirus) Stored at 4°C.	DMEM (Gibco) FBS (Gibco) Pen-Strep (Gibco) Sodium Butyrate (Merck)	1X 2% 1% 2 mM
Freezing Medium (For HEK Cells) Stored at 4°C.	Complete Medium DMSO (Sigma)	90% 10%
FBS Medium (For Astrocytes) Stored at 37°C.	DMEM FBS GlutaMax (Gibco) MITO (BD)	1X 10% 1% 0.1%
NBA Medium (For neurons) Stored at 4°C.	NBA Medium (Gibco) B-27 (Gibco) GlutaMax Pen-Strep (Gibco)	1X 2% 1% 0.2%

2.1.5. Reagents for Electrophysiology

Reagents	Constituents & Supplier	Final Concentration
10X ATP/GTP Energy Stock (pH 7.5, 370 mOsm/L) Stored at -20°C.	ATP-Mg Salt (Sigma Aldrich) GTP-Na salt (Sigma Aldrich) MgCl ₂ .6H ₂ O Creatine phosphate – Na ₂ (Sigma) Creatine phosphokinase	40 mM 3 mM 6 mM 150 mM 50 U/ml
CaCl ₂ (For intracellular Soln.) Stored at -20°C.	1M CaCl ₂ (Merck) ddH ₂ O	100 mM
EGTA-AM Stored at -20°C.	EGTA-AM (Calbiochem) DMSO	7.5 mM
Sucrose	Sucrose (Sigma) 1X Base +	1 M

Stored at -20°C, diluted to 0.5 M in 1X Base+ for experimental use.		
Tetrodotoxin	Tetrodotoxin (Tocris) ddH ₂ O	3 mM
Stored at -20°C, diluted to 300 nM in 1X Base+ for experimental use.		
1X Base + (pH 7.4, 310-320 mOsm/L) (External Solution)	KCl NaCl HEPES D-Glucose (Sigma) CaCl ₂ MgCl ₂ ddH ₂ O	2.4 mM 140 mM 10 mM 10 mM 4 mM 4 mM
Freshly prepared.		
Intracellular Solution (pH 7.4, 320 mOsm/L)	KCl HEPES K-EGTA 10X ATP/GTP energy stock	136 mM 17.8 mM 0.1 mM 1X
Stored at -20°C.		

2.1.6. Antibiotics, Media Supplements and Solutions

<u>Supplements</u>	<u>Constituents & Supplier</u>	<u>Final Concentration</u>
Ampicillin (1000X) (Amp) Stored at -20°C.	Ampicillin (Sigma) ddH ₂ O	50 mg/ml
Kanamycin (400X) (Kan) Stored at -20°C.	Kanamycin (Sigma) ddH ₂ O	10 mg/ml
Geneticin Stored at -20°C.	Geneticin (Calbiochem) PBS	50 mg/ml 1X
MITO Stored at -20°C.	DMEM + GlutaMax (Gibco) MITO serum extender (BD)	1X 1%
Pen-Strep (100X) Stored at -20°C.	Pen-Strep (Gibco)	0.2%
Trypsin-EDTA (1X) Stored at -20°C.	Trypsin-EDTA (Gibco)	0.05%
HBSS Stored at 4°C.	HBSS w/o Ca and Mg (Gibco)	1X

Papain Solution	DMEM CaCl ₂ (Merck) EDTA (Flyka Analytical) L-cysteine (Sigma)	1X 1 mM 0.5 mM 1.65 mM
<p>Papain solution was filter sterilized through a 0.22 µm filter and stored at -20°C. To 1 ml of thawed papain solution, 25 units of Papain enzyme (Worthington Biochem. Corp.) was added and bubbled with Carbogen for 20 min, to obtain a clear solution. The solution was filter sterilized and incubated at 37°C until further use in cell culture.</p>		
STOP Solution	DMEM FBS (PAA) Albumin (Sigma) Trypsin Inhibitor (Sigma Aldrich)	1X 10% (v/v) 2.5 mg/ml 2.5 mg/ml
Filter sterilized through a 0.22 µm filter and stored at -20°C.		

2.1.7. Antibodies for Western Blotting and Immunocytochemistry

Table 1 Primary Antibodies

Antibody name	Antibody working concentration
mCPX I/II 94.2 (SySy) Rabbit Polyclonal C-terminus	1:1000
mCPX III SA1896 (SySy) Rabbit Polyclonal	1:500
mCPX IV SA1897 (SySy) Rabbit Polyclonal	1:500
SNAP25 71.1 (SySy) Mouse Monoclonal	1:1,000,000
SNAP23 (SySy) Rabbit Polyclonal	1:1000
SNAP47 (SySy) Purified Rabbit Polyclonal	1:1000
SNAP29 (SySy) Affinity-Purified Rabbit Polyclonal	1:1000 (for WB)/1:500 (for ICC)
Synaptobrevin-2 69.1 (SySy) Mouse Monoclonal	1:7500
Syntaxin-1AB 78.2 (SySy) Mouse Monoclonal	1:10,000
VGLUT-1 (SySy) Guinea Pig	1:1000
β-Tubulin (SySy) Rabbit Polyclonal	1:20,000

Table 2 Secondary Antibodies

Antibody name	Antibody working concentration
GαR (Invitrogen) HRP-Coupled	1:5000
GαM (Invitrogen) HRP-Coupled	1:5000
IRD800αR (Rockland-Biomol)	1:5000
Alexa-488 (SySy) (GαR - GFP channel)	1:1000
Alexa-555 (SySy) (GαGP - Cy5 channel)	1:1000

2.1.8. Primer sequences, PCR reaction mix and programs**Cplx1 Genotyping PCR****Table 3 Primer Sequences for Cplx1**

Primer no.	Gene of interest	Sequence
1118	Cplx1 WT	5'-AGTACTTTTGAATCCCCTGGTGA -3'
1119	Cplx1 WT	5'-TAGCTATCCCTTCTTGTCCCTTGTG -3'
1111	Cplx1 KO	5'-CGCGGCGGAGTTGTTGACCTCG -3'
1112	Cplx1 KO	5'-CTGGCTTGTCCCTGAATCCTGTCC -3'

Table 4 PCR reaction mix for Cplx1 WT

Constituents	Reaction vol. (in µl)
10X RedTaq Buffer	2
2.5 mM dNTPs	1
10 pM/µl Primer 1118	1
10 pM/µl Primer 1119	1
1 u/µl RedTaq Enzyme	1
ddH ₂ O	13
DNA	1

Table 5 PCR reaction mix for Cplx1 KO

Constituents	Reaction vol. (in µl)
10X RedTaq Buffer	2
2.5 mM dNTPs	1
10 pM/µl Primer 1111	1
10 pM/µl Primer 1112	1
1 u/µl RedTaq Enzyme	1
ddH ₂ O	13
DNA	1

Table 6 PCR program for Cplx1

Steps	Temp (°C)	Time (min:sec)
1	94	03:00
2	94	00:30
3	60	00:30
4	72	01:00
5	Go to Step 2, Repeat steps 2-3-4 30 times	
6	72	07:00
7	10	Forever

Nex-Cre SNAP29 KO Genotyping PCR**Table 7 Primer sequences for Nex-Cre SNAP29**

Primer no.	Gene of interest	Sequence
20172	SNAP-29 (WT/floxed)	5'-CCACATGTAACCACCAGCCCTC -3'
20173	SNAP-29 (WT)	5'-GTTCTAGGACTCCTCGCTGCCG -3'
20176	SNAP-29 (floxed)	5'-CTTGCTATCCACCTGCCTTAG -3'

Table 8 PCR reaction mix for Nex-Cre SNAP29 KO

Constituents	Reaction vol. (in µl)
10X RedTaq Buffer	2
2.5 mM dNTPs	2
10 pM/µl Primer 20172	0.5
10 pM/µl Primer 20173	0.5
1 u/µl RedTaq Enzyme	1
ddH ₂ O	13
DNA	1

Table 8.1 PCR program for Nex-Cre SNAP29 KO ()

Steps	Temp (°C)	Time (min:sec)
1	95	03:00
2	55	00:45
3	72	01:00
4	95	00:30
5	Go to Step 2, Repeat steps 2,3,4 35 times	
6	55	01:00
7	72	10:00
8	10	Forever

Table 9 PCR reaction for Nex-Cre SNAP29 KO

Constituents	Reaction vol. (in μ l)
10X RedTaq Buffer	2
2.5 mM dNTPs	2
10 pM/ μ l Primer 20172	0.5
10 pM/ μ l Primer 20176	0.5
1 u/ μ l RedTaq Enzyme	1
ddH ₂ O	13
DNA	1

Table 9.1 PCR program for Nex-Cre SNAP29 KO

Steps	Temp ($^{\circ}$ C)	Time (min:sec)
1	95	03:00
2	49	00:30
3	72	01:00
4	95	00:30
5	Go to Step 2, Repeat steps 2,3,4 39 times	
6	55	01:00
7	72	10:00
8	10	Forever

Constitutive SNAP29 KO Genotyping PCR**Table 10 Primer sequences for Constitutive SNAP29 KO**

Primer no.	Gene of interest	Sequence
20174	SNAP-29 (WT/floxed)	5'-CACACCTCCCCCTGAACCTGAAAC -3'
20175	SNAP-29 (WT)	5'-GCAGCGTCTGCATTGGATAC -3'
20176	SNAP-29 (floxed)	5'-CTTGCTATCCACCTGCCTTAG -3'

Table 11 PCR reaction mix for SNAP29 KO

Constituents	Reaction vol. (in μ l)
10X RedTaq Buffer	2
2.5 mM dNTPs	2
10 pM/ μ l Primer 20174	0.5
10 pM/ μ l Primer 20175	0.5
10 pM/ μ l Primer 20176	0.5
1 u/ μ l RedTaq Enzyme	1
ddH ₂ O	12.5
DNA	1

Table 11.1 PCR program for SNAP29 KO

Steps	Temp (°C)	Time (min:sec)
1	95	03:00
2	49	00:30
3	72	01:00
4	95	00:30
5	Go to Step 2, Repeat steps 2,3,4 39 times	
6	55	01:00
7	72	10:00
8	10	Forever

2.2. Methods

2.2.1. Transformation of plasmid DNA into competent bacteria

The plasmid DNA transformation was performed according to the protocol detailed in Endofree Plasmid Maxi Kit from Qiagen. The plasmid DNA was diluted to a concentration of 100 ng/ μ l in order to transform into a selective strain of bacteria E.coli. For transformations, one aliquot containing 50 μ l of competent bacteria was thawed on ice, and 1 μ l of diluted DNA was added. The content was transferred to the Gene Pulser[®] cuvette and electroporated at 1.8 mV. The electroporated bacteria were collected in 1 ml plain LB medium and allowed a recovery time of 1 hr at 37°C in a shaker. After recovery, 100 μ l of transformed bacteria was plated on to an LB plate containing selective antibiotic and incubated at 37°C for up to 12 hours to obtain confluent bacterial growth on the plate.

2.2.2. Plasmid DNA “Maxi” purification

Plasmid DNA purification was performed according to the protocol detailed in Endofree Plasmid Maxi Kit from Qiagen. The Endofree procedure prevents co-purification of endotoxins, which strongly decrease transfection efficiency of DNA in primary cells. In order to purify the plasmid DNA, a single colony of transformed bacteria was picked inoculated in 2 ml of Luria Bertani (LB) medium containing selective antibiotic. The starter culture was incubated for 8 hrs at 37°C with vigorous shaking and then diluted 1/1000 in selective LB medium for 12-16 hrs at 37°C with vigorous shaking (300 rpm). Thereafter, the bacterial cells were harvested by centrifugation at 3500 rpm for 15 min at 4°C. The bacterial cell pellet was resuspended in 10 ml of cold Buffer P1 containing RNase A. To the suspension, 10 ml of buffer P2 was added and mixed thoroughly by inverting the tube 4-6 times. The mixture was incubated at RT for 5 min. In the meantime, QIAfilter cartridge was placed in a 50 ml falcon. Next, 10 ml of Buffer P3 was added to the lysate and mixed thoroughly. The lysate was poured on to the QIAfilter cartridge and incubated at RT for 10 min. The plunger was then gently inserted into the cartridge to filter the lysate in the falcon tube. To the filtered lysate, 2.5 ml of Buffer ER was added and mixed well. The mixture was incubated on ice for 30 min. The OIAGEN-tip 500 column was equilibrated by applying 10 ml of Buffer QBT and emptied by gravity flow. The filtered lysate was applied to the column and allowed to pass through the resin through gravity flow. The column was washed twice with 30 ml of Buffer QC. The DNA was eluted from the resin into a 50 ml falcon using 15 ml of Buffer QN. The DNA was precipitated by adding 10.5 ml of Isopropanol and mixed well. The solution containing the

DNA was centrifuged at 3500 rpm for 45 min at 4°C. Thereafter, the supernatant was carefully removed and the DNA pellet was washed with 1 ml of 70% Ethanol. The mix was centrifuged at 15000 rpm for 10 min and the supernatant was discarded. The DNA pellet was air dried for 10 min, re-dissolved in 100 µl of endotoxin free Buffer TE and stored at -20°C.

2.2.2.1. Determination of yield of purified DNA

To determine the yield, the DNA concentration was measured using the UV spectrophotometer. The DNA can be quantified at wavelength 260 nm and 280 nm because a solution of DNA with an optical density of 1.0 will have a concentration of 50 µg/ml (using a 10 mm pathlength cell). The A260/A280 absorbance ratio for a pure DNA solution will be 1.8, enabling an assessment of the purity and quality of the preparation. The purified DNA samples were diluted 1:100 in ddH₂O. For reference, a blank solution containing pure ddH₂O was used. The A260/A280 absorbance ratio and concentration of each of the sample was thereafter recorded.

2.2.3. Recombinant protein purification

2.2.3.1. Equilibration of beads

First, 2x6 ml of 50% Ni-NTA agarose solution (Qiagen) was transferred into a 50 ml falcon tube. The solution was centrifuged at 1000xg for 1 min. The beads were washed with 40 ml of the wash buffers 1 and 2 as well as the elution buffer for 5 min each, using a rotating wheel at RT. The beads were transferred in a final volume of 10 ml into small falcon tubes and washed once again. Both the aliquots were combined, the beads were finally re-suspended in a volume of 6 ml of wash buffer 1 and stored at 4°C.

2.2.3.2. IPTG Induction

A single colony of bacteria transformed with pET-28a plasmid containing the gene of interest was inoculated in 100 ml of LB-KAN medium and incubated overnight at 37°C in a shaker. The following day, 50 ml of the overnight culture was inoculated in 1 l of LB-KAN medium incubated for 1 hr at 37°C and subsequently for 30 min at RT, in a shaker. IPTG was added to a final concentration of 1 mM to the bacterial culture to induce protein production. The culture was further incubated at RT for 4 to 6 hrs in a shaker. The bacterial cells were collected by centrifugation at 4000 rpm for 20 min at 4°C. The pellet was washed once with

30 ml of 1X PBS and the cell suspension was collected in a 50 ml falcon tube, centrifuged at 3500 rpm for 20 min at 4°C. The supernatant was discarded and the pellet was stored at -80°C.

2.2.3.3. Preparation of protein extract and binding of protein to beads

The pellet was thawed and re-suspended in 10 ml of wash buffer 1 (without urea; containing protease inhibitors) on ice. The suspension was sonicated three times for 20 sec each and centrifuged at 15000 rpm for 30 min at 4°C. The supernatant was transferred into a fresh 50 ml falcon tube to which urea was added at a final concentration of 8 M and the volume was made up to 50 ml using wash buffer 1. Then, 2 ml of the equilibrated beads was added and the solution was incubated overnight at RT on a rotating wheel.

2.2.3.4. Wash and protein elution

The solution was centrifuged at 1000 rpm for 5 min at RT. The beads were washed three times with 40 ml of wash buffer 1 and wash buffer 2 for 5 min each respectively. The protein was finally eluted three times using 1 ml of elution buffer for 10 min each respectively. The supernatant containing the protein was flash frozen in liquid Nitrogen and stored at -80°C.

2.2.3.5. Protein precipitation

One volume of 20% precooled TCA was added to one volume of eluted protein solution and the mix was incubated at -80°C for 30 min. The solution was then transferred into a polycarbonate tube and ultra-centrifuged at 80000 rpm for 25 min. The supernatant was removed and the pellet was washed with 80% precooled Acetone and transferred into an eppendorf tube. The sample was subjected to centrifugation at 15000 rpm for 30 min. The supernatant was discarded while the pellet was dried and re-suspended in 1X PBS containing Triton X-100 at a concentration of 0.1%. The precipitated protein was stored at -80°C.

2.2.4. Genotyping of DNA samples from tissues

2.2.4.1. Equilibration of nexttec™ cleanplate96

350 µl of Prep Buffer was added on to each well of nexttec™ cleanplate96, incubated at RT for 5 min and centrifuged at 350x g for 1 min.

2.2.4.2. Lysis

To each sample of tissue, 265 µl Buffer G1, 10 µl Buffer G2 and 25 µl Buffer G3 was added and incubated at 61°C, 1100 rpm for 1 hr.

2.2.4.3. Purification of genomic DNA

Upon lysis, 120 µl of each of the lysates was transferred to the equilibrated nexttec™ cleanplate96 and incubated for 3 min at RT. The plate was centrifuged at 700x g for 1 min and the eluate contained the purified DNA.

2.2.5. Polymerase Chain Reaction

The purified DNA was incorporated into the reaction mix for PCR amplification and the PCR reaction was carried out in a PTC-225 Peltier Thermal Cycler (Tables 4, 5, and 6 for Cplx1, tables 8, 8.1, 9, and 9.1 for Nex-Cre SNAP-29 and tables 11, 11.1 for constitutive SNAP-29 KO).

2.2.6. Agarose Gel Electrophoresis

In order to analyze DNA samples and determine the genotype of the animals, the DNA samples obtained after PCR amplification were subjected to electrophoresis on a 1% Agarose gel. First, the PCR DNA samples were diluted in gel loading buffer. The gel was prepared by adding 1 g Agarose to 100 ml of 1X TBE Buffer, and the solution was microwaved at 900W for 3 min. The gel solution was incubated in a water bath at 50°C for 45 min and then poured on to the holding cassette after addition of GelRed in a final concentration of 1:20,000. The samples were then loaded on the solidified agarose gel along with the 100 bp ladder. The gel was run for 45 min at 115 V and visualized under UV illumination and the band sizes were documented. Depending on the size and presence or absence of the bands, the DNA sample was verified as knockout, heterozygous or homozygous control (Fig.10. Cplx1 PCR products, and Fig.11. SNAP29 PCR products).

2.2.6.1. Genotyping results from PCR and agarose gel electrophoresis

I performed PCR amplification of the genomic DNA isolated from tail biopsies of mice, to identify the KO and littermate heterozygote/wild type animals. PCR amplification was performed using respective primers as detailed in materials 2.1.8.

Cplx1 Genotyping

Parent mice used for breedings were Cplx1 (+/-) and Cplx2 (-/-) and Cplx3 (-/-). The tail DNA samples were subjected to electrophoresis, and genotyping results yielded a Cplx1 WT band at 333 bp, and Cplx1 KO band at 425 bp.

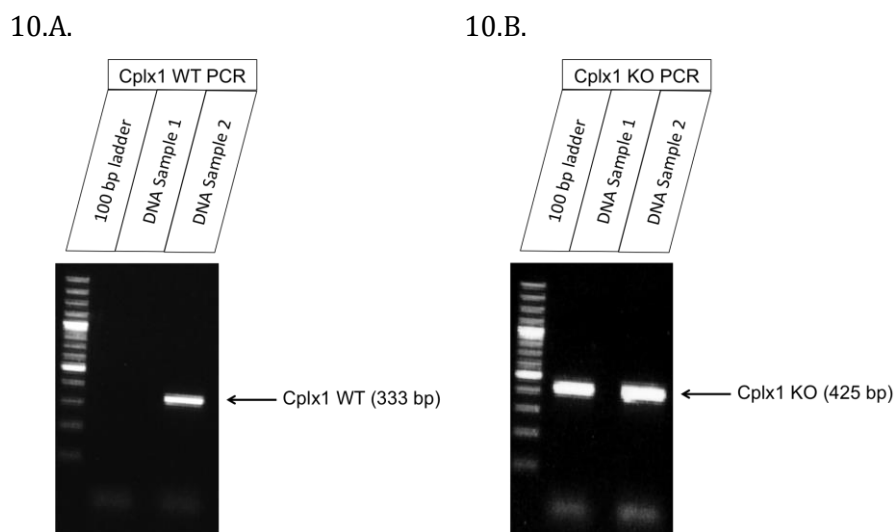


Figure 10 Genotyping results for Cplx1 PCR. (A) and (B) Cplx1 WT and Cplx1 KO PCRs respectively (Tables 4, 5 and 6) for DNA samples from P0 or E18 animals. DNA sample 1 lacks WT fragment of 333 bp, but contains Cplx1 KO fragment at 425 bp. Hence, DNA sample 1 is a Cplx1 knockout (-/-). DNA sample 2 contains a WT fragment of 333 bp and a KO fragment of 425 bp implying that it is Cplx1 Heterozygous (+/-)

SNAP-29 Genotyping

SNAP-29 conditional and constitutive KO mice were generated by Nex-Cre and EIIa-Cre mediated deletion of exon-2 on the SNAP-29 gene, respectively (Appendix 6.1.). In case of the Nex-Cre SNAP-29 KO, the exon-2 of SNAP-29 was flanked by two LoxP cassettes to obtain a floxed target allele. Nex-Cre mediated recombination of the target allele resulted in deletion of exon-2, loss of SNAP-29 protein expression. Cross-breeding mice carrying a floxed target allele and mice expressing cre-recombinase under the Nex promoter resulted in litters of animals that were wild type (620 bp), or floxed/wild-type heterozygotes (765 bp/620 bp), or

floxed/floxed KO (765 bp). Cre-recombination could be confirmed by the presence of a 450 bp fragment. Similarly, crossing mice carrying the targeted KO allele with mice expressing Cre-recombinase under the EIIa promoter, resulted in litters of animals that were homozygous SNAP-29 KO (-/-) (430 bp), or wild type (+/+) (343 bp), or heterozygous for SNAP-29 (+/-) (343 bp /430 bp).

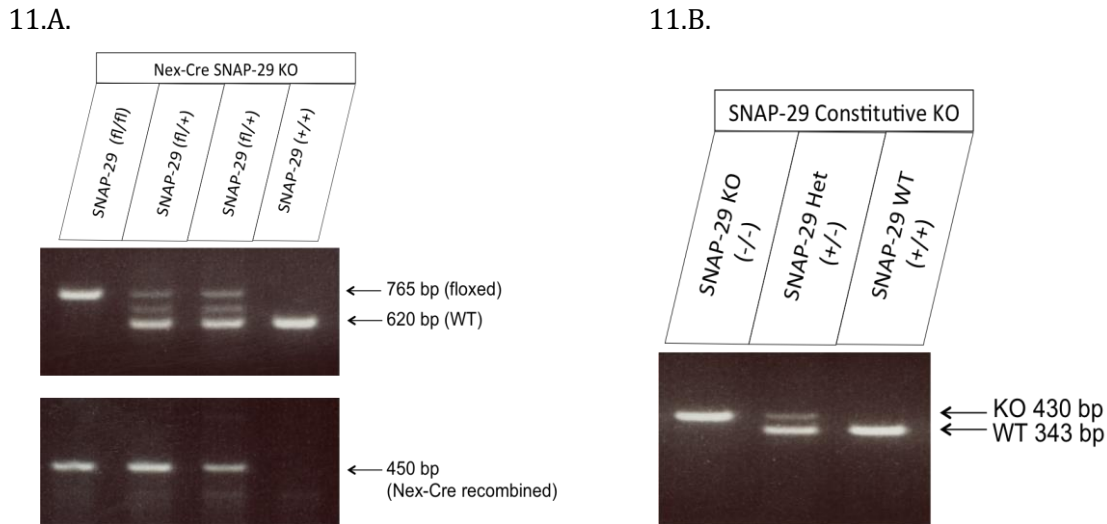


Figure 11 Genotyping results for SNAP-29 conditional and constitutive deletion. **(A)** Floxed SNAP-29 gene is 765 bp in size, while SNAP-29 wild type is 620 bp in size. Nex-Cre mediated recombination results in loss of SNAP-29 exon-2 yielding a 450 bp fragment. Since Cre-recombinase targets the gene in the presence of LoxP sites, no recombination is observed in case of SNAP-29 wild type (+/+). **(B)** EIIa-Cre mediated recombination results in the constitutive loss of SNAP-29 exon-2. SNAP-29 homozygous knockouts (-/-) are 430 bp in size, while the wild type is 343 bp in size.

2.2.7. SDS - Polyacrylamide Gel Electrophoresis

SDS-Polyacrylamide Gel Electrophoresis is a technique used to separate a complex mixture of proteins, and to verify the homogeneity of samples. In order to ensure dissociation of proteins into their individual polypeptide subunits and to minimize aggregation, a strongly reducing agent such as SDS is added to aid the migration of the SDS-polypeptide complexes according to the size of the polypeptide through the pores formed via cross-linking of the polymerized bisacrylamide (Laemmli, UK, 1972).

2.2.7.1. Preparation of SDS-Polyacrylamide Gels

The glass plates were first assembled according to manufacturer's instructions. The appropriate volume of resolving gel was prepared and poured in between the plates, leaving sufficient space for the stacking gel and space for the comb. The gel solution was overlaid with water-saturated Butanol. After 30 min, the Butanol was poured off and the solidified gel surface was washed with water. Next, the appropriate volume of stacking gel was prepared and poured over the polymerized resolving gel. A Teflon comb was immediately inserted into the stacking gel solution to create wells for loading samples.

2.2.7.2. Preparation of samples

All samples were heated at 100°C for 5 min in laemmli buffer prior to loading on SDS-gels in order to denature the proteins and ensure optimal band resolution.

2.2.7.3. Electrophoresis of gels

After the polymerization of the stacking gel, the comb was removed and the wells were washed with water. The gel was mounted on the electrophoresis apparatus and the running buffer was added to the top and bottom reservoirs. The samples were loaded on to the wells using a Hamilton microlitre syringe. The electrophoresis apparatus was attached to a power supply and a current of 25 mA was applied to one gel until the samples reached the bottom of the resolving gel. Thereafter, the power supply was turned off, and the gel plates were disassembled to obtain the electrophoresed gel for staining or blotting purposes.

2.2.8. Coomassie Staining of proteins in SDS-PAGE gels

The Coomassie Brilliant Blue staining procedure helps in easy and rapid detection of proteins on the gel. For staining, the gel was placed in a plastic container, covered with 5 volumes of Coomassie staining solution and agitated on an orbital shaker for 20 min. Thereafter, the solution was discarded and the gel was covered with destaining solution for 2 hrs. The destaining solution was changed several times to obtain a clear background against the protein bands.

2.2.9. Western Blotting

2.2.9.1. Protein transfer from gel to nitrocellulose membrane

After completion of electrophoresis, the gel sandwich was disassembled and the stacking gel was discarded. The transfer sandwich comprised of nitrocellulose membrane of pre-cut size in contact with the resolving gel, both surrounded by Whatmann papers of pre-cut size, porous pads and plastic supports. The transfer was performed with the gel towards the cathode in a tank containing two electrode panels. The transfer of proteins from gel to the nitrocellulose membrane was achieved by applying a current of 250 mA for 2 hrs or 40 mA overnight at 4°C (Towbin et al., 1979).

2.2.9.2. Ponceau S staining of proteins

Upon completion of protein transfer, the nitrocellulose membrane was carefully removed from the transfer sandwich. It was stained with Ponceau S for a few minutes at RT. Thereafter the membrane was washed with water to destain Ponceau S and air-dried at RT.

2.2.9.3. Immunoblotting for ECL analysis

The Enhanced Chemiluminescence (ECL) Western Blotting analysis system is a non-radioactive method used for detection of antigen epitopes on the immobilized target protein, conjugated directly or indirectly with horseradish peroxidase (HRP)-labelled antibodies. In this procedure, the non-specific binding sites on the nitrocellulose membrane anchoring the proteins were blocked by immersing the membrane in 10 ml of blocking buffer (buffer A) for 30 min on an orbital shaker. The primary antibody was diluted in fresh buffer A at the appropriate concentration, after which it was added on to the membrane and incubated for 1 hr at RT. Next, the membrane was washed 5 times for 5 min each with buffer B at RT. The HRP-labelled secondary antibody was diluted in buffer B and incubated on the membrane for 1 hr at RT. The membrane was washed 4 times for 5 min each with buffer B at RT. Then the membrane was washed with buffer C and buffer D once each for 5 min at RT. The membrane was placed on a glass plate with the protein side upwards and the excess buffer was drained off. The detection reagents were mixed in a 1:1 proportion and added to the surface of the membrane. The reagent mixture was incubated for 1 min at RT without any agitation, and then drained off. The membrane was covered with a transparency and air bubbles were smoothed out. The membrane was exposed to sheets of Hyperfilm ECL for different time periods ranging from 5 sec to 5 min in the dark room. The films were removed and developed in the developer.

2.2.9.4. Immunoblotting for Odyssey® analysis

The Infrared Imaging system Odyssey® developed by LI-COR Biosciences is a widely used protein detection system, which employs Infrared fluorescence dyes IRDye® coupled secondary antibodies to label proteins. The system uses the digital software Image Studio™ Lite, for quantitative analysis of Western Blots thereby eliminating the need for films, dark rooms and associated costs yet providing a sensitive and accurate method for detecting strong as well as weak protein bands. This procedure involved the following steps.

The non-specific sites on the nitrocellulose membrane were blocked using the blocking buffer for 1 hr at RT. The primary antibody was diluted in the required concentration in the antibody buffer and added to the membrane after removal of blocking buffer. The membrane was slowly agitated on an orbital shaker for 1 hr at RT. Then, the membrane was washed 5 times for 5 min each with the wash buffer. The IRDye® coupled secondary antibody was diluted in fresh antibody buffer at required concentration and incubated on the membrane for 1 hr at RT in the dark in order to prevent photobleaching of the fluorescent IRDye®. The membrane was then washed 3 times for 5 min each with the wash buffer in the dark and subsequently washed 2 times for 5 min each with 1X PBS. The membrane was then analyzed with Odyssey®.

2.2.10. Growth and maintenance of HEK293FT cell line

The growth and maintenance of the HEK293FT cell line was done in accordance with the protocol from Invitrogen.

2.2.10.1. Thawing cells

One vial of HEK293FT cells was thawed in a 37°C water bath. The vial was decontaminated on the outside with 70% Ethanol and the cells were transferred to a 15 ml sterile tube containing 1X PBS. The cells were briefly centrifuged at 150-200 xg and resuspended in 2 ml of complete medium lacking Geneticin®. The cells were transferred into a T-75 cm² flask containing 10 ml of complete medium lacking Geneticin®. The flask was incubated overnight at 37°C to allow the cells to attach to the base of the flask. The medium was aspirated the following day and replaced with fresh complete medium containing Geneticin®. The flask was incubated at 37°C until the cells were 80-90% confluent.

2.2.10.2. Subculturing cells

The cells were passaged when they were at least 80% confluent. The medium from the flask was aspirated and the cells were washed once with 10 ml of 1X PBS to remove any excess medium. Then 2 ml of Trypsin-EDTA was added to the monolayer of cells and incubated for 1 min at 37°C for the cells to detach from the base of the flask. About 8 ml of complete medium containing Geneticin® was added and the cell suspension was transferred to a 15 ml sterile conical tube. The total cell count was determined using a hemocytometer. The cells were seeded at recommended densities after diluting in pre-warmed medium. The cells were maintained in adherent monolayer cultures over a few passages before transfections.

2.2.10.3. Freezing cells

The HEK293FT cells were grown to 90% confluency after which the medium was aspirated and the cells were washed once with 10 ml of 1X PBS to remove any excess medium. Then 2 ml of Trypsin-EDTA was added to the monolayer of cells and incubated for 1 min at 37°C for the cells to detach. About 8 ml of complete medium containing Geneticin® was added and the cell suspension was transferred to a 15 ml sterile conical tube. The total cell count was determined using a hemocytometer. The cell suspension was centrifuged at 250 xg for 5 min at RT. The medium was carefully aspirated and the cell pellet was re-suspended in a pre-determined volume of chilled freezing medium comprising of 90% complete medium and 10% DMSO. The suspension was dispensed as aliquots in cryovials and the cells were frozen at a density of 3×10^6 viable cells per ml in a controlled-rate freezing apparatus where the freezing rate was decreased at 1°C per minute. The vials were transferred into liquid nitrogen for long-term storage.

2.2.11. Lentivirus Production

The protocol for lentivirus production was optimized from the standard protocol offered by Invitrogen.

2.2.11.1. Coating dishes

For coating 15 cm dishes, a mixture of Poly-L-Lysine and PBS was used in a ratio of 1:11 respectively. The mixture was mixed well and added to 15 cm dishes to cover the surface. The plates were incubated at 37°C for at least 1 day for the PLL to layer coat the plate entirely.

2.2.11.2. Transfection into HEK293FT cells

About 1.6×10^7 cells were seeded on day 1 on a PLL-coated 15 cm dish containing OptiMEM medium with 10% FBS. After 24 hours on day 2, the cells were 90% confluent and were used for transfections with the plasmid DNA of interest. First, a mixture of 60 μ l Lipofectamine[®] 2000 and 6 ml plain OptiMEM medium was prepared. Simultaneously, 25 μ g the DNA of interest was added to 6 ml of plain OptiMEM medium along with 6 μ g of the enveloping DNA and 6 μ g of packaging DNA and incubated at RT for 5 min. The Lipofectamine[®] 2000 and DNA mixtures were combined and incubated at RT for 1 hr. The mixture was then added to the dish containing the HEK293FT cells and 10 mM of Sodium Butyrate was added to inhibit further cell proliferation and induce expression of the DNA of interest. The cells were incubated at 37°C for 7 hours, after which the medium was replaced with fresh DMEM medium containing FCS, Pencillin-Streptomycin, and Sodium Butyrate.

2.2.11.3. Harvesting Lentivirus

Lentiviruses were produced according to S2 level biosafety regulations from HEK293FT cells. After 48 hours of transfection, the cells were found to detach from the plate surface implicating virus production and consequent cell death. The virus containing medium from the dish was transferred into a 50 ml falcon tube and centrifuged at 2000 rpm for 5 min at 4°C. The supernatant was filtered through a Luer-Lock syringe system and a 0.45 μ m filter into a fresh 50 ml falcon tube and the cell pellet was discarded. 10 ml of the filtered supernatant solution was transferred into an AMICON filter system tube. The solution was centrifuged at 4300 rpm for 10 min at 4°C and the flow-through was discarded. The procedure was repeated for the remaining supernatant solution and the virus was washed twice with 10 ml of plain Neurobasal medium. Subsequently, the virus was washed twice with 5 ml of 1X TBS and the virus was concentrated to 500 μ l in the filter. The lentivirus was dispensed as aliquots in cryovials, flash-frozen in Liquid Nitrogen and stored at -80°C for long-term use.

2.2.11.4. Lentiviral Infections in neurons

The lentivirus prepared was thawed to RT and added to neurons at DIV 2 for the optimal infection and protein expression.

2.2.12. Mouse Strains

The respective mutant and control mice for individual neuron culture experiments were obtained from one litter. Cplx TKO mice (Xue et al., 2008) were generated by interbreeding Cplx I^{+/-} Cplx II^{-/-} Cplx III^{-/-} parent mice. Littermates Cplx I^{+/-} Cplx II^{-/-} Cplx III^{-/-} served as controls for some experiments. Nex-Cre SNAP29 KO mice (Goebbels et al., 2006) and constitutive SNAP-29 KO mice were generated by Dr Sandra Goebbels and Georg Wieser (MPI Experimental Medicine, Göttingen, Germany).

2.2.13. Autaptic Neuron Culture

The autaptic neuron culture was prepared according to standard published protocol (Burgalossi et al., 2012).

2.2.13.1. Preparation of glass coverslips

The glass coverslips were immersed in a glass beaker containing 1N HCl and swirled gently overnight. The HCl was drained and any debris was rinsed off using distilled water. The coverslips were then washed twice for 10 min in 70% Ethanol and once for 10 min in 100% Ethanol. The coverslips were then stored in 100% Ethanol.

2.2.13.2. Preparation of plates

The coverslips were taken one at a time and placed slanted towards the wall of the well in order to allow them to dry off the Ethanol. This procedure was done on the sterile bench and the coverslips were air-dried for at least 15 min before being placed horizontally on the well surface. A solution of 0.15% Agarose was made in water and microwaved for 3 min for complete dissolution. About 2 ml of the Agarose solution was added to each well and removed after 10 sec. The coating of Agarose was allowed to air dry for 15 min after which the plates were sterilized under UV for 30 min.

2.2.13.3. Stamping the agarose coated coverslips

In order to stamp the agarose coated coverslips, a mixture of 3 parts acetic acid, one part collagen and one part PDL was used for preparation of a stamping medium. About 1.5 ml of the medium was added on to small folded tissues and the stamp was dipped on this stamping

pad to get just enough medium on. The agarose layer on the well was gently stamped and the procedure was repeated to stamp all the wells. The plates were allowed to air dry for 20 min and sterilized under UV for 30 min. The plates were ready to be used for cultures.

2.2.13.4. Culturing Cortical Astrocytes in T-75 cm² flasks

The cortical astrocytes adhere well to the PDL-Collagen stamp islands to form a feeder layer for the growth of autaptic neurons. To culture cortical astrocytes, the cortices from the P0 mouse brain were dissected in ice-cold HBSS removing the meninges and hippocampi. The cortices were transferred into 1 ml of 0.05% Trypsin-EDTA and were incubated on a shaker at 450 rpm for 15 min at 37°C. The solution was then discarded and the cortices were washed twice with 500 µl of FBS medium. Then cortices were dissociated by trituration for about 30 times in 500 µl of FBS medium. About 13 ml of FBS medium was added to the T-75 cm² and the triturated cortices were added to the flask and mixed gently. The flask was incubated at 37°C, 5% CO₂ and the medium was changed to fresh FBS after 24 hours to allow the growth of astrocytes. The astrocytes were ready to use after 1 week when they were 70% confluent.

2.2.13.5. Preparation of astrocyte micro-islands

The stamped culture plates were sterilized for 1 hour under UV. The T-75 cm² was removed and vortexed for 2 min at high speed. The medium containing all detached non-astrocytic cells was removed. The astrocytes were rinsed twice with 10 ml of sterile PBS. 5 ml of 0.05% Trypsin-EDTA was added to the astrocytes for 30 sec and removed. The flask was incubated for 10 min at 37°C, 5% CO₂. Simultaneously, the sterile culture plates were filled with 2 ml of FBS per well. After 10 min, the trypsinization was stopped in the flask using 10 ml of FBS; the astrocytes were carefully washed down the flask and removed into a 50 ml falcon. The cells were triturated using a 10 ml pipette and counted using a hemocytometer. Upon counting, the astrocyte cells were seeded on to the wells of the plates at an appropriate density depending on the stamp size. The plates were shaken for about 2 min in order to ensure homogenous distribution of cells. The plates were kept in the incubator for up to 2 days and used for neuron culture.

2.2.13.6. Preparation of neurons for autaptic culture

For neuron culture, the hippocampi were dissected from the brain of a E18/P0 mouse and placed in 500 µl of papain solution in a 1.5 ml eppendorf tube. They were digested for 1 hour

at 37°C under constant agitation at 450 rpm. Next, the papain solution was removed and 500 µl of the STOP solution was added and incubated for 15 min at 37°C, 450 rpm. The STOP solution was removed and the hippocampi were washed twice with 500 µl of NBA medium. The hippocampal neurons were then gently triturated in 200 µl of NBA medium and the tube was kept undisturbed for 1 min to allow the cell debris to settle at the bottom of the tube. The cell supernatant was extracted and mixed with 1 ml of fresh NBA medium. The neurons were counted using a hemocytometer and seeded at the appropriate density on to the plates.

2.2.14. Electrophysiology of autaptic neurons

Whole-cell voltage clamp measurements were performed on single neurons over astrocyte microislands (autapses) using Multiclamp 200B (Molecular devices) under the control of Clampex 10.1 (Molecular devices). Neurons were clamped at -70 mV, the series resistance was compensated and action-potential (AP) induced evoked responses were triggered by a 2 ms somatic depolarization to 0 mV. Neurons were stimulated at 0.2 Hz to measure basal evoked responses (EPSCs/IPSCs) in the standard external solution. A perfusion system was used to apply hypertonic sucrose solution directly on the patched neuron for duration of 5 s in order to measure the size of the readily releasable vesicle pool from the charge transfer of the sucrose-induced transient synaptic current. Evoking 50 and 100 synaptic responses at high-frequency stimulations of 10 Hz and 40 Hz respectively determined the short-term synaptic plasticity. Quantal release (mEPSCs and mIPSCs) was measured for duration of 100 s by directly perfusing standard external solution containing 300 nM TTX on to the neuron. In order to detect miniature events, traces were digitally filtered at 5 kHz offline and events were automatically detected using a defined template function in Axograph 1.0. All data were analyzed offline using Axograph 1.0 (Axograph Scientific) and Kaleidagraph (Synergy Software). Statistical significance was tested using Student's t-test.

2.2.15. Collagen-PDL coating of 24 well plates and 6 cm dishes

A combination of Acetic acid, Collagen and Poly-D-Lysine at predetermined concentrations was prepared and mixed well. The solution was uniformly spread on to the surface of the wells using a cotton swab. The plated were air-dried and UV-sterilized for 1 hr under the airflow hood. The plates were closed and stored at RT and UV-sterilized for 1 hr before use.

2.2.16. Continental Neuron Culture

In order to make continental cultures of neurons, the brain of a Embryonic day 18 (E18) or Postnatal day 0 (P0) mouse pup was dissected to remove the hippocampi. Both the hippocampi were incubated in 500 μ l of papain solution for 45 min or 1 hr respectively at 37°C with constant agitation at 450 rpm after which the solution was removed and 500 μ l of the STOP solution was added. The hippocampi were incubated for 15 min at 37°C in a shaker at 450 rpm. The STOP solution was removed and the hippocampi were washed twice with 500 μ l of NBA+B27 medium. Then, 200 μ l of the NBA+B27 medium was added and the hippocampi were gently triturated for 20 times. The cell debris was allowed to settle for 1 to 2 min. About 180 μ l of the supernatant containing the neurons was removed and added to 1 ml of fresh NBA+B27 medium. The cell suspension was mixed well by inversion and the total cell count was determined using a hemocytometer. After determination of the cell count, the neurons were plated out at a density of 1,000,000 cells per 6 cm coated dish in order to obtain a confluent continental neuron culture. The media in the wells was changed after 48 hours to remove cell debris.

2.2.17. Immunocytochemistry of continental neuron cultures

Neurons cultured on 24-well coverslips were used after 14 days *in-vitro* for immunocytochemical staining. The medium was aspirated and the cells were briefly washed with 1X PBS. 4% PFA containing sucrose in PB buffer was added to RT and incubated at RT for 7 min. The cells were washed for 4 times, 5 min each with 1X PBS. The cells were permeabilized using PBS solution containing goat serum and Triton-X 100 for 30 min. The cells were washed twice with 1X PBS. The blocking solution made of 1X PBS and goat serum was added to the cells and incubated for 30 min. The blocking solution was aspirated and fresh blocking solution containing the primary antibodies were added and incubated overnight at 4°C. The cells were washed 3 times the next day with 1X PBS. The Alexa-fluorophore labeled secondary antibodies were diluted in the blocking solution and added to cells. The cells were incubated for 90 min in the dark at RT, and were further washed 3 times with 1X PBS. The coverslips were mounted onto glass slides using the aquamount solution and analyzed using an epifluorescent microscope.

2.2.18. Harvesting proteins from continental neuron cultures

After 14 days of neuron growth, the medium from the plate was aspirated and the neurons were washed once with 1X PBS to remove any excess medium. Then, 30 μ l of PBS containing a cocktail of protease inhibitors was added to one well and the cells were vigorously scraped

using a cell scraper. The cell suspension was transferred into a small eppendorf tube and briefly homogenized using a 30G needle and a 1 ml syringe. A small aliquot of the homogenized cell suspension was taken for estimation of the protein concentration using Bradford's assay and the remaining sample was stored at -80°C.

2.2.19. Bradford's Assay

The Bradford's assay was performed for all samples such as cortical homogenates, cell lysates and recombinant proteins to ascertain the concentration of proteins in a given volume of sample. BSA was used as protein standard in concentrations of 0, 0.025, 0.05, 0.075, 0.1, 0.125 µg/ml in a total volume of 200 µl of ddH₂O. The dye reagent was diluted 5 times in ddH₂O, filtered and stored in the dark at 4°C. The samples were diluted in the ratios of 1:100 and 1:200 in 200 µl of ddH₂O. The wavelength for absorbance was set at 595 nm in the spectrophotometer. Each of the standards was mixed with 800 µl of the dye reagent and the mixture was transferred into disposable plastic cuvettes of 1 ml capacity. The absorbance was recorded in the spectrophotometer and the procedure was repeated for the protein samples. A hyperbolic graph was obtained plotting the absorbance values at 595 nm against the protein concentrations. The slope of the graph was used to determine the protein concentration of the sample from its respective absorbance value.

3. Results

3.1. Results - SNAP-29

3.1.1. Insights into the role of SNAP-29 at neuronal synapses

SNAP-29, as many studies have indicated, is a ubiquitously expressed protein and also a closely related paralog of neuronal SNAP-25. In my study, I investigated the physiological role of SNAP-29 at synapses in the mouse brain.

For this purpose, two genetic mouse mutants of SNAP-29 were generated (See Appendix 6.1). First, targeted deletion of the SNAP-29 gene from forebrain glutamatergic neurons was performed via Nex-Cre (Goebbels et al., 2006) driven recombination of a conditional SNAP-29 KO allele. The conditional loss of SNAP-29 from the hippocampus and the cerebral cortex did not cause any morphological or behavioral abnormalities in newborn mice. Subsequently, SNAP-29 constitutive KO mice were generated. These mice exhibited a strong keratoderma phenotype, as observed in patients suffering from the CEDNIK syndrome, and survived only a few hours after birth. The perinatal lethality was thus an intriguing characteristic that motivated my study on synaptic function in SNAP29 KO neurons.

3.1.1.1. Protein composition in the Nex-Cre SNAP-29 KO mice

I prepared cortical homogenates and neuronal lysates from KO and WT littermate animals for biochemical studies. Using Western blotting and enhanced chemiluminescence (ECL), I analyzed the expression levels of SNAP-29 and the SNARE proteins namely SNAP-25, Syntaxin-1, and Synaptobrevin-2. I found that the expression of SNAP-29 was strongly reduced in Nex-Cre KO cortex when compared with littermate WT cortex (Fig.12.A.) however, expression of other SNARE proteins was unaltered (Fig.12.C.). Furthermore, I analyzed the protein expression levels in cultured hippocampal neurons and found that the KO neurons exhibited a clear reduction in SNAP-29 (Fig.12.B.). In all cases, β -Tubulin was used as loading control, and no apparent changes were observable.

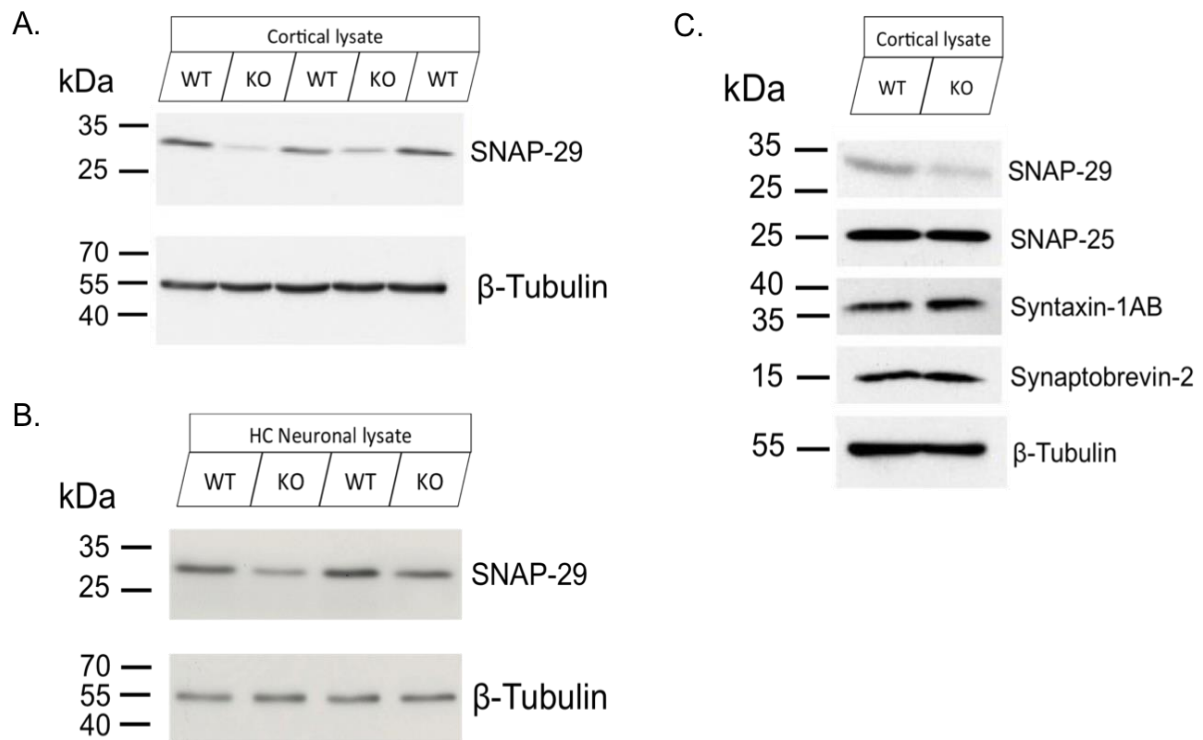


Figure 12.

Biochemical analysis of the protein composition in the

Nex-Cre SNAP-29 KO neurons. (A) Expression levels of SNAP-29 (~29 kDa) in the cortex of 3 WT and 2 NexCre SNAP29 KO animals as assessed by Western blotting **(B)** Expression levels of SNAP-29 in cultured hippocampal neurons of 2 WT and 2 NexCre SNAP29 KO animals as assessed by Western blotting **(C)** Expression levels of SNAP-29 and neuronal SNARE proteins SNAP-25 (25 kDa), Syntaxin-1AB (~35 kDa), and Synaptobrevin-2 (15 kDa) in the cortex of WT and NexCre SNAP29 KO mice. KO animals exhibited a strong reduction in SNAP-29 levels in cortex and hippocampal neurons. Loading control β -Tubulin (55 kDa) was used for all experiments.

3.1.1.2. Normal glutamatergic synaptic transmission in Nex-Cre SNAP29 KO mice

Exogenous addition and over-expression of SNAP-29 was previously shown to inhibit synaptic release in neurons in an activity dependent manner (Su et al., 2001; Pan et al., 2005). However, several questions were raised on the role of endogenous SNAP-29. As the Nex-Cre mediated deletion of SNAP-29 drastically lowered the endogenous SNAP-29 protein levels in the forebrain, I studied the basic parameters of synaptic transmitter release by performing whole-cell patch clamp recordings in autaptic hippocampal neurons from NexCre SNAP29 KO mice and WT littermates. The amplitudes of evoked excitatory post-synaptic currents (EPSC), the size of the readily releasable pool of vesicles and the vesicular release probability in KO and WT neurons were not significantly different (Fig.13. A. B. and C.).

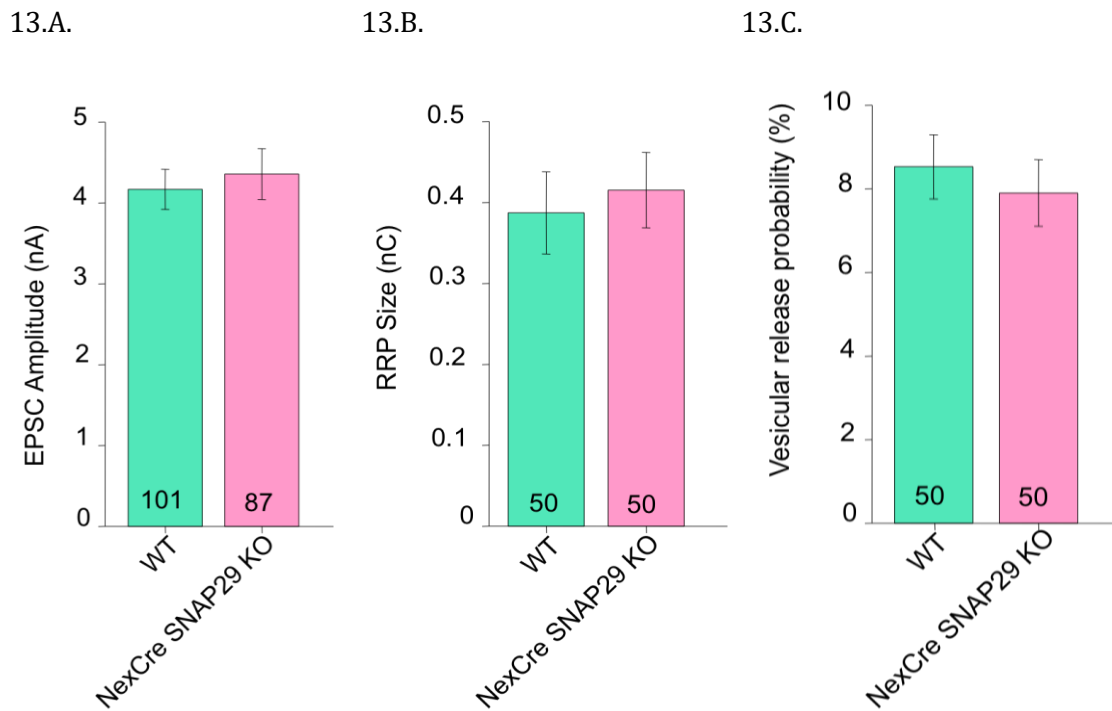


Figure 13. Normal excitatory synaptic transmission in hippocampal neurons of Nex-Cre SNAP-29 KO. (A) Mean EPSC amplitude of WT and SNAP29 deficient neurons was similar **(B)** Mean RRP size measured as charge triggered by the application of 0.5 M sucrose solution was similar **(C)** Mean vesicular release probability estimated as the ratio of charge of the evoked EPSC to the charge of the RRP was similar. Error bars indicate standard error of mean. Numbers of neurons analyzed are indicated on bars. Absolute values are indicated in Table 12. No statistically significant differences were observed (Students t-test).

I measured the short-term plasticity by applying stimulations of 10 Hz and 40 Hz, but found both the WT and KO synapses to depress similarly (Fig.14.A. and B.).

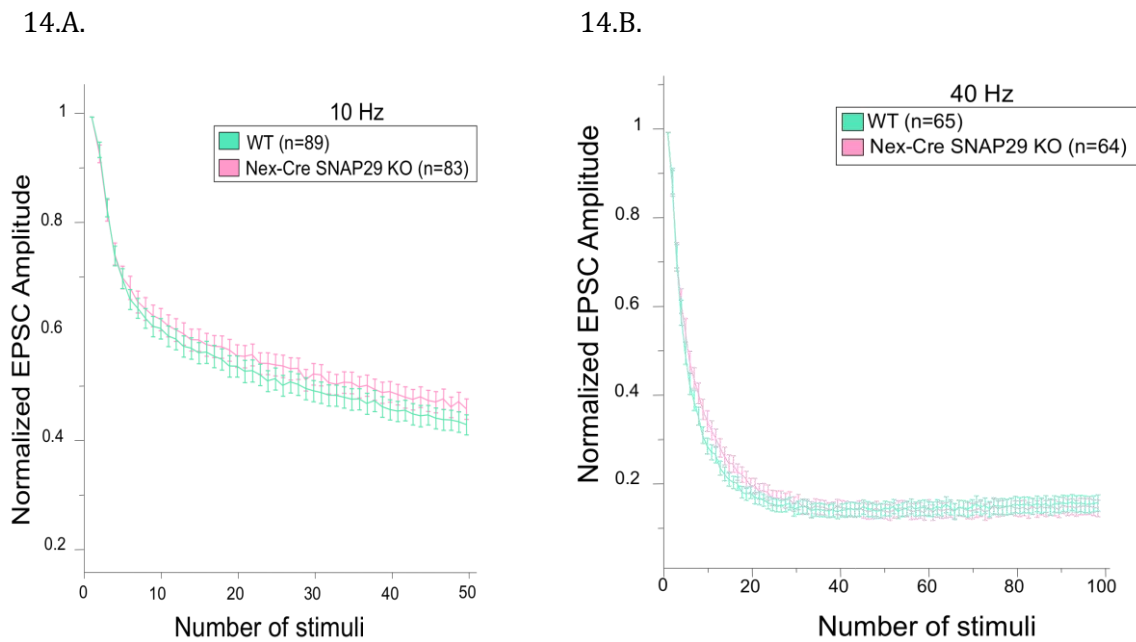


Figure 14. **Normal short-term plasticity in hippocampal neurons of Nex-Cre SNAP-29 KO.** (A) and (B) Normalized synaptic responses observed upon stimulation of WT and SNAP29 deficient neurons at frequencies of 10 Hz and 40 Hz, respectively.

Down-regulation of SNAP-29 was indicated to increase the rate of turnover of the vesicle pool (Pan et al., 2005). In order to test this claim, I measured the spontaneous release by exogenous application of 300 nM TTX immediately after a train stimulation of 40 Hz. Since high-frequency stimulations increase residual calcium in the terminal, spontaneous release of release-ready vesicles increases manifold as newly primed vesicles join the pool. The increased basal Ca^{2+} does not have an effect on the amplitudes of spontaneous miniature events. In my study, I found that immediately after stimulation at 40 Hz, the frequency of mEPSC events increased approximately three-fold (compared to the mEPSC frequency at resting conditions) in both the WT and KO neurons (Fig.15.A.) and no significant differences observable. The frequency of spontaneous miniature currents measured at resting conditions was similar in WT and KO neurons (Fig.15.B.). The mEPSC amplitudes remained unchanged in both conditions (Fig.15.C. and Fig.15.D.).

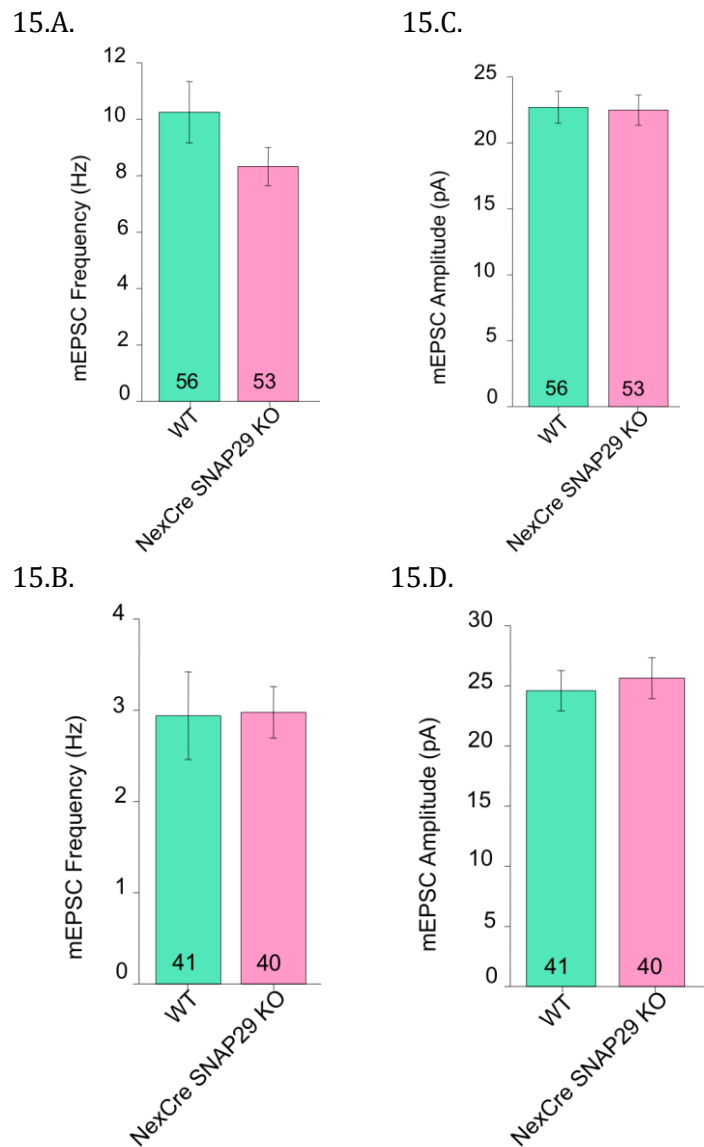


Figure 15.

Normal mEPSC release in excitatory hippocampal

neurons of Nex-Cre SNAP-29 KO. Miniature responses measured in the presence of 300 nM TTX to block APs. **(A)** and **(C)** Mean mEPSC frequency and amplitudes immediately after high-frequency stimulation of 40 Hz, **(B)** and **(D)** Mean mEPSC frequency and mEPSC amplitudes at rest. Error bars indicate standard error of mean. Numbers of neurons analyzed are indicated on bars. Absolute values are indicated in Table 12. No statistically significant differences were observed (Students t-test).

Table 12. Synaptic parameters measured from excitatory autaptic hippocampal neurons of WT and Nex-Cre SNAP29 KO mice

Parameters	WT	Nex-Cre SNAP29 KO
Mean EPSC Amplitudes (nA) ± S.E.M.	4.1696 ± 0.24786 (n=101)	4.3589 ± 0.31405 (n=87)
Mean RRP Size (nC) ± S.E.M.	0.387190 ± 0.05073 (n=50)	0.41526 ± 0.046521 (n=50)
Mean Pvr (%) ± S.E.M.	8.5279 ± 0.76799 (n=50)	7.9025 ± 0.79510 (n=50)
Mean mEPSC Frequency (After 40 Hz) (Hz) ± S.E.M.	10.252 ± 1.0882 (n=56)	8.3309 ± 0.67503 (n=53)
Mean mEPSC Amplitude (After 40 Hz) (pA) ± S.E.M.	22.698 ± 1.2046 (n=56)	22.486 ± 1.1481 (n=53)
Mean mEPSC Frequency (At rest) (Hz) ± S.E.M.	2.9407 ± 0.47954 (n=41)	2.9765 ± 0.28224 (n=40)
Mean mEPSC Amplitude (At rest) (pA) ± S.E.M.	24.602 ± 1.6743 (n=41)	25.646 ± 1.7048 (n=40)

S.E.M. is standard error of mean n is total number of cells pooled from multiple cultures.

3.1.1.3. Protein composition in the brain of constitutive SNAP-29 KO mice

As the constitutive SNAP-29 KO mice exhibited the Keratoderma phenotype, they could be visually distinguished from WT littermates. I prepared cortical homogenates from the WT and KO animals and subjected the samples to biochemical analysis. I found that the constitutive deletion of SNAP-29 gene resulted in a complete loss of the SNAP-29 protein (also corroborated by tail genotyping and PCR). I tested the expression levels of cognate SNAREs and the paralogs of SNAP-29 namely, SNAP-25, SNAP-23 and SNAP-47 and found that loss of SNAP-29 did not up-regulate the expression of other paralogs or SNAREs (Fig.16.).

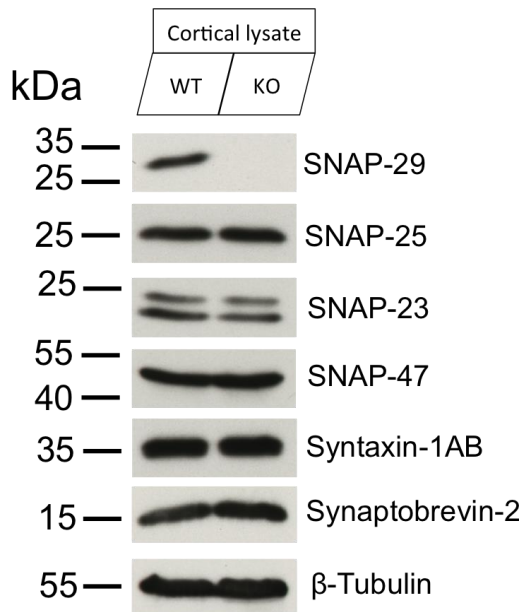
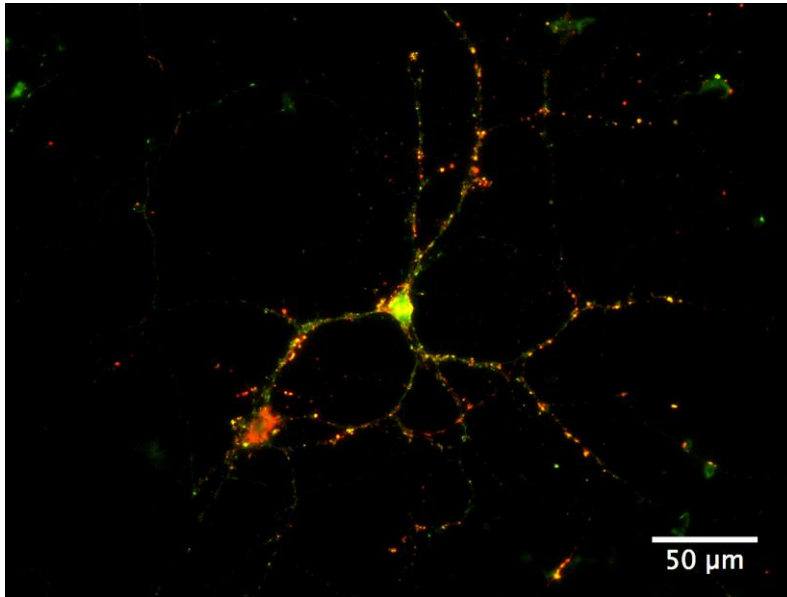


Figure 16. Protein composition in SNAP-29 constitutive KO mouse brain. Expression levels of SNAP-29 and other candidate proteins in WT and constitutive SNAP-29 KO cortical lysates. Complete loss of SNAP-29 in the KO cortex but normal expression in WT was observed, while Syntaxin-1AB (35 kDa), Synaptobrevin-2 (15 kDa), and SNAP-25 (25 kDa) were expressed normally, along with SNAP-47 (47 kDa) and SNAP-23 (two likely alternative splice variants detected as two bands at ~23 kDa) in both WT and KO animals. β -Tubulin (55 kDa) was used as loading control.

3.1.1.4. Immunocytochemical analysis of SNAP-29 in hippocampal neurons

SNAP-29 was previously shown to co-localize with the presynaptic marker Synaptophysin (Su et al., 2001). However, the corresponding experiments lacked a valid control. In my study, I performed immunostaining on cultured hippocampal neurons (DIV: 14) from SNAP-29 KO and WT animals to check for presynaptic expression of SNAP-29 in neurons, and used VGLUT-1 as a presynaptic marker. Although visibly diffuse expression of SNAP-29 (in green) is observable throughout the soma and the neuronal processes in the WT animals, a co-localization with VGLUT-1 (in red) in the presynaptic compartment was not detectable (Fig.17.A). KO neurons were completely devoid of the SNAP-29 staining (Fig.17.B.).

17.A. SNAP-29 WT



17.B. SNAP-29 KO

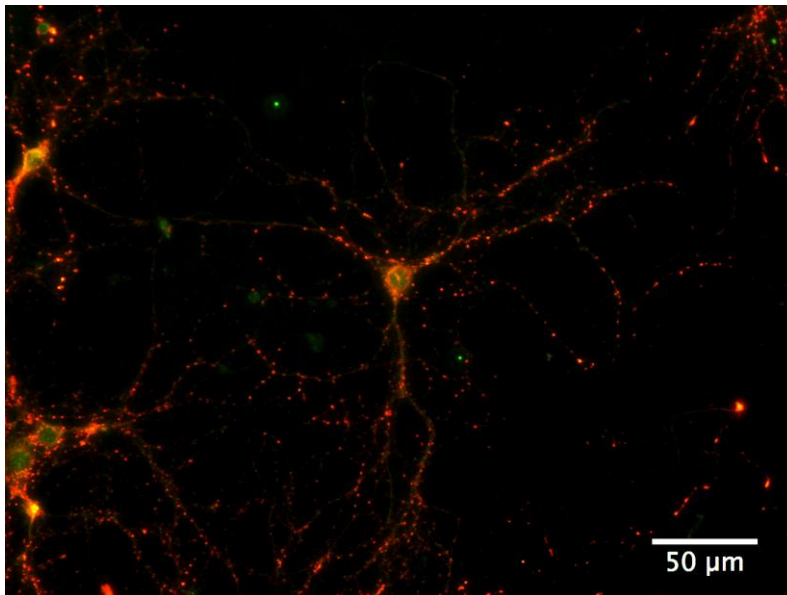


Figure 17.

Immunocytochemical analysis of SNAP-29 localization in neurons. (A) WT cultured hippocampal neurons stained for SNAP-29 (Alexa-488-green) and VGLUT-1 (Alexa-555-red). Visibly diffuse SNAP-29 expression is observed in soma, axons and dendrites. **(B)** KO hippocampal neurons stained for SNAP-29 and VGLUT-1, complete loss of expression of SNAP-29 is observable.

3.1.1.5. Normal glutamatergic synaptic transmission in Constitutive SNAP-29 KO mice

Obvious absence of synaptic deficits in NexCre SNAP29 KO mice and the perinatal lethal phenotype of the constitutive SNAP29 KO animals prompted me to verify the synaptic parameters in the glutamatergic neurons of the hippocampus of the constitutive SNAP29 KOs. In both WT and KO animals, all measured parameters such as evoked EPSC amplitudes, RRP size, and vesicular release probability were not significantly different (Fig.18.A. B. and C., Table 13). Short-term plasticity measured upon high-frequency stimulation also showed normal EPSC depression in both SNAP29 WT and SNAP29 KO neurons (Fig.19.A. and B.).

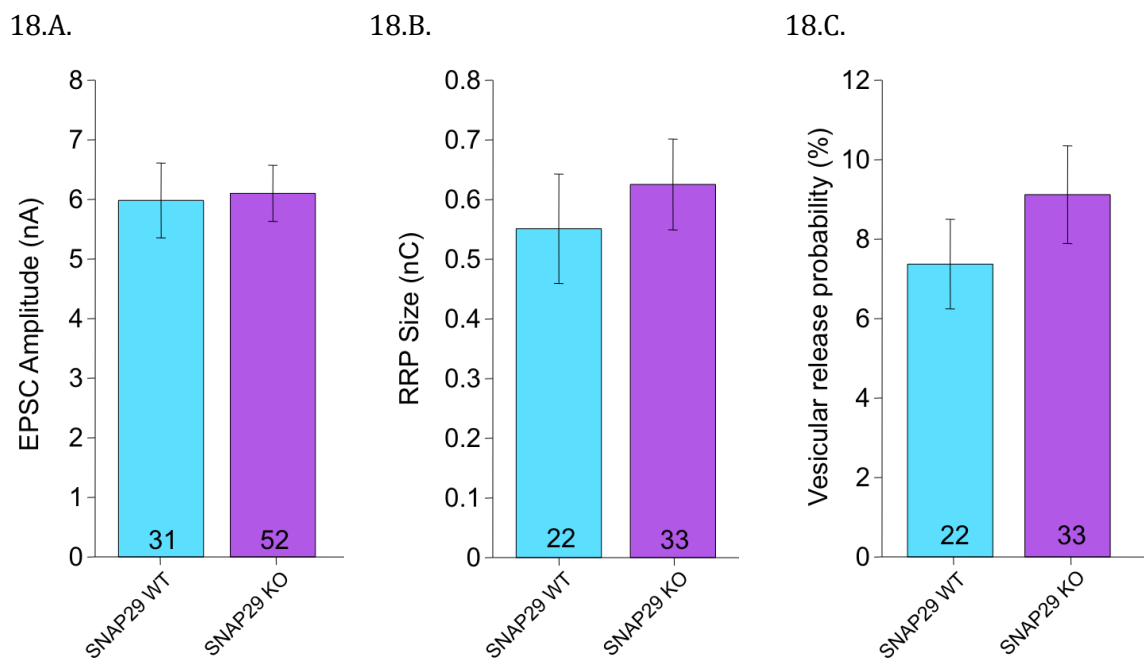


Figure 18. Normal excitatory synaptic transmission in hippocampal neurons of SNAP-29 KO. **(A)** Mean EPSC amplitude of WT and SNAP29 KO neurons was similar **(B)** Mean RRP size measured as charge triggered by the application of 0.5 M sucrose solution was similar **(C)** Mean vesicular release probability estimated as the ratio of charge of the evoked EPSC to the charge of the RRP was similar. Error bars indicate standard error of mean. Numbers of neurons analyzed are indicated on bars. Absolute values are indicated in Table 13. No statistically significant differences were observed (Students t-test).

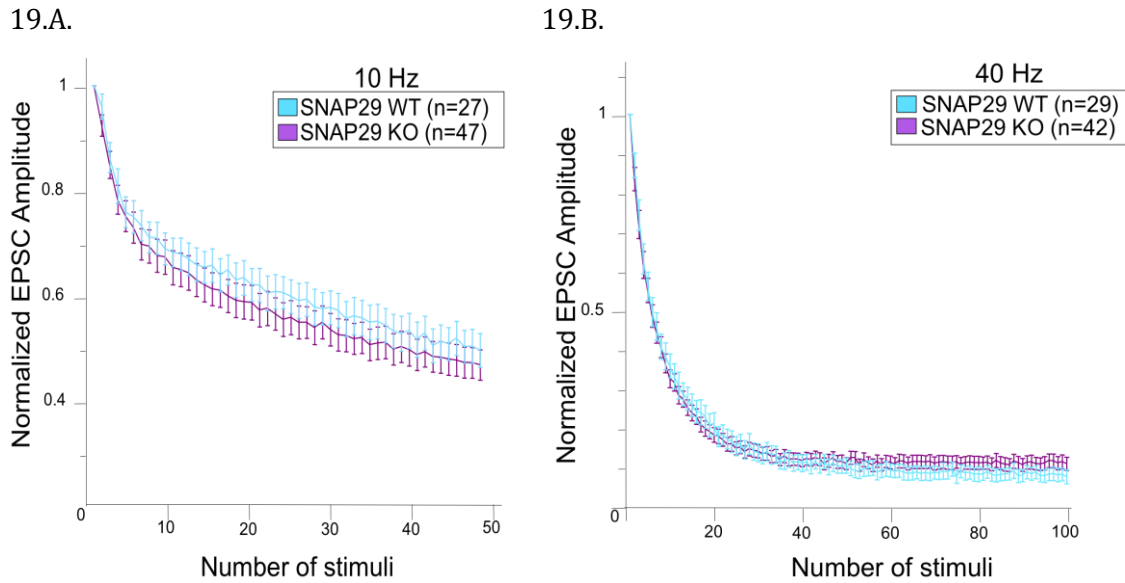
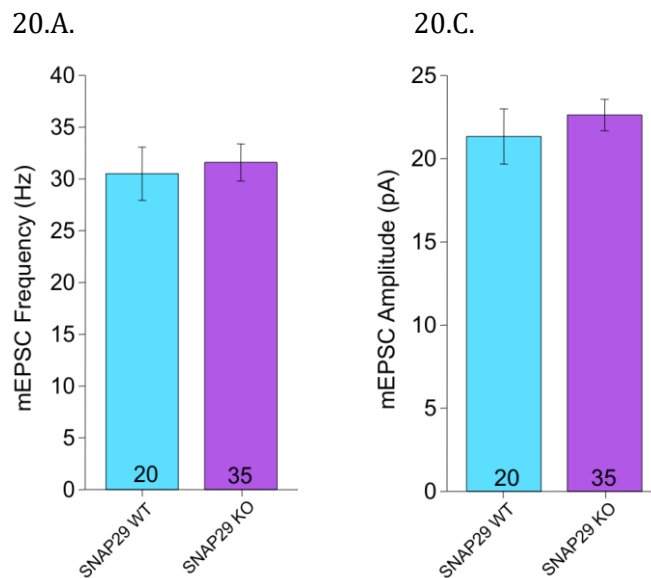


Figure 19. Normal short-term plasticity in hippocampal neurons of SNAP-29 KO. (A) and (B) Normalized synaptic responses observed upon stimulation of WT and SNAP29 KO neurons at frequencies of 10 Hz and 40 Hz, respectively.

Frequency of spontaneous release measured after high-frequency activity was markedly higher (approximately three-fold compared to resting conditions) in both WT and KO neurons but did not significantly vary between the genotypes (Fig.20.A. and B., Table 13). There were no visible differences in mEPSC amplitudes (Fig.20.C. and D., Table 13).



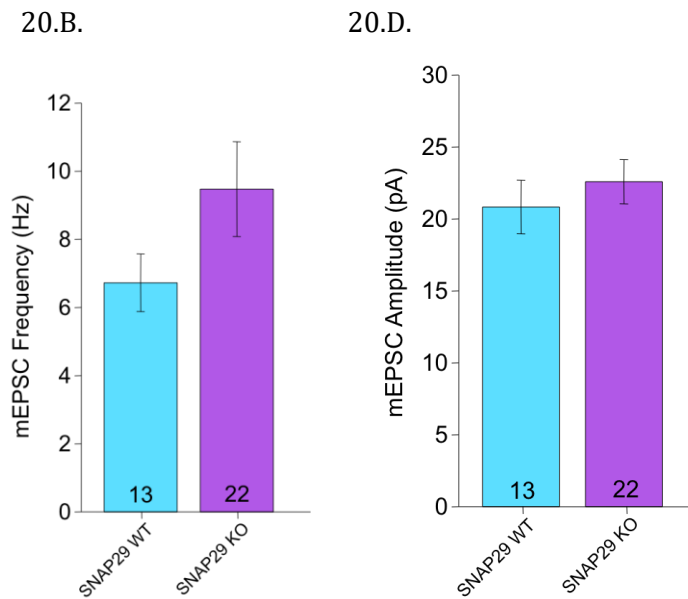


Figure 20. Normal mEPSC release in excitatory hippocampal neurons of SNAP-29 KO. Exogenous application of 300 nM TTX to block AP and measure miniature release - **(A)** and **(C)** Mean mEPSC frequency and amplitudes immediately after high-frequency stimulation of 40 Hz, **(B)** and **(D)** Mean mEPSC frequency and mEPSC amplitudes after low frequency stimulation of 0.2 Hz. Error bars indicate standard error of mean. Numbers of neurons analyzed are indicated on bars. Absolute values are indicated in Table 13. No statistically significant differences were observed (Students t-test used to test statistical significance).

Table 13. Synaptic parameters measured from excitatory autaptic hippocampal neurons of WT and constitutive SNAP29 KO mice

Parameters	WT	SNAP29 KO
Mean EPSC Amplitudes (nA) ± S.E.M.	5.9830 ± 0.62848 (n=31)	6.1046 ± 0.47024 (n=52)
Mean RRP Size (nC) ± S.E.M.	0.55125 ± 0.091682 (n=22)	0.62544 ± 0.075976 (n=33)
Mean Pvr (%) ± S.E.M.	7.3743 ± 1.1273 (n=22)	9.1212 ± 1.2280 (n=33)
Mean mEPSC Frequency (After 40 Hz) (Hz) ± S.E.M.	30.508 ± 2.5736 (n=20)	31.613 ± 1.7891 (n=35)
Mean mEPSC Amplitude (After 40 Hz) (pA) ± S.E.M.	21.341 ± 1.6585 (n=20)	22.628 ± 0.94515 (n=35)
Mean mEPSC Frequency (At rest) (Hz) ± S.E.M.	6.7292 ± 0.84912 (n=13)	9.4768 ± 1.3896 (n=22)
Mean mEPSC Amplitude (At rest) (pA) ± S.E.M.	20.843 ± 1.8612 (n=13)	22.602 ± 1.5345 (n=22)

S.E.M. is standard error of mean n is total number of cells pooled from multiple cultures.

3.1.1.6. Normal GABAergic synaptic transmission in Constitutive SNAP-29 KO mice.

Since the excitatory glutamatergic neurons showed no deficits in synaptic release, and because inhibitory neurons were reported to express lower levels of SNAP-25 than excitatory neurons (Frassoni et al., 2005), I tested the inhibitory neurons in the striatum of the SNAP-29 KO mice to identify possible functional deficits due to reduced endogenous SNAP-25 levels and total loss of SNAP-29. Major synaptic parameters such as evoked IPSC amplitudes, short-term plasticity and vesicular release probability were similar in WT and KO striatal GABAergic neurons (Fig.21.A. and C. and Fig.22.A. and B.). Although the RRP size was seemingly larger in the KO neurons than in the WT neurons, the difference was not significant (Fig.21.B.). The frequency and amplitude of mIPSCs measured at rest were also similar between the WT and KO neurons (Fig.23.A. and B.).

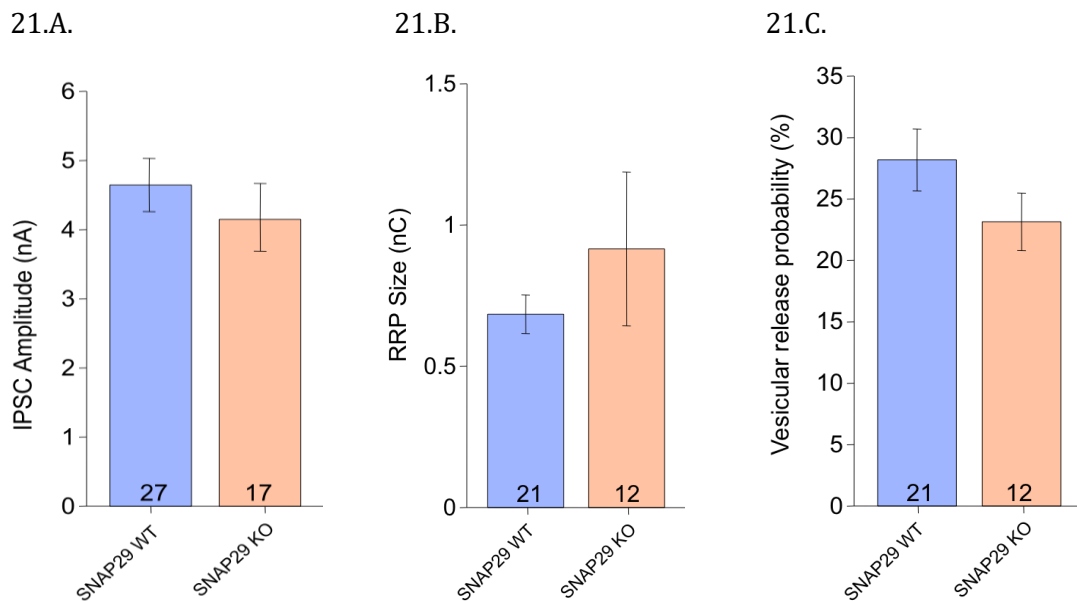


Figure 21.

Normal inhibitory synaptic transmission in striatal neurons of SNAP-29 KO. (A) Mean IPSC amplitude of WT and SNAP29 deficient neurons was similar **(B)** Mean RRP size measured as charge triggered by the application of 0.5 M sucrose solution was similar **(C)** Mean vesicular release probability estimated as the ratio of charge of the evoked EPSC to the charge of the RRP was similar. Error bars indicate standard error of mean. Numbers of neurons analyzed are indicated on bars. Absolute values are indicated in Table 14. No statistically significant differences were observed (Students t-test used to test statistical significance).

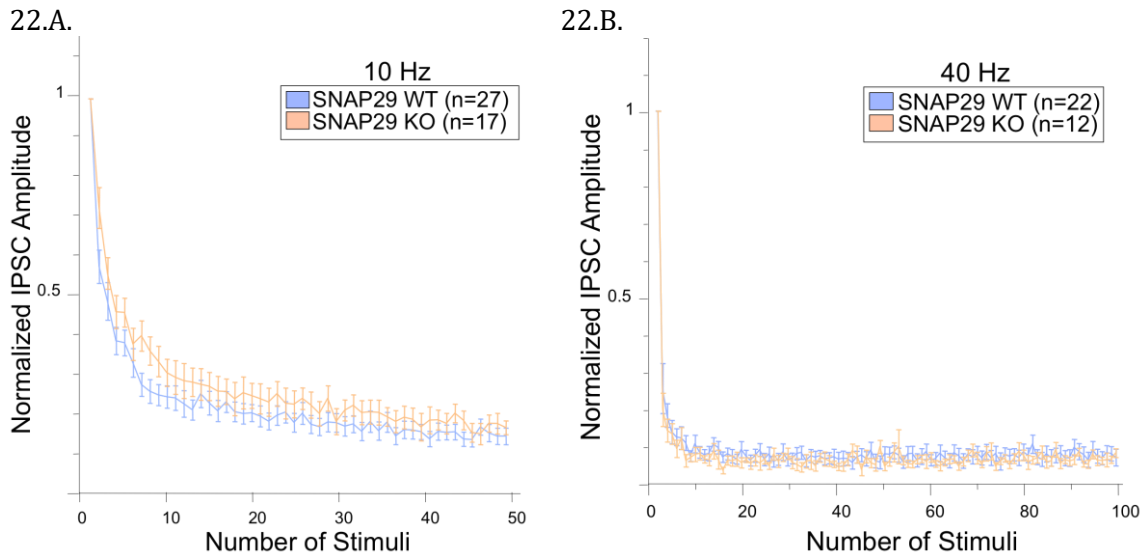


Figure 22. **Normal short-term plasticity in striatal neurons of SNAP-29 KO.** **(A)** and **(B)** Normalized synaptic depression observed upon stimulation of WT and SNAP29 KO neurons at high-frequencies of 10 Hz and 40 Hz, respectively.

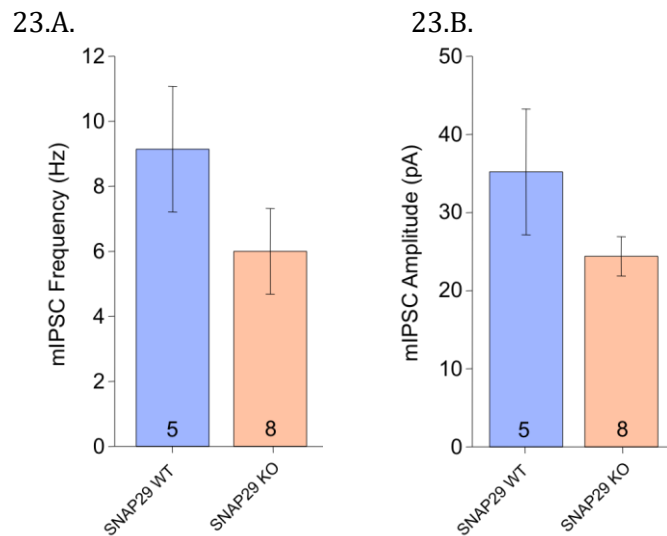


Figure 23. **Normal miniature release in inhibitory striatal neurons of SNAP-29 KO.** Exogenous application of 300 nM TTX to block AP and measure miniature release **(A)** and **(B)** Mean mIPSC frequency and amplitudes after low-frequency stimulation of 0.2 Hz. Error bars indicate standard error of mean. Numbers of neurons analyzed are indicated on bars. Absolute values are indicated in Table 14. No statistically significant differences were observed (Students t-test used to test statistical significance).

Table 14. Synaptic parameters measured from inhibitory autaptic striatal neurons of WT and constitutive SNAP29 KO mice

Parameters	WT	SNAP29 KO
Mean IPSC Amplitudes (nA) \pm S.E.M.	4.6467 \pm 0.38514 (n=27)	4.1507 \pm 0.49095 (n=17)
Mean RRP Size (nC) \pm S.E.M.	0.68431 \pm 0.06837 (n=21)	0.91578 \pm 0.27234 (n=12)
Mean Pvr (%) \pm S.E.M.	28.183 \pm 2.5166 (n=21)	23.141 \pm 2.3342 (n=12)
Mean mIPSC Frequency (At rest) \pm S.E.M.	9.1420 \pm 1.9316 (n=5)	6.0012 \pm 1.3180 (n=8)
Mean mIPSC Amplitude (At rest) (pA) \pm S.E.M.	35.206 \pm 8.0420 (n=5)	24.403 \pm 2.5223 (n=8)

S.E.M. is standard error of mean

n is total number of cells pooled from one culture.

3.2. Results - Complexins

3.2.1. Wild-type mammalian Complexins facilitate glutamatergic synaptic transmission

Multiple studies have extensively discussed the role of Complexins in different model systems. The mammalian Complexins are the most intriguing due to the presence of different paralogs, variations in their structures, and different affinities to the neuronal SNAREs. In the literature, mammalian Complexins have been shown to facilitate Ca²⁺-evoked transmitter release but a systematic comparative structure-function analysis of the various paralogs has never been done. Also, the role of Complexins in synchronizing vesicle fusion and release has not been clearly defined. In my study, I performed a comparative and detailed analysis of the various Complexin paralogs and examined the differences in their efficacies to modulate neurotransmitter release at central glutamatergic synapses.

3.2.1.1. Endogenous Complexin-1 is essential for Ca²⁺-triggered release of vesicles but not for vesicle priming

Many previous studies have shown that mammalian Complexin-1 (Cplx1) is an effective facilitator of synaptic release (Reim et al., 2001; Xue et al., 2008). I have been able to confirm these results using the Cplx-TKO autaptic neuron culture system, in which I performed whole-cell patch clamp recordings to measure transmitter release in a homogenous population of synapses. As control (Cplx-CTRL), I used neurons from littermate Cplx1 heterozygotes (Cplx1 +/- Cplx2 -/- Cplx3 -/-), which share the same phenotype as wild-type animals. Also, as a part of my study, I analyzed the kinetics of EPSCs in these neurons to better understand the role of Complexins in synchronizing vesicle fusion.

I measured the amplitudes of AP-evoked EPSCs in Cplx-CTRL and Cplx-TKO neurons and found that the absence of Complexins resulted in a 50% reduction of the peak EPSC amplitudes (mean EPSC: 4.195 ± 0.595 nA) compared to control neurons expressing Cplx1 (mean EPSC: 2.032 ± 0.38 nA) (Fig.24.A.). However, the size of the readily releasable primed pool of vesicles was similar at synapses of Cplx-CTRL (mean RRP: 0.28 ± 0.068 nC) and Cplx-TKO neurons (mean RRP: 0.27 ± 0.079 nC) (Fig.24.B.). A deficit in Ca²⁺-triggered release in the absence of Cplx despite the presence of a normal releasable vesicle pool implied a reduction in the vesicular release probability (P_vr) at the affected synapses. The vesicular

release probability in Cplx-TKO neurons (mean Pvr: $9.54 \pm 0.953\%$) was reduced by 60% compared to Cplx-CTRL (mean Pvr: $3.38 \pm 0.382\%$) (Fig.24.C.).

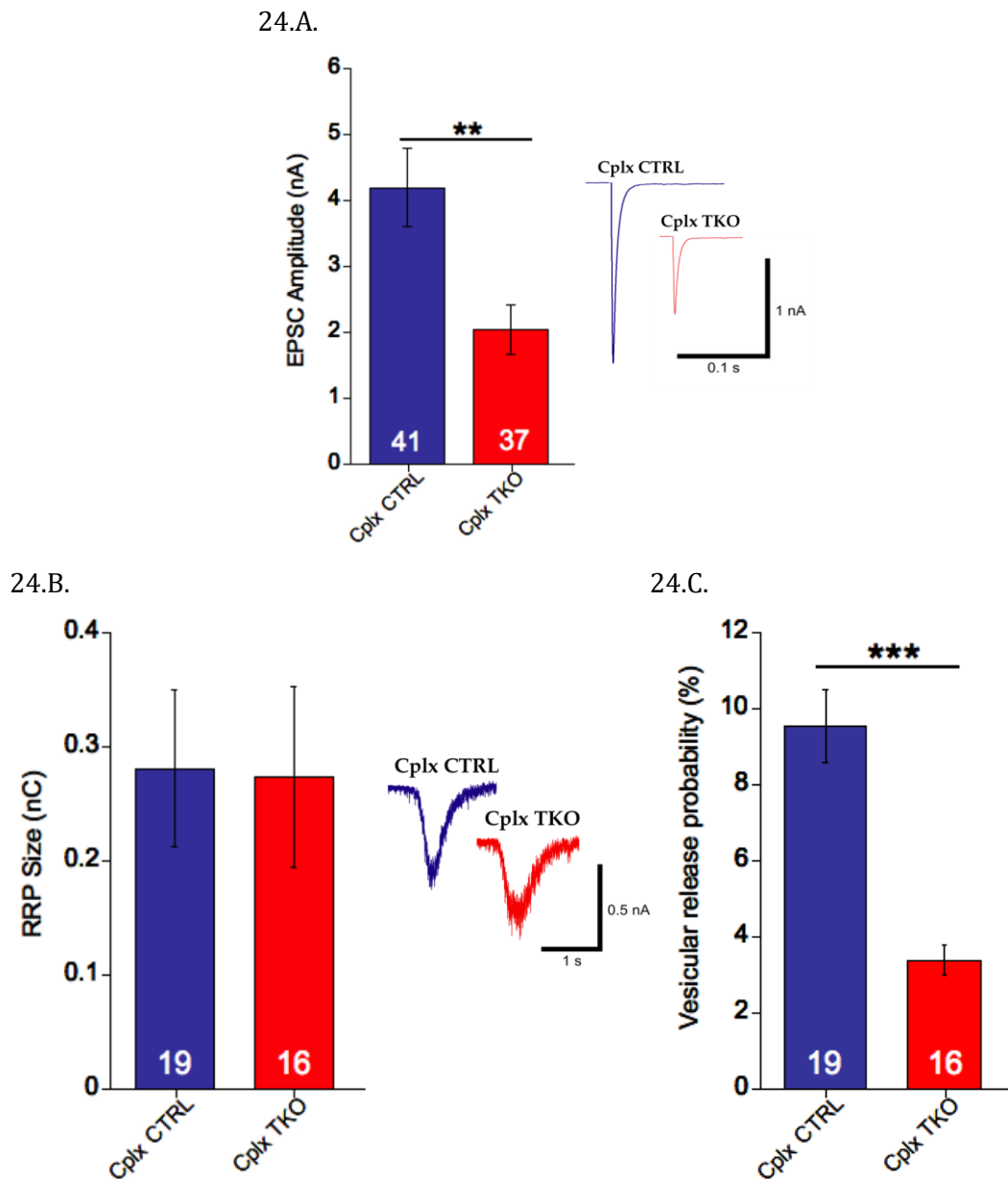


Figure 24.A.,B.,C.

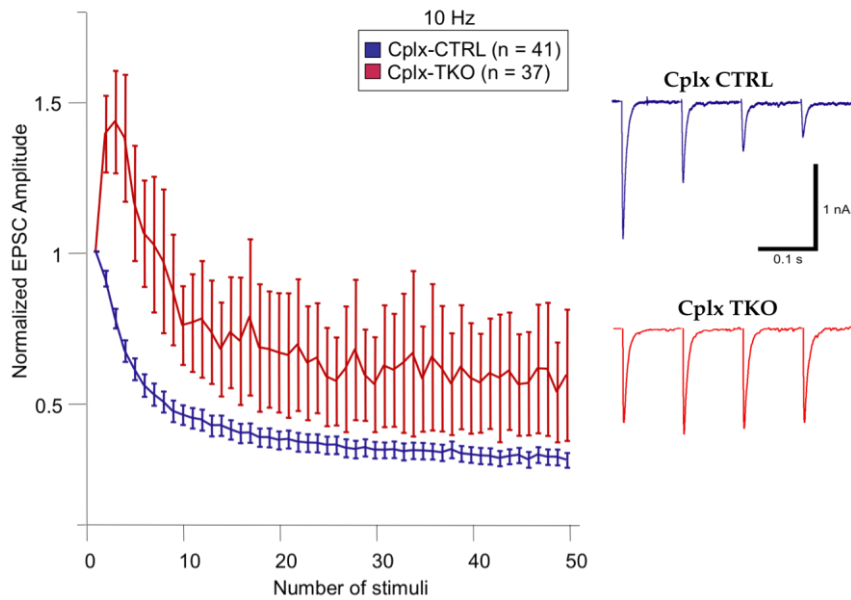
Evoked synaptic transmission in autaptic hippocampal neurons of Cplx CTRL and Cplx TKO mice.

Cplx CTRL (Cplx1+/-, Cplx2-/-, Cplx3-/-) and Cplx TKO (Cplx1-/-, Cplx2-/-, Cplx3-/-) cultured neurons were used in the study. **(A)** Mean excitatory post-synaptic current (EPSC) amplitudes \pm S.E.M. of CTRL and TKO neurons - EPSC was reduced by 50% in the absence of Complexins, $**p < 0.01$ compared with Cplx CTRL, representative traces for Cplx CTRL and TKO are included. **(B)** Mean RRP size \pm S.E.M. measured as charge elicited due to release of the primed vesicle pool, induced by application of 0.5 M sucrose solution - RRP size was unaltered in CTRL and TKO neurons, representative traces for Cplx CTRL and TKO are

included. **(C)** Mean vesicular release probability (Pvr) \pm S.E.M. in CTRL and TKO neurons estimated as the percentage ratio of charge of the evoked EPSC to the charge of the RRP – Pvr was reduced by 60% in the absence of Complexins, ***p<0.001 compared with Cplx CTRL. Error bars indicate standard error of mean (S.E.M.). Numbers of neurons analyzed are indicated on bars. Students t-test was used to test statistical significance.

Short-term plasticity analysis further corroborated the reduced vesicular release probability in the absence of Complexins. A high initial facilitation of EPSCs was observed in the Cplx-TKO neurons at high-frequency stimulation (10 Hz and 40 Hz), indicative of low initial vesicular release probability when compared to a fast depression of EPSCs in the Cplx-CTRL neurons (Figs.24.D. and 24.E.).

24.D.



24.E.

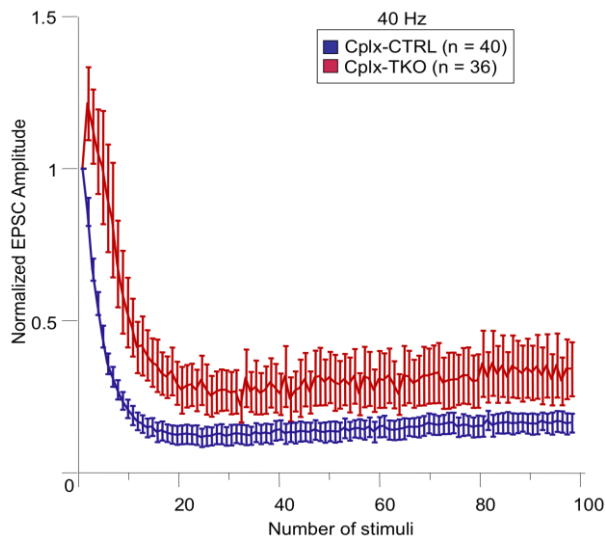


Figure 24.D.,E.

Short-term plasticity in autaptic hippocampal neurons of Cplx CTRL and Cplx TKO mice. (D) and (E) Amplitudes of the synaptic responses evoked by a train of stimulation at 10 Hz and 40 Hz (for EPSCs) were normalized to the amplitude of the first response and plotted against the stimulus number. Representative traces for Cplx CTRL and TKO are included for 10 Hz stimulation. Data are expressed as mean \pm S.E.M. Numbers of neurons analyzed are indicated. Normalized EPSC depression observed in CTRL neurons implies high initial vesicular release probability, while initial facilitation of normalized EPSC amplitudes in TKO neurons indicates lower initial release probability.

3.2.1.2. Loss of Complexins does not dramatically affect spontaneous vesicle fusion.

I measured the frequency and amplitudes of miniature excitatory post-synaptic currents (mEPSC) spontaneously occurring at the Cplx-CTRL and Cplx-TKO neuronal synapses (by blocking action-potentials using TTX). The mEPSC frequency was reduced to a small extent in the absence of Complexins (mean mEPSC frequency: 3.19 ± 0.483 Hz) compared to the controls (mean mEPSC frequency: 4.858 ± 0.593 Hz), although the amplitude of miniature release was not significantly different between the Cplx-CTRL (mean mEPSC Amplitude: 25.644 ± 2.727 pA) and Cplx-TKO (mean mEPSC Amplitude: 18.64 ± 2.5 pA) (Fig.24.F. and 24.G.).

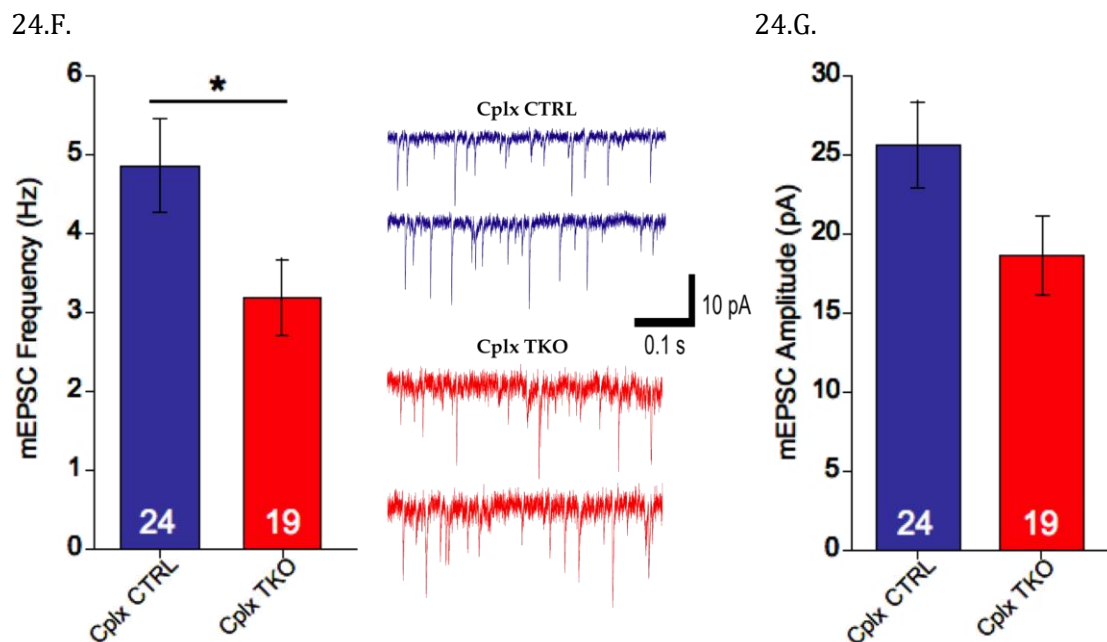


Figure 24.F.,G.

Spontaneous neurotransmitter release (mEPSC) in autaptic hippocampal neurons of Cplx CTRL and Cplx TKO mice. 300 nM Tetrodotoxin was exogenously applied using the fast perfusion system

to neurons in order to block Na⁺-channel driven action potentials while measuring miniature excitatory post-synaptic currents. **(F)** Mean mEPSC frequency - a small but significant reduction of mEPSC frequency was observed in the Cplx TKO neurons, *p<0.05 compared with CTRL; representative traces for Cplx CTRL and TKO are included. **(G)** Mean mEPSC amplitudes of Cplx CTRL and Cplx TKO - no significant differences were observed. Error bars indicate standard error of mean. Numbers of neurons analyzed are indicated on bars. Students t-test was used to test statistical significance.

3.2.1.3. Role of endogenous Complexin-1 in synchronous and asynchronous vesicle release.

Integral of the average EPSC charge clearly delineates the two kinetic phases of release - the fast synchronous phase and the slower asynchronous phase. Previously, it was shown that loss of Cplx1 and Cplx2 reduced the synchronous component of release while the asynchronous component of release was unchanged (Reim et al., 2001). This finding led to the conclusion that Complexins do not play a role in mediating asynchronous release of vesicles. I analyzed the two components of the cumulative and normalized EPSC charge in Cplx CTRL as well as TKO neurons to confirm the previously published effects. I found that in the absence of Complexins, the synchronous component of release is reduced, while the asynchronous component persists at similar levels I observed in the presence of Complexins (Fig.25.A. and 25.B.).

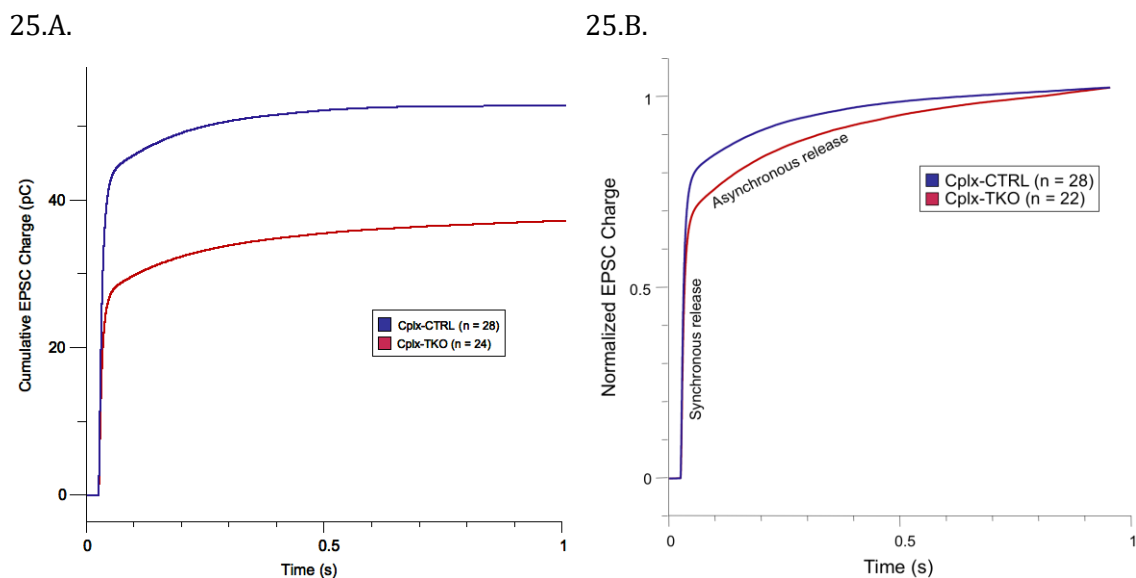


Figure 25.A.,B. Asynchronous neurotransmitter release in autaptic hippocampal neurons of Cplx CTRL and Cplx TKO mice. (A) and (B) Cumulative and normalized integrals of the EPSC charge versus time, respectively. The fast rising component indicates synchronous release of vesicles

and the slowly rising component indicates the asynchronous component of release. Synchronous release is higher in CTRL neurons when compared with TKO neurons, but the asynchronous component persists in both CTRL and TKO neurons. Numbers of neurons analyzed are indicated.

Next, I attempted to find out if and why the loss of Complexins has little effect on the asynchronous release of vesicles. For this purpose, I exogenously applied the slow Ca^{2+} -chelating buffer EGTA-AM to neurons and recorded evoked EPSCs at low frequency of 0.2 Hz (Fig.25.C.).

25.C.

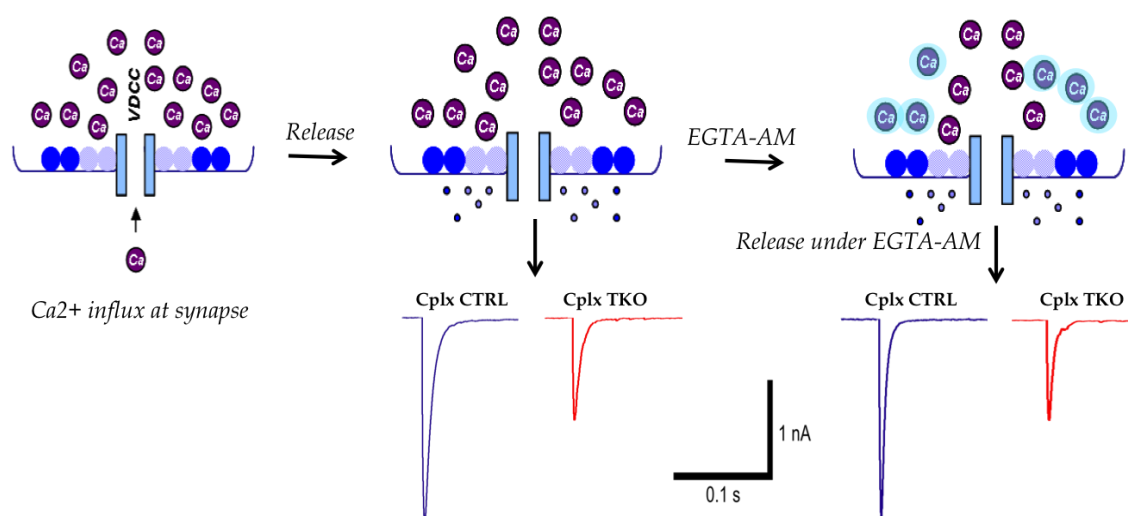


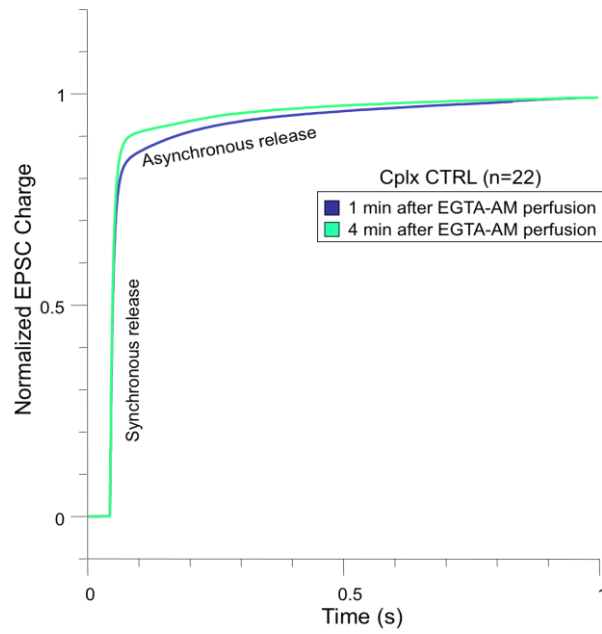
Figure 25.C.

Representation of synchronous and asynchronous neurotransmitter release under the effect of exogenously applied EGTA-AM in autaptic hippocampal neurons of Cplx CTRL and Cplx TKO mice. When an AP arrives at the presynaptic terminal, Ca^{2+} -influx releases a fraction of the primed vesicles resulting in the excitatory post-synaptic current that typically reflects two kinetic components of release - a fast synchronous release phase occurring within tens of milliseconds, and a slow asynchronous phase (or delayed release) occurring for a few hundred milliseconds as the Ca^{2+} in the terminal is cleared. Application of EGTA-AM, a slow Ca^{2+} -binding buffer chelates the Ca^{2+} ions that cause delayed release. In Cplx CTRL neurons, the synchronous release is not affected but the asynchronous phase is selectively reduced 4 minutes upon application of EGTA-AM, whereas EGTA-AM does not affect the release kinetics of Cplx TKO neurons.

In the Cplx CTRL neurons, no reduction in the synchronous and asynchronous release was observable within one minute after perfusion of EGTA-AM. After four minutes of application, the asynchronous component of release was reduced while the synchronous component remained unaltered (Fig.25.D.). In the Cplx TKO neurons, one minute after perfusion, EGTA-

AM did not alter the synchronous and asynchronous release. Four minutes after perfusion of EGTA-AM also resulted in no changes to both the asynchronous and synchronous components of release (Fig.25.E.) indicating that the loss of Complexins likely causes desynchronization of vesicle fusion.

25.D.



25.E.

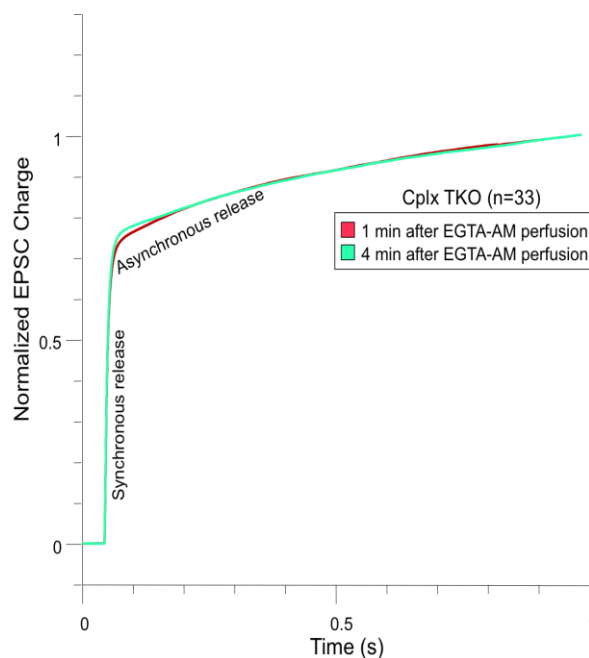


Figure 25.D.,E.

Synchronous and asynchronous neurotransmitter release under the effect of exogenously applied buffer EGTA-AM in autaptic hippocampal neurons of Cplx CTRL and Cplx TKO mice. Integral of normalized EPSC charge versus time shows a fast rising component indicating synchronous release of vesicles and a slowly rising

component for the asynchronously released vesicles. **(D)** Cplx CTRL - EPSC charge integral 1 min after application of EGTA-AM (in blue) and 4 min after application of EGTA-AM (in green) - the synchronous component of release is increased and asynchronous release is decreased in CTRL neurons **(E)** Cplx TKO - EPSC charge integral 1 min after application of EGTA-AM (in red) and 4 min after application of EGTA-AM (in green) - no changes of the synchronous and asynchronous component is apparent in TKO neurons. Numbers of neurons analyzed are indicated.

3.2.1.4. Lentiviral expression of wild-type Complexins can restore efficient transmitter release in Cplx-TKO neurons

The Cplx-DKO mutant neurons derived from the Cplx-DKO mice (lacking Cplx1 and Cplx2) exhibited similar deficits in synaptic parameters as the Cplx-TKO mice (Reim et al., 2001; Xue et al., 2008). Over-expression of three Complexin paralogs - Cplx1, Cplx3 and Cplx4 - via Semliki-Forest-virus (SFV) transduction in Cplx-DKO mutant neurons could efficiently restore the EPSC amplitudes and the vesicular release probability (Reim et al., 2005).

I decided to conduct a detailed comparative analysis of the functions of all mammalian Complexins, which had not been done before. For this purpose, I used the lentiviral delivery system for expression of the different Cplx paralogs. This approach circumvents the notorious toxicity and possible overexpression artifacts of the SFV system that was used in the previous studies. All the lentiviral expression constructs used in the present study were kindly prepared by Dr. Kerstin Reim. The pFUGW-lentiviral vector was used for expressing the Cplx genes under the control of a Synapsin promoter for neuronal expression, and the vector contained a reporter gene (EGFP) insert expressed under the control of a ubiquitin promoter. Unlike the SFV-mediated over-expression, lentiviral transduction of neurons causes integration of the gene of interest into the host genome and typically results in protein expression at levels comparable to the endogenous proteins. In the present study, the autaptic Cplx TKO neurons were infected with the lentiviruses and were allowed to grow up to 10 days *in-vitro* (DIV) for gene integration and protein expression. The neurons were used for whole-cell patch clamp recordings after visible expression of EGFP between DIV 10 and 14.

I found that all wild type Complexins were able to efficiently rescue the synchronous Ca²⁺-triggered EPSCs in the Cplx TKO neurons. Expression of all Cplx-WTs in the Cplx TKO neurons resulted in more than a 65% increase of the EPSC peak amplitudes as compared to TKO neurons expressing only EGFP (Fig.26.A.). Analysis of the kinetics of EPSCs substantiated

further that the synchronous component of release was higher in the presence of the Cplx-WT isoforms, whereas the asynchronous component remained unaltered for all conditions (Fig.26.B.).

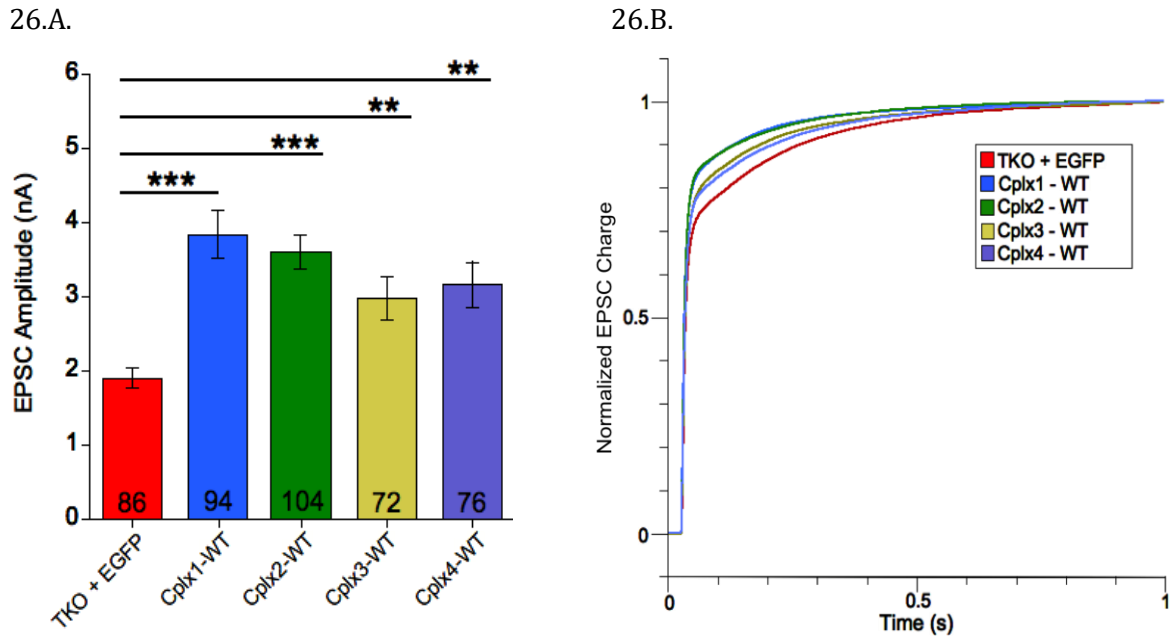
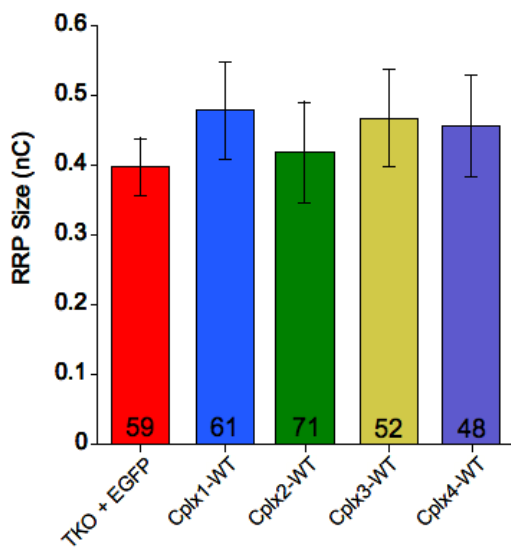


Figure 26.A.,B. Evoked EPSC amplitudes and synchronous release in autaptic hippocampal Cplx TKO neurons expressing Cplx wild type proteins (A) Mean excitatory post-synaptic current (EPSC) amplitudes. Peak EPSC amplitudes were completely rescued in the presence of all Complexin wild type paralogs, *** $p < 0.0001$, ** $p < 0.001$ compared with TKO neurons transduced with EGFP. Absolute values are included in Table 15. Error bars indicate standard error of mean. Numbers of neurons analyzed are indicated on bars. Students t-test was used to test statistical significance. **(B)** Synchronous and asynchronous release depicted as integral of EPSC charge - The synchronous component of EPSCs is enhanced in Cplx TKO neurons expressing the various wild type Complexins.

The size of the primed vesicle pool ready for release was similar in all cases (Fig.26.C.). The vesicular release probability at synapses was diminished in the absence of Complexins but significantly increased in neurons expressing Cplx1, Cplx2, Cplx3 and Cplx4 (Fig.26.D.). Cplx-TKO neurons expressing the wild-type Complexins exhibited faster depression of EPSCs under high frequency stimulations, indicative of higher initial vesicular release probability in the presence of Complexins (Fig.26.E. and 26.F.). A small increase in the frequency of miniature EPSCs was observable in Cplx-TKO neurons expressing Cplx1, but not in the presence of the other Cplx paralogs (Fig.26.G.), whereas the amplitudes of the miniature EPSCs were unaltered in the presence of all the Cplx isoforms (Fig.26.H.).

26.C.



26.D.

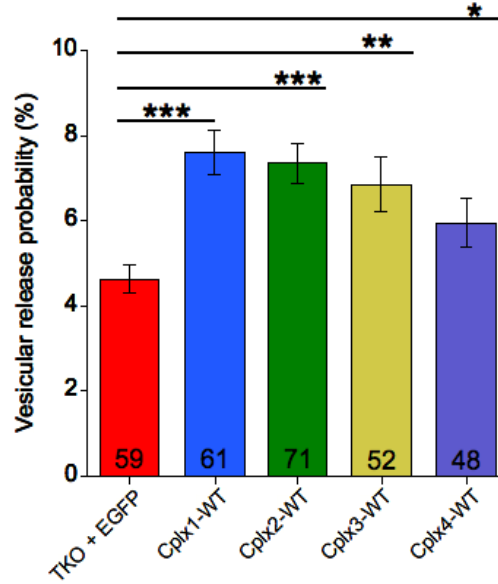
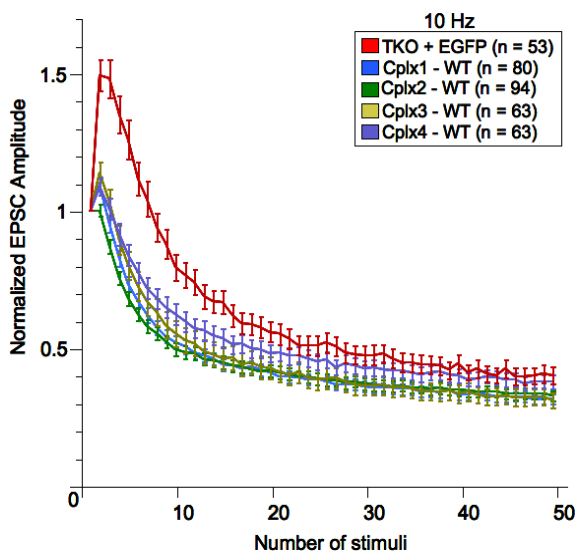


Figure 26.C.,D.

RRP size and vesicular release probability in autaptic hippocampal Cplx TKO neurons expressing Cplx wild type proteins (C) Mean RRP size was measured as charge elicited due to release of the primed vesicle pool, induced by application of 0.5 M sucrose solution - RRP size was unaltered in TKO neurons irrespective of the construct expressed **(D)** Mean vesicular release probability (Pvr) was estimated as the ratio of charge of the evoked EPSC to the charge of the RRP - Pvr was enhanced in the presence of all wild type Complexins, *** $p < 0.0001$, ** $p < 0.001$, * $p < 0.05$ compared with TKO neurons expressing EGFP. Absolute values are included in Table 15. Error bars indicate standard error of mean. Numbers of neurons analyzed are indicated on bars. Students t-test was used to test statistical significance.

26.E.



26.F.

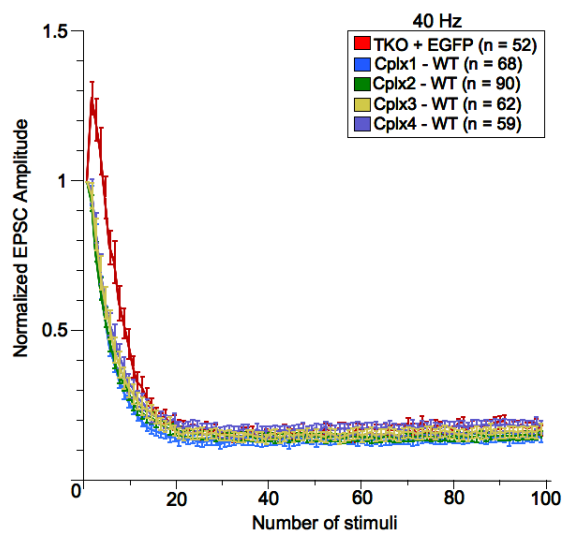
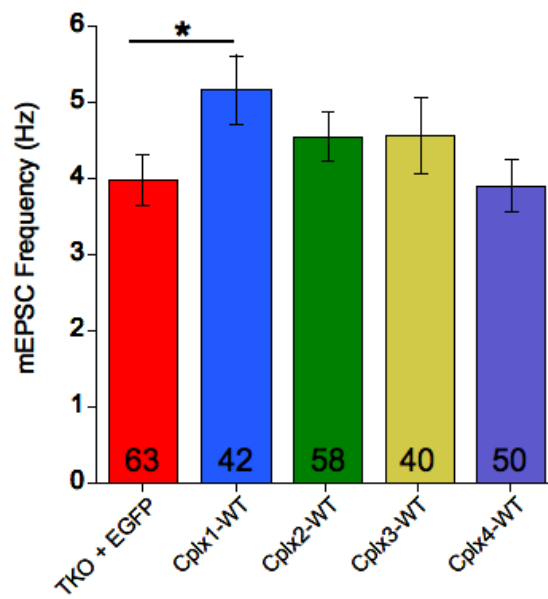


Figure 26.E.,F.

Short-term plasticity in autaptic hippocampal Cplx TKO neurons expressing Cplx wild type proteins (E) and (F) Amplitudes of the synaptic responses evoked by a train of stimulation at 10 Hz and 40 Hz (for EPSCs) were normalized to the amplitude of the first response and plotted against the stimulus number. Data are expressed as mean \pm S.E.M. Numbers of neurons analyzed are indicated. EPSC depression was observed in TKO neurons expressing Cplx wild type paralogs implying high initial vesicular release probability, while high initial facilitation of EPSC amplitudes was observed in TKO neurons expressing EGFP indicating lower initial release probability.

26.G.



26.H.

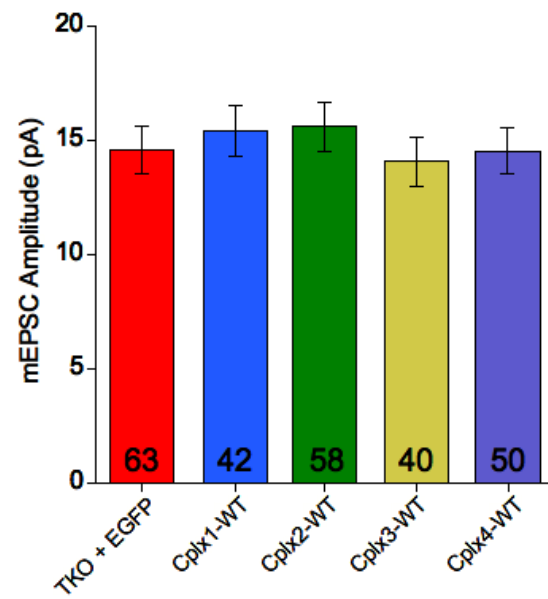


Figure 26.G.,H.

Spontaneous neurotransmitter release (mEPSC) in autaptic hippocampal Cplx TKO neurons expressing EGFP and Cplx wild type proteins. 300 nM Tetrodotoxin was exogenously applied to neurons in order to block Na⁺-channel driven action potentials while measuring miniature excitatory post-synaptic currents. **(G)** Mean mEPSC frequency - a small but significant increase of mEPSC events was observed only in the Cplx TKO neurons expressing Cplx1-WT protein, *p<0.05 compared with Cplx TKO **(H)** Mean mEPSC amplitudes of Cplx TKO neurons expressing Cplx wild type paralogs - no significant differences were observed. Absolute values are included in Table 15. Error bars indicate standard error of mean. Numbers of neurons analyzed are indicated on bars. Students t-test was used to test statistical significance.

Table 15. Synaptic parameters measured from excitatory Cplx TKO neurons expressing EGFP and Cplx1, Cplx2, Cplx3, Cplx4 WT lentiviral proteins.

Parameter (Mean \pm S.E.M.)	Cplx TKO (+)				
	EGFP	Cplx1-WT	Cplx2-WT	Cplx3-WT	Cplx4-WT
EPSC Amplitude (nA)	1.90 \pm 0.136 (n=86)	3.84 \pm 0.322 (n=94)	3.59 \pm 0.23 (n=104)	2.97 \pm 0.285 (n=72)	3.17 \pm 0.30 (n=76)
RRP Size (nC)	0.397 \pm 0.041 (n=59)	0.478 \pm 0.07 (n=61)	0.418 \pm 0.07 (n=71)	0.467 \pm 0.07 (n=52)	0.456 \pm 0.07 (n=48)
Pvr (%)	4.64 \pm 0.326 (n=59)	7.6 \pm 0.51 (n=61)	7.34 \pm 0.46 (n=71)	6.84 \pm 0.644 (n=52)	5.95 \pm 0.577 (n=48)
mEPSC Frequency (Hz)	3.99 \pm 0.33 (n=63)	5.16 \pm 0.45 (n=42)	4.55 \pm 0.32 (n=58)	4.56 \pm 0.49 (n=40)	3.89 \pm 0.34 (n=50)
mEPSC Amplitude (pA)	14.6 \pm 1.03 (n=63)	15.4 \pm 1.12 (n=42)	15.6 \pm 1.07 (n=58)	14.08 \pm 1.08 (n=40)	14.54 \pm 0.99 (n=50)

S.E.M. is standard error of mean

n is number of cells pooled from multiple cultures

3.2.2. Mutation of the SNARE-binding domain and Farnesylation domain in Complexins impedes glutamatergic synaptic transmission.

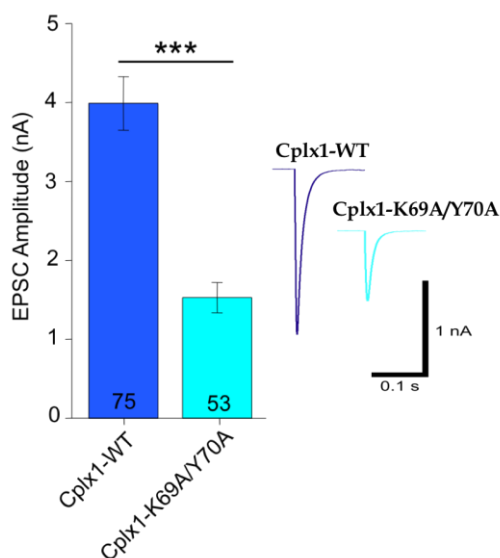
The Complexin domain structure is intriguing with different parts of the protein accounting for different functions. In this study, I have investigated the central α -helical SNARE binding domain and the farnesylation domains of the various Complexins. Multiple studies have examined deletions or point mutations on these domains to comprehend their role in the Ca²⁺-triggered and constitutive transmitter release processes. The central α -helical SNARE binding domain from amino acid residues 48-70 is highly conserved across the various Complexin paralogs and among different species (Reim et al., 2005; Xue et al., 2007). Point mutation of an Arginine residue at position 63, Lysine residue at position 69 and Tyrosine residue at position 70 on Cplx1 were previously shown to completely abolish SNARE complex binding in co-sedimentation assays (Xue et al., 2007). Of particular interest was the double point mutation of lysine and tyrosine residues on Cplx1, which not only abolished Cplx1 binding to the SNARE complex but also failed to rescue synaptic transmission upon SFV-mediated over-expression in Cplx-DKO neurons. Although the lysine-tyrosine amino acid duo is conserved across the Complexin homologs in many species, this double point mutation was previously tested only on Cplx1. Therefore, I assessed the effect of double point mutations of lysine (K) to alanine (A) and tyrosine (Y) to alanine (A) in the SNARE-binding central α -

helical on all four Complexins: Cplx1-K69A/Y70A, Cplx2-K69A/Y70A, Cplx3-K79A/Y80A, and Cplx4-K80A/Y81A. Also, one cysteine (C) to serine (S) point mutation was introduced in the farnesylation 'CAAX' motif of both Cplx3 (C155S) and Cplx4 (C157S) to block farnesylation. In order to systematically compare the physiological effects of all the Complexin mutants at the Cplx-TKO synapses, I used the respective Complexin wild type and mutant lentiviruses to infect Cplx-TKO neurons and perform whole-cell patch clamp recordings on the neurons expressing the proteins.

3.2.2.1. Rescue efficacies of Complexin-1 wild type (Cplx1-WT) and Complexin-1 SNARE binding domain mutant (Cplx1-K69A/Y70A) proteins in Cplx TKO neurons.

SFV-mediated over-expression of the SNARE binding domain mutant of Cplx1 was unable to rescue the deficits in synaptic transmission in Cplx-DKO neurons, while similar over-expression of Cplx1-WT did rescue the deficits (Xue et al., 2007). Given the possible problems associated with SFV mediated overexpression, I set out to assess the role of the α -helical SNARE binding domain of the different Complexins, using lentiviral delivery. I first tested the efficacies of Cplx1-WT and Cplx1-K69A/Y70A proteins in rescue of the Cplx-TKO phenotype. In this experiment, I found that the peak amplitude of EPSC elicited by the expression of Cplx1-WT in the Cplx-TKO neurons was significantly higher when compared with the EPSCs elicited after expression of Cplx1-K69A/Y70A (Fig.27.A.). This was further corroborated by a clear augmentation in the synchronous component of release in the neurons expressing Cplx1-WT measured by the integral of the EPSC charge (Fig.27.B.).

27.A.



27.B.

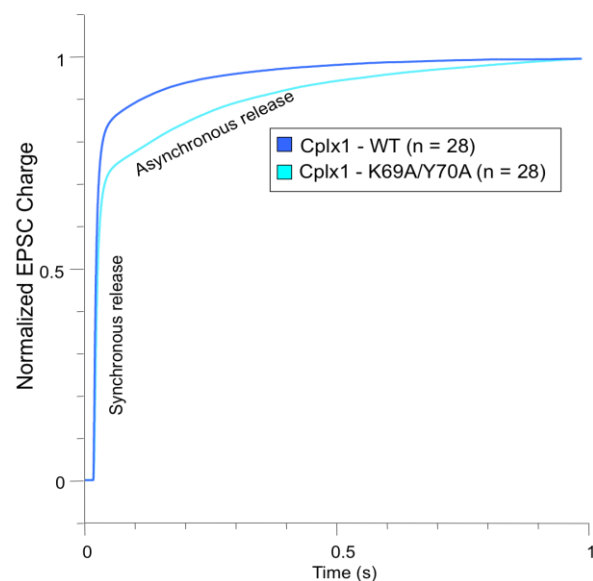
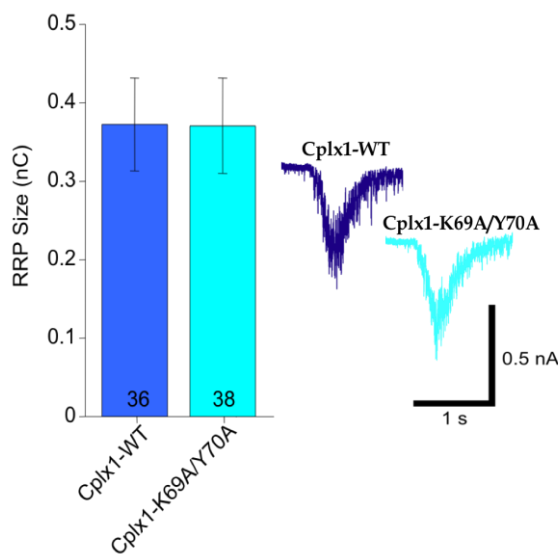


Figure 27.A.,B.

Evoked EPSC amplitudes and synchronous release in autaptic hippocampal Cplx TKO neurons expressing Cplx1-WT and Cplx1-K69A/Y70A proteins. (A) Mean excitatory post-synaptic current (EPSC) amplitudes. Peak EPSC amplitude in Cplx TKO neurons expressing Cplx1-K69A/Y70A was dramatically reduced compared with neurons expressing Cplx1-WT, *** $p < 0.0001$ between the neurons of the groups compared. Absolute values are included in Table 16. Representative traces are included. Error bars indicate standard error of mean. Numbers of neurons analyzed are indicated on bars. Students t-test was used to test statistical significance. **(B)** Synchronous and asynchronous release depicted as integral of EPSC charge - Synchronous component of EPSC is decreased in Cplx TKO neurons expressing Cplx1-K69A/Y70A compared with Cplx1-WT; the asynchronous component was unaltered. Numbers of neurons analyzed are indicated.

As the readily releasable vesicle pool size was nearly equal in neurons expressing the Cplx1 WT and Cplx1 SNARE binding mutant (Fig.27.C.), the vesicular release probability in the Cplx1-WT expressing neurons was 90% higher when compared to the neurons expressing Cplx1-K69A/Y70A, implying that the SNARE binding domain mutant of Cplx1 was unable to alleviate the deficits in the release of vesicles at Cplx-TKO synapses (Fig.27.D.). Similarly, the short-term plasticity at synapses expressing Cplx1-WT showed a marked depression of the EPSC amplitudes while those expressing the SNARE mutant showed a dramatic facilitation of initial EPSCs indicative of high and low initial release probabilities, respectively (Fig.27.E. and 27.F.). The miniature EPSC frequency and amplitude were similar in neurons expressing Cplx1-WT and Cplx1-K69A/Y70A (Fig.27.G. and 27.H.).

27.C.



27.D.

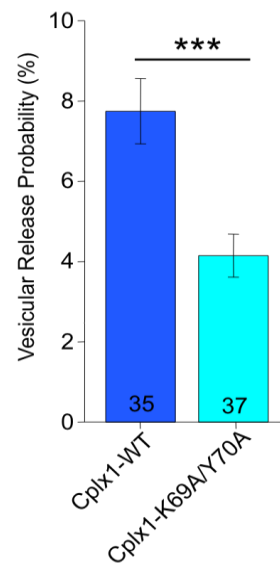
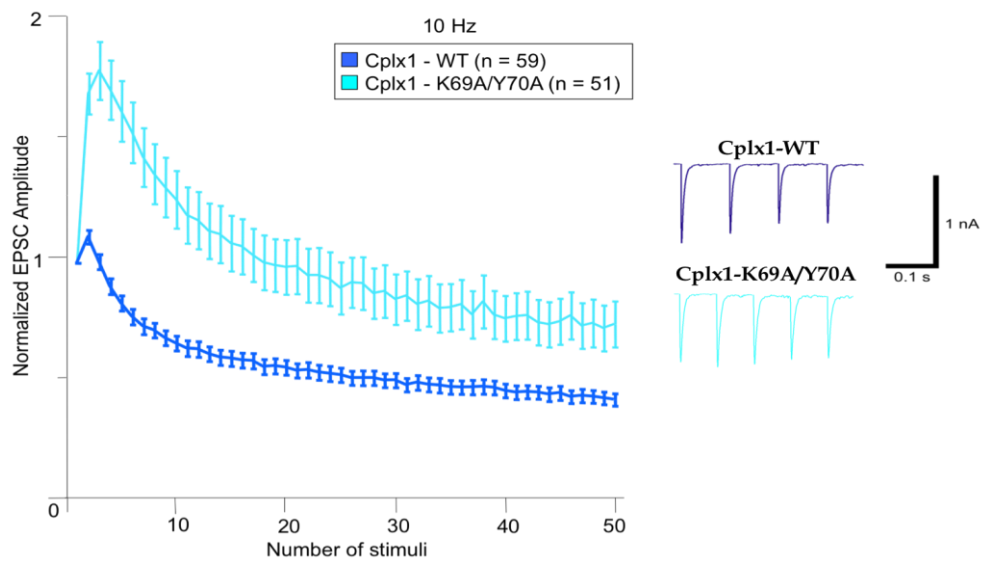


Figure 27.C.,D.

RRP size and vesicular release probability in autaptic hippocampal Cplx TKO neurons expressing Cplx1-WT and Cplx1-K69A/Y70A proteins. (C) Mean RRP size was measured as charge elicited due to release of the primed vesicle pool, induced by application of 0.5 M sucrose solution - RRP size was unaltered in TKO neurons irrespective of the construct expressed, representative traces are included. **(D)** Mean vesicular release probability (Pvr) estimated as the ratio of charge of the evoked EPSC to the charge of the RRP - Pvr was reduced by 50% in the neurons expressing Cplx1-K69A/Y70A compared with Cplx1-WT expressing neurons, *** $p < 0.0001$ between the neurons of the groups compared. Absolute values are included in Table 16. Error bars indicate standard error of mean. Numbers of neurons analyzed are indicated on bars. Students t-test was used to assess statistical significance.

27.E.



27.F.

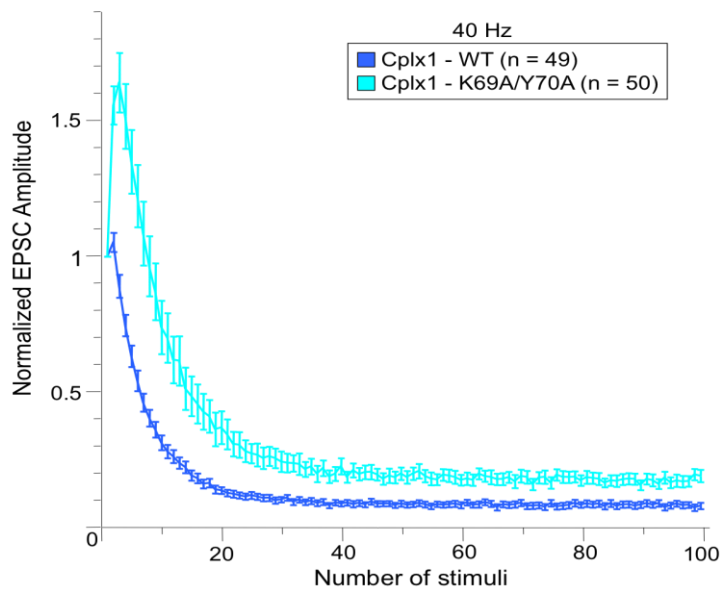


Figure 27.E.,F.

Short-term plasticity in autaptic hippocampal Cplx TKO neurons expressing Cplx1-WT and Cplx1-K69A/Y70A proteins. (E) and (F) EPSC amplitudes of the synaptic responses evoked by a train of stimulation at 10 Hz and 40 Hz (for EPSCs) were normalized to the amplitude of the first response and plotted against the stimulus number. Representative traces of EPSCs at the beginning of the 10 Hz stimulation train are shown. Data are expressed as mean \pm S.E.M. Numbers of neurons analyzed are indicated. Depression of EPSCs was observed in TKO neurons expressing Cplx1-WT, and initial facilitation of EPSCs was observed in TKO neurons expressing Cplx1-K69A/Y70A, indicating high and low initial release probabilities, respectively.

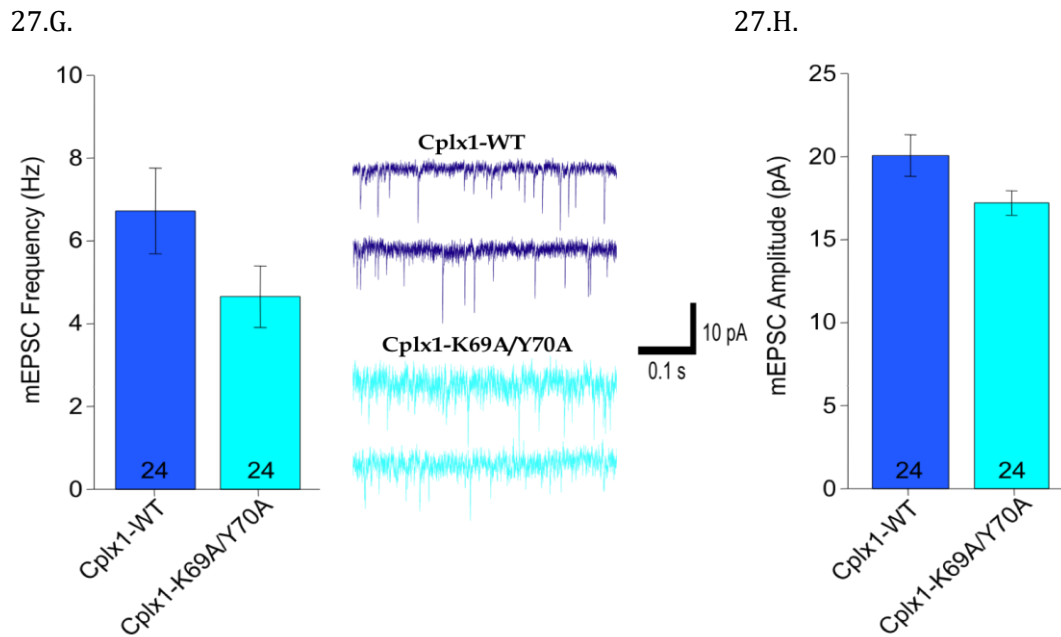


Figure 27.G.,H.

Spontaneous neurotransmitter release (mEPSC) in autaptic hippocampal Cplx TKO neurons expressing Cplx1-WT and Cplx1-K69A/Y70A proteins. 300 nM Tetrodotoxin was exogenously applied to neurons in order to block Na⁺-channel driven action potentials while measuring miniature excitatory post-synaptic currents. Representative traces are included (G) Mean mEPSC frequency, and (H) Mean mEPSC amplitudes in Cplx TKO neurons expressing Cplx1-WT and Cplx1-K69A/Y70A - no significant differences were observed. Absolute values are included in Table 16. Error bars indicate standard error of mean. Numbers of neurons analyzed are indicated on bars. Students t-test was used to test statistical significance.

Table 16. Synaptic parameters measured from excitatory Cplx TKO neurons expressing Cplx1-WT and Cplx1-K69A/Y70A lentiviral proteins.

Parameter (Mean \pm S.E.M.)	Cplx TKO (+)	
	Cplx1-WT	Cplx1-K69A/Y70A
EPSC Amplitude (nA)	3.99 \pm 0.339 (n=75)	1.53 \pm 0.192 (n=53)
RRP Size (nC)	0.372 \pm 0.059 (n=36)	0.373 \pm 0.060 (n=38)
Pvr (%)	7.747 \pm 0.813 (n=35)	4.148 \pm 0.537 (n=37)
mEPSC Frequency (Hz)	6.72 \pm 1.03 (n=24)	4.65 \pm 0.74 (n=24)
mEPSC Amplitude (pA)	20.075 \pm 1.25 (n=24)	17.214 \pm 0.74 (n=24)

S.E.M. is standard error of mean n is number of cells pooled from multiple cultures

3.2.2.2. Rescue efficacies of Complexin-2 wild type (Cplx2-WT) and Complexin-2 SNARE binding domain mutant (Cplx2-K69A/Y70A) proteins in Cplx TKO neurons.

Complexin-2 is the other major Complexin paralog present in the brain. Loss of Cplx2 has been shown to impair long-term potentiation of synapses in the CA1 stratum radiatum and CA3 mossy-fibre terminals of the hippocampus with no effect on short-term plasticity (Takahashi et al., 1999). In adrenal chromaffin cells, large dense-core vesicle (LDCV) secretion triggered by UV-flash photolysis of caged-Ca²⁺ was dramatically reduced in the absence of Cplx2, implying that Cplx2 is essential for secretion in chromaffin cells (Cai et al., 2008). In the same study, it was also found that mutation of the lysine (K69) and tyrosine (Y70) residues on the SNARE-binding domain of Cplx2 blocked Cplx2 activity, indicating a key role of Cplx2-SNARE binding in LDCV exocytosis.

I expressed the Cplx2-WT and its SNARE binding domain mutant Cplx2-K69A/Y70A in Cplx TKO neurons to determine the effect on synaptic release. In presence of Cplx2-WT, the Ca²⁺-evoked EPSCs in Cplx-TKO neurons are significantly higher compared to neurons expressing Cplx2-K69A/Y70A (Fig.28.A.). Correspondingly, the synchronous component of EPSCs was higher in presence of Cplx2-WT while the asynchronous component of release was similar in presence of both Cplx2 variants (Fig.28.B.). The RRP size was unchanged between neurons expressing wild type Cplx2 and SNARE domain mutant Cplx2; however, the vesicular release probability was significantly higher in the former (Fig.28.C. and 28.D.). Consistent with the release probability features, neurons expressing Cplx2-WT exhibited fast depression of EPSCs when stimulated at high frequencies, but those expressing the Cplx2-K69A/Y70A exhibited

an initial facilitation (Fig.28.E. and 28.F.). In the presence of Cplx2-WT and the Cplx2-K69A/Y70A, the frequency and the average amplitude of miniature EPSCs were at comparable levels (Fig.28.G. and 28.H.).

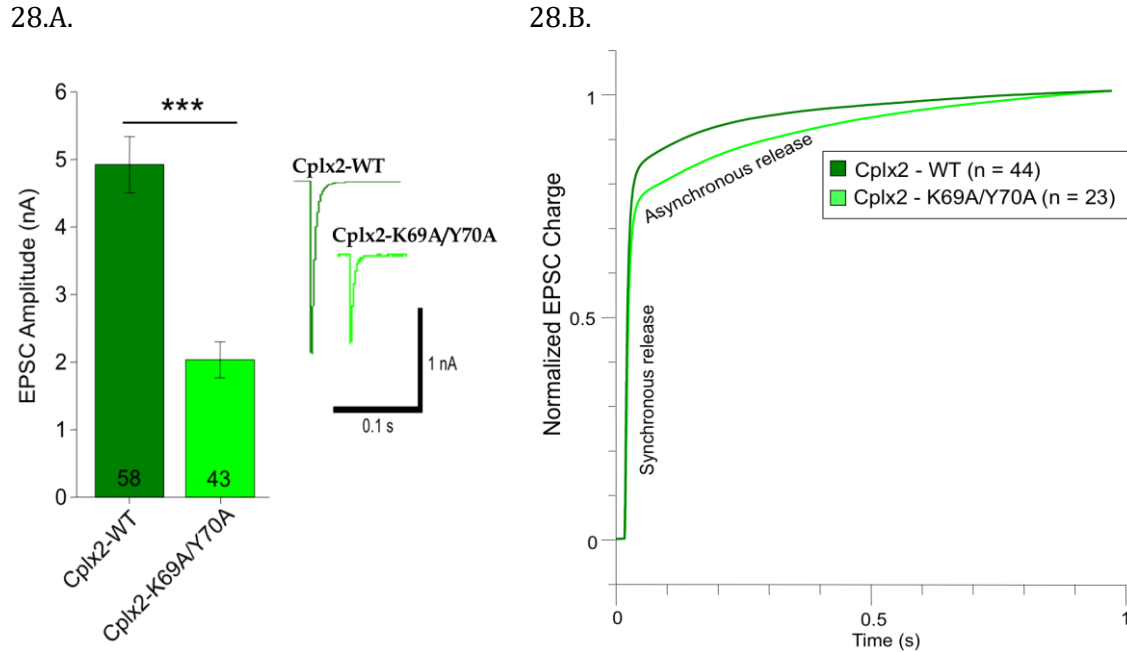
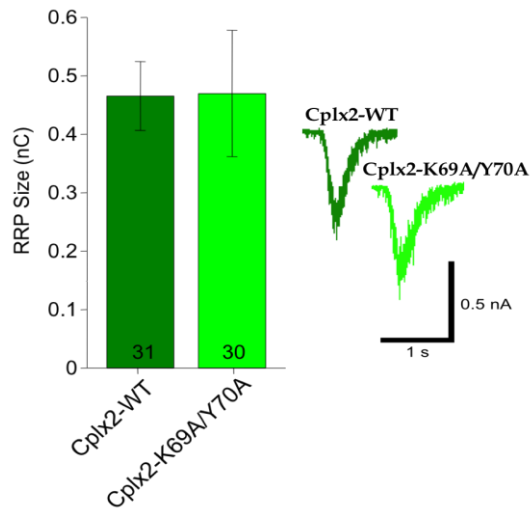


Figure 28.A.,B.

Evoked EPSC amplitudes and synchronous release in autaptic hippocampal Cplx TKO neurons expressing Cplx1-WT and Cplx1-K69A/Y70A proteins. (A) Mean excitatory post-synaptic current (EPSC) amplitudes. Peak EPSC amplitude in Cplx TKO neurons expressing Cplx2-K69A/Y70A was dramatically reduced compared with neurons expressing Cplx2-WT, *** $p < 0.0001$ between the neurons of the groups compared. Absolute values are included in Table 17. Representative traces are included. Error bars indicate standard error of mean (S.E.M.). Numbers of neurons analyzed are indicated on bars. Students t-test was used to test statistical significance. **(B)** Synchronous and asynchronous release depicted as Integral of EPSC charge – The synchronous component of EPSC is lower in Cplx TKO neurons expressing the Cplx2-K69A/Y70A compared with Cplx2-WT; the asynchronous component was unaltered. Numbers of neurons analyzed are indicated.

28.C.



28.D.

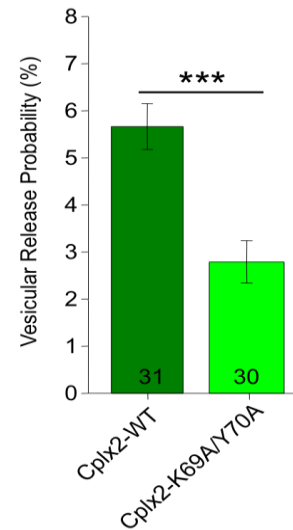
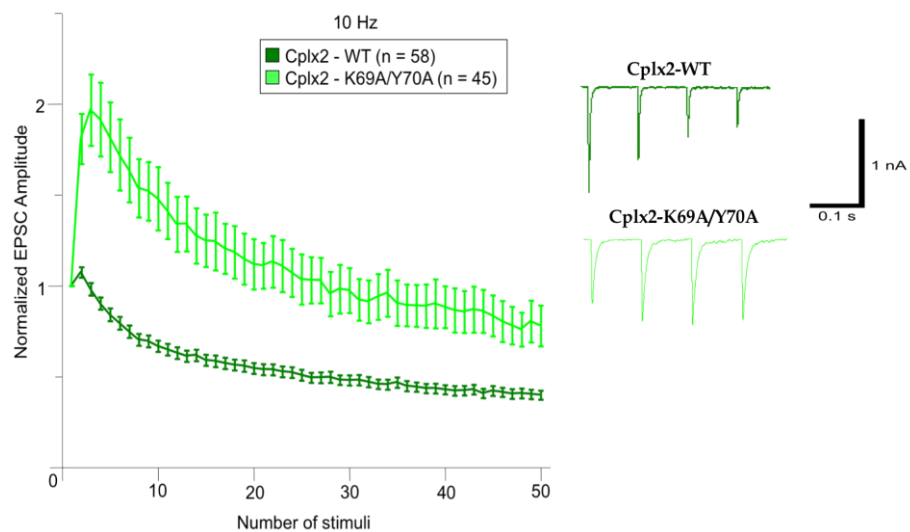


Figure 28.C.,D.

RRP size and vesicular release probability in autaptic hippocampal Cplx TKO neurons expressing Cplx2-WT and Cplx2-K69A/Y70A proteins (C) Mean RRP size measured as charge elicited due to release of the primed vesicle pool, induced by application of 0.5 M sucrose solution – RRP size was unaltered in neurons irrespective of the construct expressed; representative traces are included. **(D)** Mean vesicular release probability (Pvr) estimated as the ratio of charge of the evoked EPSC to the charge of the RRP - Pvr was reduced by 50% in the neurons expressing Cplx2-K69A/Y70A compared with Cplx2-WT expressing neurons, *** $p < 0.0001$ between the neurons of the groups compared. Absolute values are included in Table 17. Error bars indicate standard error of mean (S.E.M.). Numbers of neurons analyzed are indicated on bars. Students t-test was used to assess statistical significance.

28.E.



28.F.

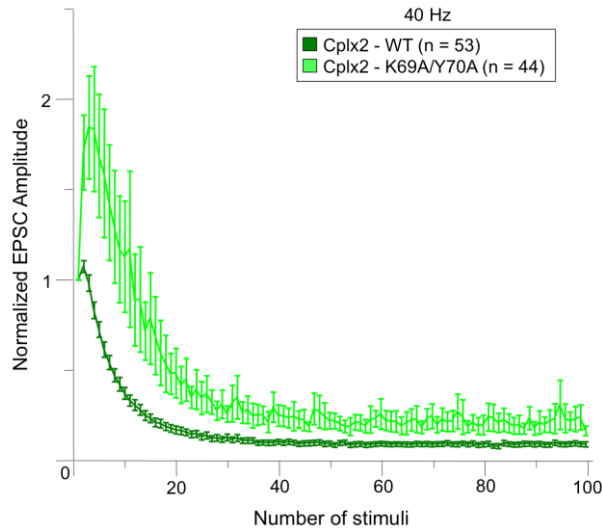
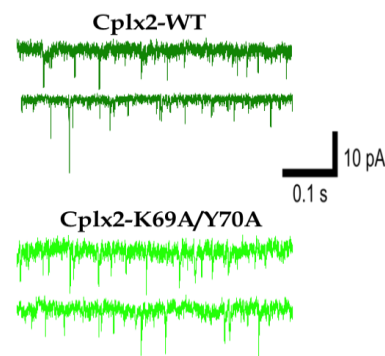
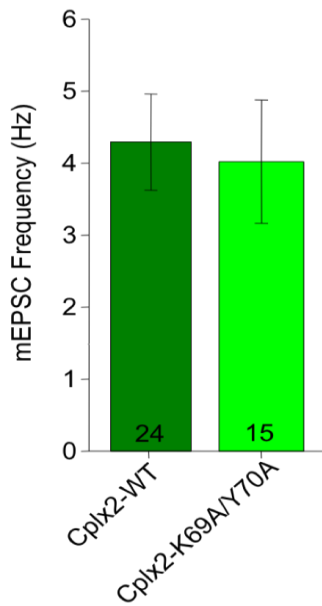


Figure 28.E.,F.

Short-term plasticity in autaptic hippocampal Cplx TKO neurons expressing Cplx2-WT and Cplx2-K69A/Y70A proteins. (E) and (F) Amplitudes of the synaptic responses evoked by a train of stimulation at 10 Hz and 40 Hz (for EPSCs) were normalized to the amplitude of the first response and plotted against the stimulus number. Representative traces of EPSCs at the beginning of the 10 Hz stimulation train are shown. Data are expressed as mean \pm S.E.M. Numbers of neurons analyzed are indicated. Depression of EPSCs was observed in TKO neurons expressing Cplx2-WT, and initial facilitation of EPSCs was observed in TKO neurons expressing Cplx2-K69A/Y70A indicating high and low initial release probabilities, respectively.

28.G.



28.H.

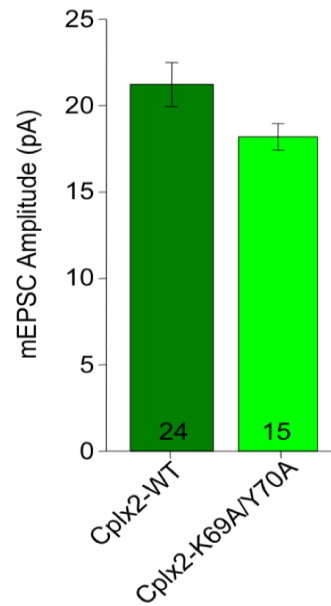


Figure 28.G.,H. Spontaneous neurotransmitter release (mEPSC) in autaptic hippocampal Cplx TKO neurons expressing Cplx2-WT and Cplx2-K69A/Y70A proteins. 300 nM Tetrodotoxin was exogenously applied to neurons in order to block Na⁺-channel driven action potentials while measuring miniature excitatory post-synaptic currents. Representative traces are included **(G)** Mean mEPSC frequency, and **(H)** Mean mEPSC amplitudes in Cplx TKO neurons expressing Cplx2-WT and Cplx2-K69A/Y70A - no significant differences were observed. Absolute values are included in Table 17. Error bars indicate standard error of mean. Numbers of neurons analyzed are indicated on bars. Students t-test was used to test statistical significance.

Table 17. Synaptic parameters measured from excitatory Cplx TKO neurons expressing Cplx2-WT and Cplx2-K69A/Y70A lentiviral proteins.

Parameter (Mean ± S.E.M.)	Cplx TKO (+)	
	Cplx2-WT	Cplx2-K69A/Y70A
EPSC Amplitude (nA)	4.924±0.416 (n=58)	2.036±0.267 (n=43)
RRP Size (nC)	0.465±0.058 (n=31)	0.469±0.108 (n=30)
Pvr (%)	5.66±0.49 (n=31)	2.79±0.452 (n=30)
mEPSC Frequency (Hz)	4.295±0.667 (n=24)	4.022±0.857 (n=15)
mEPSC Amplitude (pA)	21.225±1.278 (n=24)	18.193±0.773 (n=15)

S.E.M. is standard error of mean n is number of cells pooled from multiple cultures

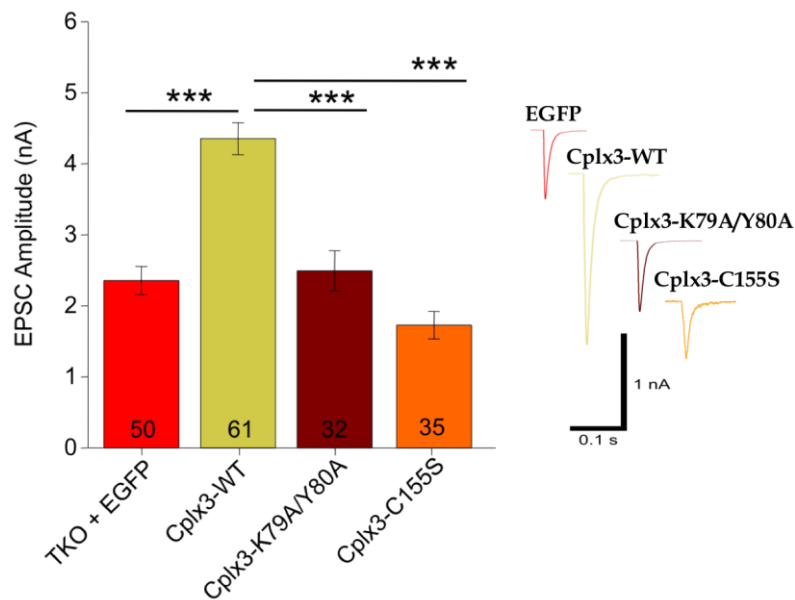
3.2.2.3. Rescue efficacies of Complexin-3 wild type (Cplx3-WT), Complexin-3 SNARE binding domain mutant (Cplx3-K79A/Y80A) and Complexin-3 Farnesylation domain mutant (Cplx3-C155S) proteins in Cplx TKO neurons.

Complexin-3 is prominently expressed in the retina; low Cplx3 expression is detectable in the cortex and hippocampus of murine brain (Reim et al., 2005), but not in cultured cortical or hippocampal neurons. Although hardly via biochemical methods, the possibility that Cplx3 may affect release at neuronal synapses could not be disregarded. The binding affinity of Cplx3 to the cognate SNARE complex is lower as compared to Cplx1 and Cplx2. However, the lysine and tyrosine residues essential for binding to the SNARE complex are conserved. Furthermore, Cplx3 contains a CAAX motif on the C-terminal end that is farnesylated (addition of a 15-carbon moiety to translated protein product) *in-vivo* and targets Cplx3 to membranes (Reim et al., 2005). Hence, I compared the rescue efficacies of the Cplx3-WT against its SNARE binding domain mutant (Cplx3-K79A/Y80A) and farnesylation domain

mutant (Cplx3-C155S) by lentiviral expression of the respective proteins in Cplx-TKO neurons. As a negative control, I also used Cplx-TKO neurons infected with an EGFP expressing lentivirus.

I found that lentiviral expression of Cplx3-WT in the Cplx-TKO neurons efficiently rescued the evoked EPSC amplitudes, vesicular release probability and short-term plasticity. However, expression of the Cplx3-K79A/Y80A and Cplx3-C155S did not rescue the transmitter release deficits in the Cplx-TKO neurons. Also, compared to Cplx3-WT, the evoked EPSCs in cells expressing Cplx3-K79A/Y80A and Cplx3-C155S was significantly lower (Fig.29.A. and 29.B.).

29.A.



29.B.

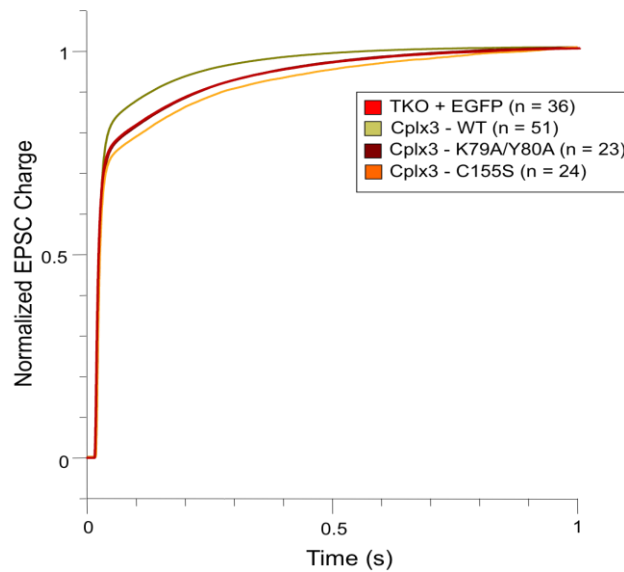
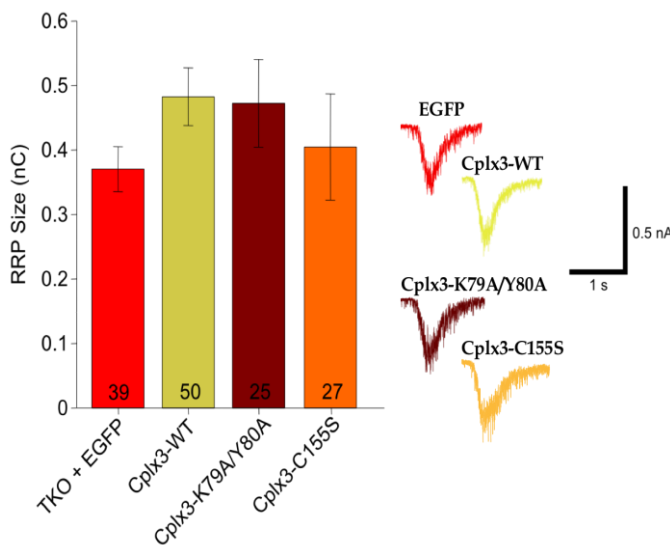


Figure 29.A,B.

Evoked EPSC amplitudes and synchronous release in autaptic hippocampal Cplx TKO neurons expressing EGFP, Cplx3-WT, Cplx3-K79A/Y80A and Cplx3-C155S proteins. (A) Mean excitatory post-synaptic current (EPSC) amplitudes. Peak EPSC amplitudes in Cplx TKO neurons expressing Cplx3-WT were significantly higher when compared with neurons expressing EGFP, Cplx3-K79A/Y80A and Cplx3-C155S. *** $p < 0.0001$ between the neurons of the groups in comparison. Absolute values are included in Table 18. Representative traces are included. Error bars indicate standard error of mean (S.E.M.). Numbers of neurons analyzed are indicated on bars. Students t-test used to test statistical significance. (B) Synchronous and asynchronous release depicted as integral of EPSC charge - The synchronous component of EPSCs was lower in Cplx TKO neurons expressing EGFP, Cplx3-K79A/Y80A and Cplx3-C155S compared with Cplx3-WT; the asynchronous component was unaltered. Numbers of neurons analyzed are indicated.

Likewise, the vesicular release probability of TKO neurons expressing Cplx3-K79A/Y80A and Cplx3-C155S was low compared to data from cells expressing Cplx3-WT although the RRP sizes were relatively similar (Fig.29.C. and 29.D.).

29.C.



29.D.

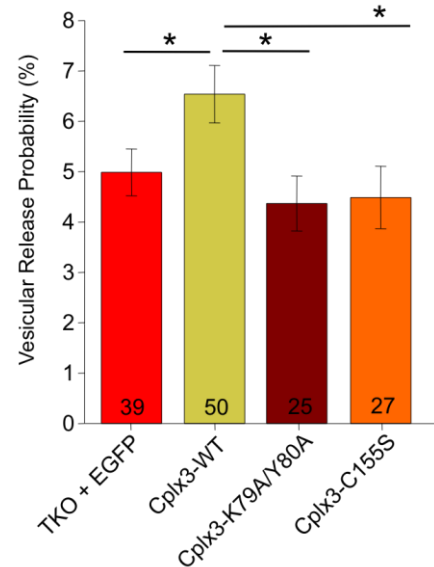


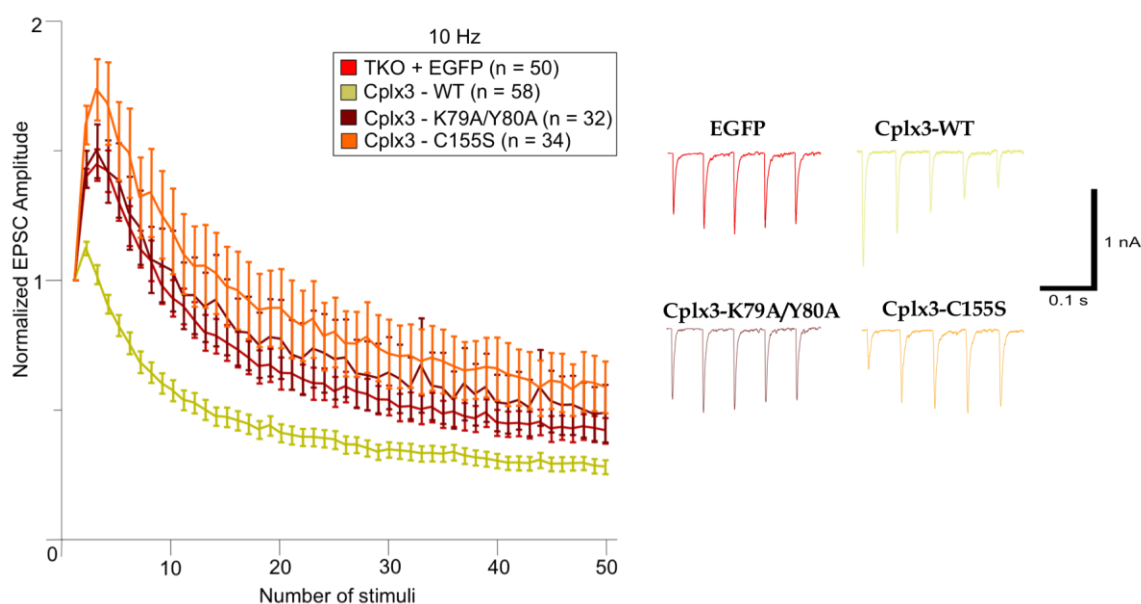
Figure 29.C.,D.

RRP size and vesicular release probability in autaptic hippocampal Cplx TKO neurons expressing EGFP, Cplx3-WT, Cplx3-K79A/Y80A and Cplx3-C155S proteins (C) Mean RRP size measured as charge elicited due to release of the primed vesicle pool, induced by application of 0.5 M sucrose solution - RRP size was unaltered in neurons irrespective of the construct expressed, representative traces are included. (D) Mean vesicular release probability (Pvr) estimated as the ratio of charge of the evoked EPSC to the charge of the RRP - Pvr was enhanced by 30% in the neurons expressing Cplx3-WT compared with neurons expressing EGFP, Cplx3-

K79A/Y80A and Cplx3-C155S, * $p < 0.05$ between the neurons of the groups compared. Absolute values are included in Table 18. Error bars indicate standard error of mean. Numbers of neurons analyzed are indicated on bars. Students t-test was used to assess statistical significance.

High frequency stimulations at 10 Hz and 40 Hz resulted in EPSC depression in neurons expressing Cplx3-WT and a marked initial facilitation in neurons expressing the Cplx3 SNARE binding domain mutant or farnesylation domain mutant (Fig.29.E. and 29.F.).

29.E.



29.F.

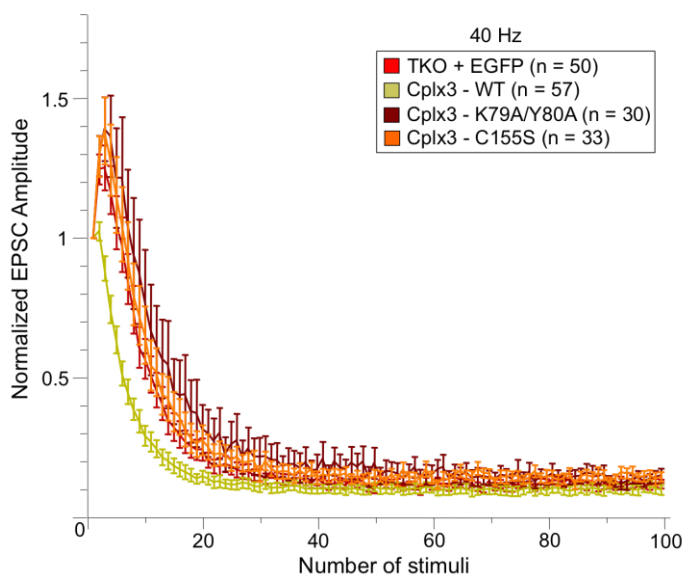


Figure 29.E.,F.

Short-term plasticity in autaptic hippocampal Cplx TKO neurons expressing EGFP, Cplx3-WT, Cplx3-K79A/Y80A and Cplx3-C155S

proteins. (E) and (F) Amplitudes of the synaptic responses evoked by a train of stimulation at 10 Hz and 40 Hz (for EPSCs) were normalized to the amplitude of the first response and plotted against the stimulus number. Representative traces of EPSCs at the beginning of the 10 Hz stimulation train are shown. Data are expressed as mean \pm S.E.M. Numbers of neurons analyzed are indicated. Depression of EPSCs was observed in TKO neurons expressing Cplx3-WT indicating high initial release probability, while initial facilitation of EPSCs was observed in TKO neurons expressing EGFP, Cplx3-K79A/Y80A and Cplx3-C155S indicating low initial release probabilities.

The miniature EPSCs frequency and amplitude elicited by the neurons expressing the different Cplx3 variants remained unaltered (Fig.29.G. and 29.H.).

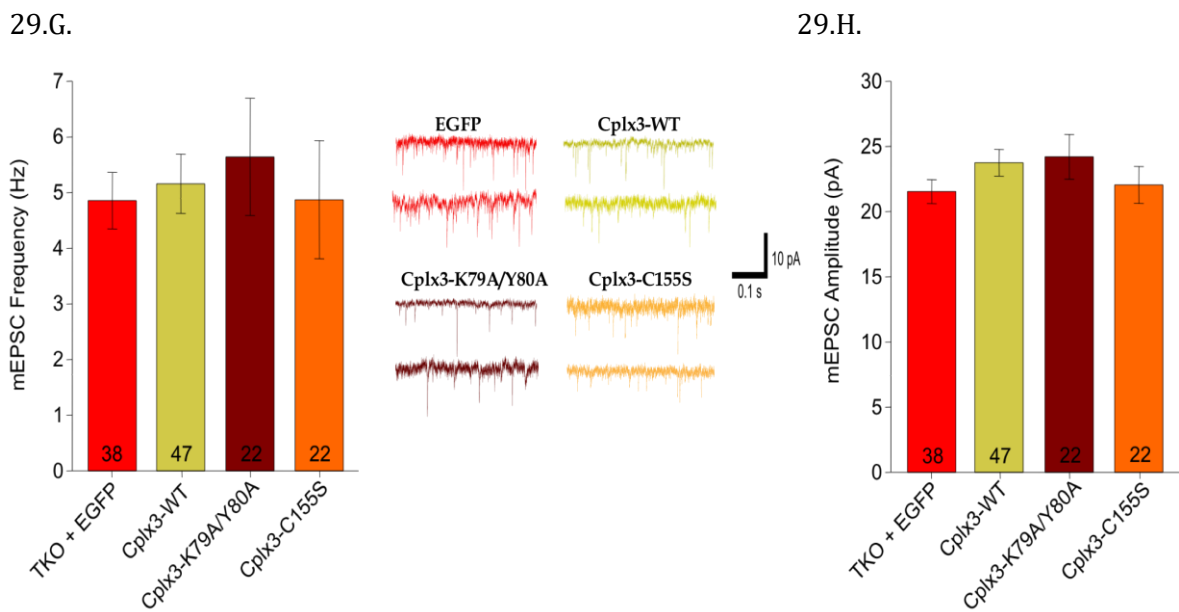


Figure 29.G.,H.

Spontaneous neurotransmitter release (mEPSC) in autaptic hippocampal Cplx TKO neurons expressing EGFP, Cplx3-WT, Cplx3-K79A/Y80A and Cplx3-C155S proteins. 300 nM Tetrodotoxin was exogenously applied to neurons in order to block Na⁺-channel driven action potentials while measuring miniature excitatory post-synaptic currents. Representative traces are included. No significant differences were found in **(G)** Mean mEPSC frequency, and **(H)** Mean mEPSC amplitudes in any of the groups compared. Absolute values are included in Table 18. Error bars indicate standard error of mean. Numbers of neurons analyzed are indicated on bars. Students t-test was used to test statistical significance.

Table 18. Synaptic parameters measured from excitatory Cplx TKO neurons expressing EGFP, Cplx3-WT, Cplx3-K79A/Y80A, and Cplx3-C155S lentiviral proteins.

Parameter (Mean \pm S.E.M.)	Cplx TKO (+)			
	EGFP	Cplx3-WT	Cplx3- K79A/Y80A	Cplx3-C155S
EPSC Amplitude (nA)	2.359 \pm 0.197 (n=50)	4.355 \pm 0.225 (n=61)	2.495 \pm 0.283 (n=32)	1.729 \pm 0.193 (n=35)
RRP Size (nC)	0.371 \pm 0.035 (n=39)	0.483 \pm 0.044 (n=50)	0.472 \pm 0.067 (n=25)	0.405 \pm 0.082 (n=27)
Pvr (%)	4.98 \pm 0.465 (n=39)	6.54 \pm 0.569 (n=50)	4.370 \pm 0.546 (n=25)	4.488 \pm 0.619 (n=27)
mEPSC Frequency (Hz)	4.856 \pm 0.507 (n=38)	5.158 \pm 0.529 (n=47)	5.641 \pm 1.054 (n=22)	4.872 \pm 1.06 (n=22)
mEPSC Amplitude (pA)	21.539 \pm 0.922 (n=38)	23.752 \pm 1.025 (n=47)	24.209 \pm 1.715 (n=22)	22.055 \pm 1.422 (n=22)

S.E.M. is standard error of mean

n is number of cells pooled from multiple cultures

3.2.2.4. Rescue efficacies of Complexin-4 wild type (Cplx4-WT), Complexin-4 SNARE binding domain mutant (Cplx4-K80A/Y81A) and Complexin-4 Farnesylation domain mutant (Cplx4-C157S) proteins in Cplx TKO neurons.

Complexin-4 is exclusively expressed in the mammalian retina. It is found at the rod photoreceptor (in the outer plexiform layer) and bipolar cell (in the inner plexiform layer) ribbon synapses (Reim et al., 2005). SFV-mediated over-expression of wild type Cplx4 in Cplx-DKO neurons could partly restore the amplitudes of evoked EPSCs and the vesicular release probability to levels comparable to that of Cplx1 SFV-mediated over-expression (Reim et al., 2005). Previously, it was shown that Cplx4 possesses a farnesylation motif similar to Cplx3, and SFV-mediated over-expression of non-farnesylated mutant Cplx4 could not rescue the deficits in EPSC amplitudes as well as the release probability in Cplx-DKO neurons (Reim et al., 2005). Although the interaction of Cplx4 with the native SNARE complex in the neurons is not detectable (Appendix 6.2.), I studied the functional effects of the lysine-tyrosine double point mutation in the conserved central α -helical domain (Cplx4-

K80A/Y81A) of Cplx4 and I also examined the effect of the farnesylation domain of Cplx4 (Cplx4-C157S) in regulating transmitter release.

I found that the evoked EPSC amplitudes in the Cplx-TKO neurons expressing Cplx4-WT were significantly higher compared to the EPSCs evoked in Cplx-TKO neurons expressing EGFP, Cplx4-K80A/Y81A and Cplx4-C157S, respectively (Fig.30.A.). In congruence, the synchronous component of EPSCs was higher in the neurons expressing Cplx4-WT (Fig.30.B.).

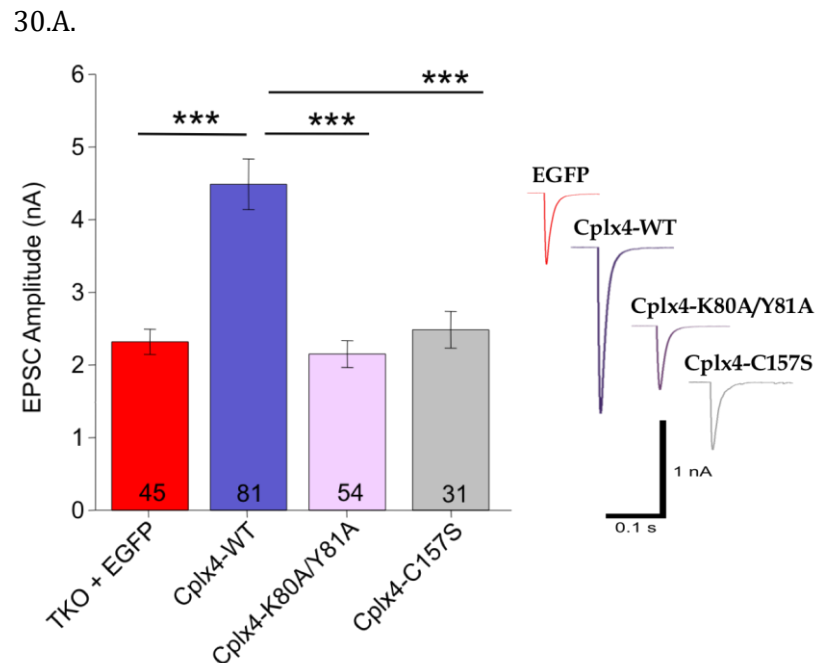


Figure 30.A.

Evoked EPSC amplitudes in autaptic hippocampal Cplx TKO neurons expressing EGFP, Cplx4-WT, Cplx4-K80A/Y81A and Cplx4-C157S proteins. Mean excitatory post-synaptic current (EPSC) amplitudes. Representative traces are included. Peak EPSC amplitude in Cplx TKO neurons expressing Cplx4-WT was significantly higher when compared with neurons expressing EGFP, Cplx4-K80A/Y81A and Cplx4-C157S. *** $p < 0.0001$ between the neurons of the groups in comparison. Absolute values are included in Table 19. Error bars indicate standard error of mean. Numbers of neurons analyzed are indicated on bars. Students t-test was used to test statistical significance.

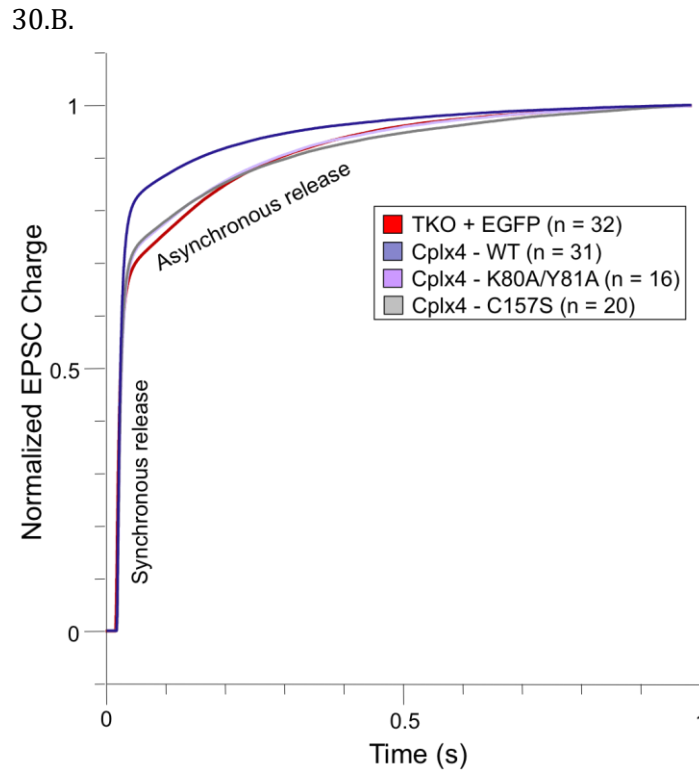
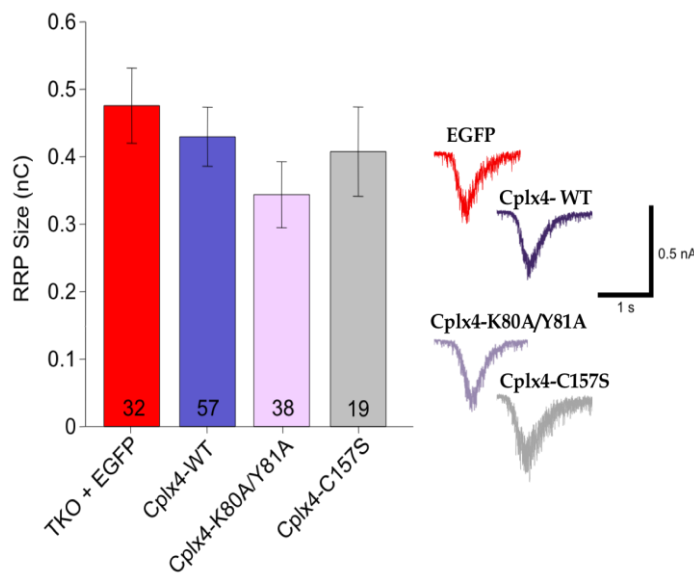


Figure 30.B. Synchronous release in autaptic hippocampal Cplx TKO neurons expressing EGFP, Cplx4-WT, Cplx4-K80A/Y81A and Cplx4-C157S proteins. Synchronous and asynchronous release depicted as integral of EPSC charge – The synchronous component of EPSC was lower in Cplx TKO neurons expressing EGFP, Cplx4-K80A/Y81A and Cplx4-C157S compared with Cplx4-WT; the asynchronous component was unaltered. Numbers of neurons analyzed are indicated.

The RRP size was not significantly different in the neurons irrespective of the constructs expressed (Fig.30.C.). However, the vesicular release probability was significantly higher in TKO neurons expressing Cplx4-WT, which also exhibited faster EPSC depression at high-frequency stimulation. To the contrary, the vesicular release probability in neurons expressing Cplx4-K80A/Y81A or Cplx4-C157S was nearly the same as in TKO neurons expressing EGFP. Also, an initial facilitation under high frequency stimulation implied the absence of rescue efficacy of the mutants (Fig.30.D., 30.E. and 30.F.).

30.C.



30.D.

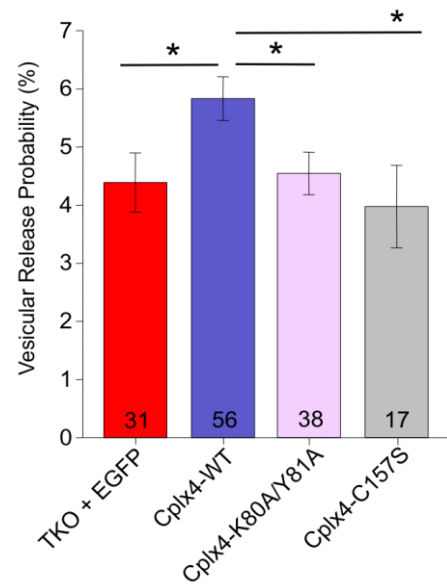
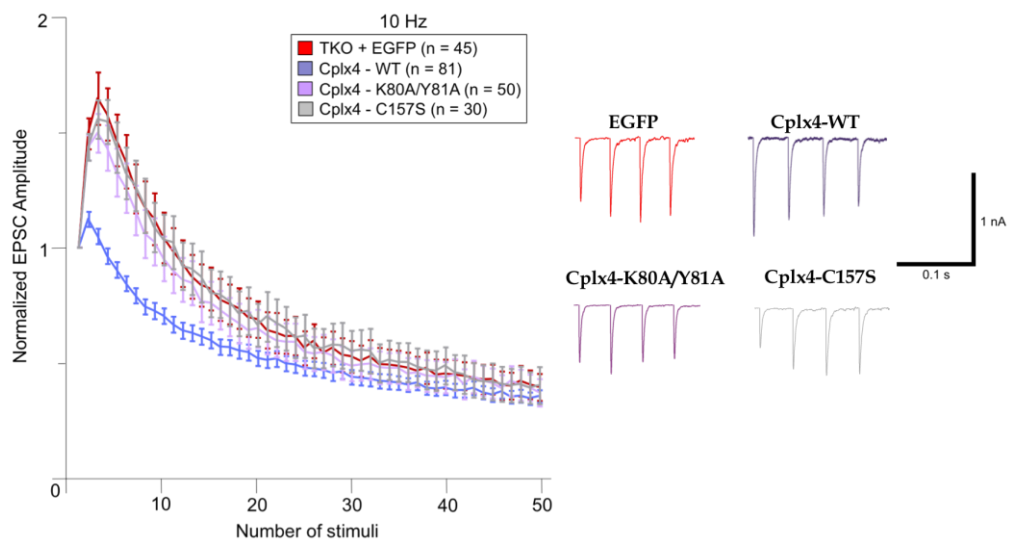


Figure 30.C.,D.

RRP size and vesicular release probability in Cplx TKO neurons expressing EGFP, EGFP, Cplx4-WT, Cplx4-K80A/Y81A and Cplx4-C157S proteins. (C) Mean RRP size measured as charge elicited due to release of the primed vesicle pool, induced by application of 0.5 M sucrose solution - RRP size was unaltered in neurons irrespective of the construct expressed, representative traces are included. **(D)** Mean vesicular release probability (Pvr) estimated as the ratio of charge of the evoked EPSC to the charge of the RRP - Pvr was enhanced by 30% in the neurons expressing Cplx4-WT compared with neurons expressing EGFP, Cplx4-K80A/Y81A and Cplx4-C157S, * $p < 0.05$ between the neurons of the groups compared. Absolute values are included in Table 19. Error bars indicate standard error of mean (S.E.M.). Numbers of neurons analyzed are indicated on bars. Students t-test was used to assess statistical significance.

30.E.



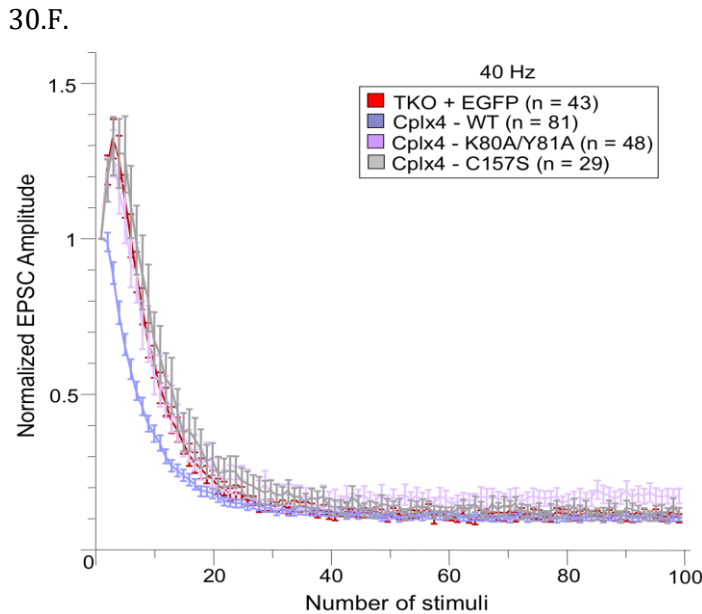


Figure 30.E.,F. **Short-term plasticity in autaptic hippocampal Cplx TKO neurons expressing EGFP, Cplx4-WT, Cplx4-K80A/Y81A and Cplx4-C157S proteins. (E) and (F)** Amplitudes of the synaptic responses evoked by a train of stimulation at 10 Hz and 40 Hz (for EPSCs) were normalized to the amplitude of the first response and plotted against the stimulus number. Representative traces of EPSCs at the beginning of the 10 Hz stimulation train are shown. Data are expressed as mean \pm S.E.M. Numbers of neurons analyzed are indicated. Depression of EPSCs was observed in TKO neurons expressing Cplx4-WT indicating high initial release probability, while initial facilitation of EPSCs was observed in TKO neurons expressing EGFP, Cplx4-K80A/Y81A and Cplx4-C157S indicating low initial release probabilities.

The mEPSC frequency elicited by the neurons expressing the different Cplx4 variants remained unaltered (Fig.30.G.). To a small extent, the miniature amplitude was reduced in the neurons expressing the SNARE-domain mutant Cplx4-K80A/Y81A and increased in the presence of farnesylation mutant Cplx4-C157S (Fig.30.H.).

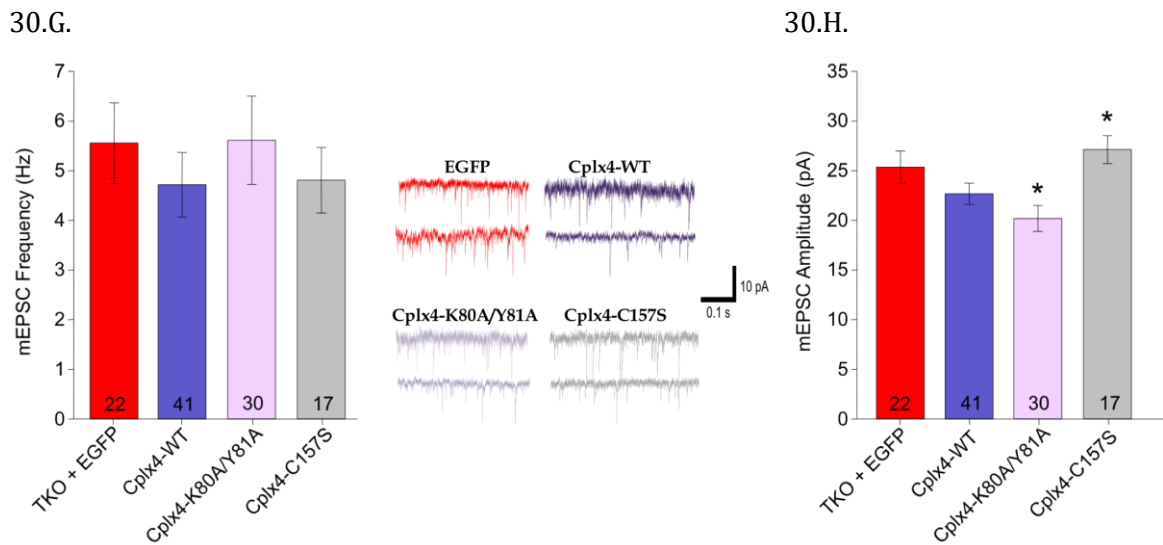


Figure 30.G.,H. Spontaneous neurotransmitter release (mEPSC) in autaptic hippocampal Cplx TKO neurons expressing EGFP, Cplx4-WT, Cplx4-K80A/Y81A and Cplx4-C157S. 300 nM Tetrodotoxin was exogenously applied to neurons in order to block Na⁺-channel driven action potentials while measuring miniature excitatory post-synaptic currents. **(G)** Mean mEPSC frequency - no significant differences were found in within all the groups compared, representative traces are included. **(H)** Mean mEPSC amplitudes - no significant variation between EGFP and Cplx4-WT expressing neurons but a slight decrease of mEPSC amplitude in the Cplx4-K80A/Y81A SNARE mutant expressing neurons and a small increase in mEPSC amplitude in the Cplx4-C157S farnesylation mutant expressing neurons, was apparent. *p<0.05 compared with EGFP and Cplx4-WT, respectively. The Absolute values are included in Table 19. Error bars indicate standard error of mean. Numbers of neurons analyzed are indicated on bars. Students t-test was used to assess statistical significance.

Table 19. Synaptic parameters measured from excitatory Cplx TKO neurons expressing EGFP, Cplx4-WT, Cplx4-K80A/Y81A, and Cplx4-C157S lentiviral proteins.

Parameter (Mean ± S.E.M.)	Cplx TKO (+)			
	EGFP	Cplx4-WT	Cplx4-K80A/Y81A	Cplx4-C157S
EPSC Amplitude (nA)	2.32±0.173 (n=45)	4.488±0.348 (n=81)	2.152±0.184 (n=54)	2.485±0.252 (n=31)
RRP Size (nC)	0.476±0.055 (n=32)	0.429±0.044 (n=57)	0.343±0.049 (n=38)	0.407±0.066 (n=19)
Pvr (%)	4.39±0.508	5.83±0.374	4.54±0.364	3.970±0.709

	(n=31)	(n=56)	(n=38)	(n=17)
mEPSC Frequency (Hz)	5.55±0.809 (n=22)	4.716±0.649 (n=41)	5.613±0.889 (n=30)	4.808±0.659 (n=17)
mEPSC Amplitude (pA)	25.352±1.628 (n=22)	22.671±1.082 (n=41)	20.184±1.3 (n=30)	27.124±1.406 (n=17)

S.E.M. is standard error of mean

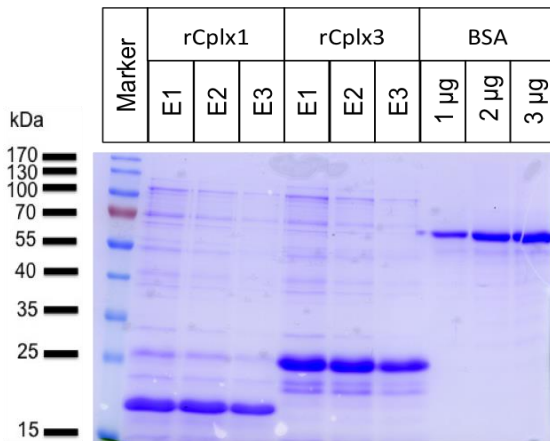
n is number of cells pooled from multiple cultures

3.2.3. Lentiviral expression and quantification of wild type and mutant Complexin proteins in Cplx-TKO neurons

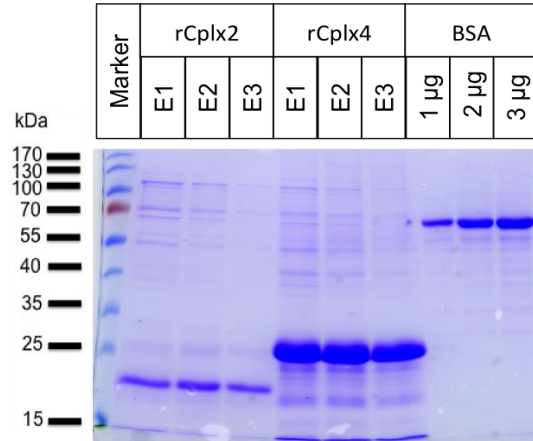
Lentivirus mediated transduction of genes in non-dividing cells has been shown to cause efficient gene integration and expression (Naldini et al., 1996). In the present study, the lentiviral pFUGW vector comprising of dual promoters - the neuron-specific Synapsin promoter for Complexins and the Ubiquitin promoter for the reporter gene EGFP, was used to express the respective Complexin genes upon transduction in neurons (Gascon et al., 2008). This lentiviral system of expression allows stable gene expression at moderate levels, and I attempted to quantify the protein expression levels from the transduced neurons and compare them with endogenous protein levels in wild type neurons.

To estimate the protein expression in the neurons, I prepared recombinant wild type Complexin proteins (rCplx1, rCplx2, rCplx3 and rCplx4) (Methods 2.2.3.) that had been cloned in the pET-28a vector for a T7 promoter driven bacterial expression of the proteins with a His₆-tag. Presence of the His₆-tag is a useful tool for affinity purification of recombinant proteins expressed in *E. coli*. After preparation of recombinant proteins, I performed SDS-PAGE and Coomassie staining to verify the purification of recombinant proteins (Fig.31.A. and B.). Subsequently, I quantified the recombinant proteins to obtain respective standard curves (31.C.).

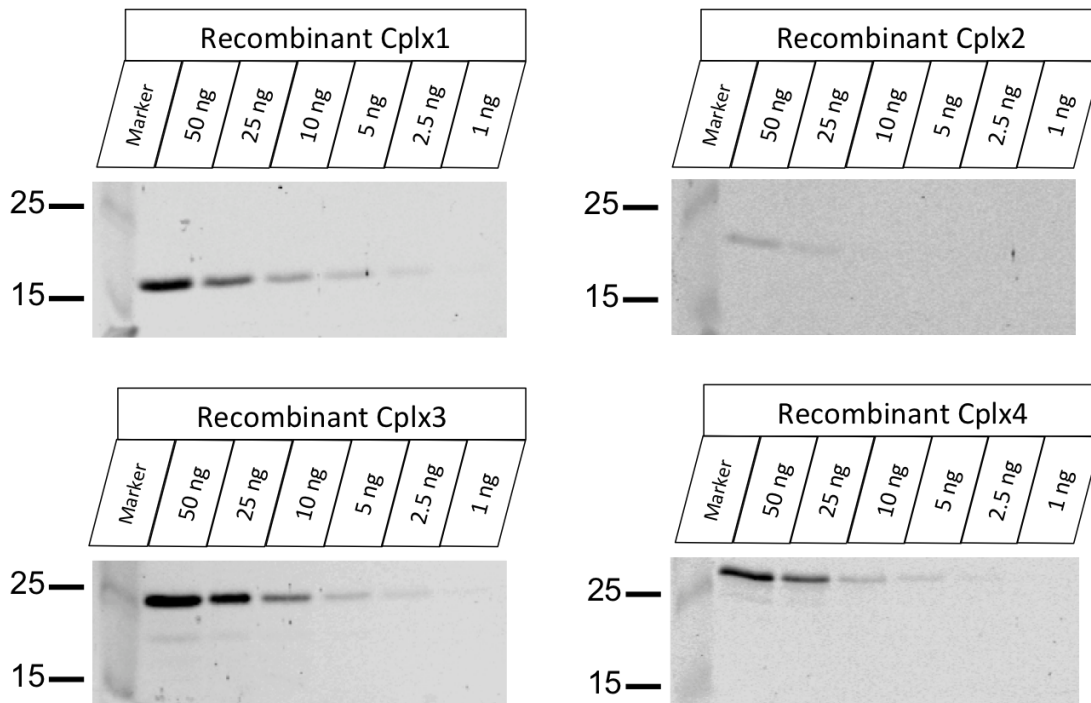
31.A.



31.B.



31.C.

**Figure 31.A.,B.,C.**

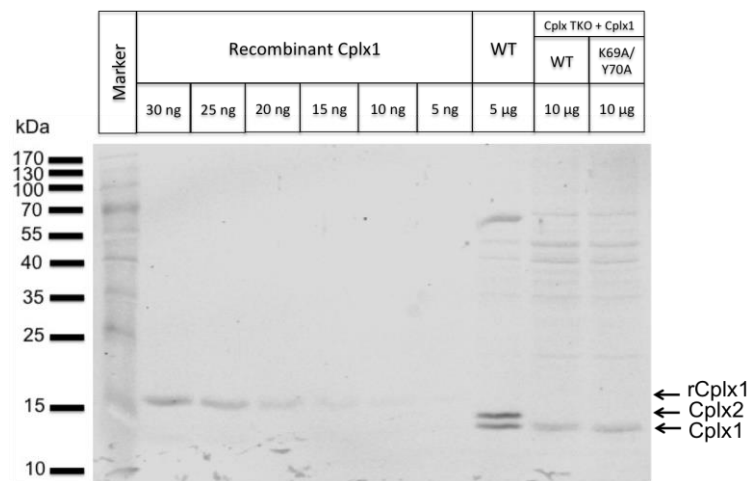
Recombinant His₆-tagged Cplx proteins. Coomassie staining of SDS-Gels. **(A)** Cplx1 and Cplx3 recombinant proteins were prepared simultaneously and eluted in three fractions E1, E2 and E3 and tested for expression against BSA standards of 1 µg, 2 µg and 3 µg (Refer Methods 2.2.3.). **(B)** Cplx2 and Cplx4 recombinant proteins were prepared simultaneously and eluted in three fractions E1, E2 and E3 and tested for expression against BSA standards of 1 µg, 2 µg and 3 µg (Refer Methods 2.2.3.). The four recombinant Cplx proteins had molecular mass in the range of 15 kDa to 25 kDa. **(C)** The recombinant proteins rCplx1, rCplx2, rCplx3 and rCplx4 were diluted to various concentrations of 50 ng, 25 ng, 10 ng, 5 ng, 2.5 ng and 1 ng and subjected to SDS-PAGE and Western blotting. The intensities of the protein bands were recorded using the Odyssey Infrared Scanner and

a standard curve was generated for each of the four recombinant Complexins.

3.2.3.1. Cplx1 protein estimation

Since Cplx1 is prominently expressed in hippocampal neurons, I calculated the protein concentrations of Cplx1-WT and Cplx1-K69A/Y70A in infected Cplx-TKO neurons in comparison to the endogenous levels of Cplx1 present in wild type hippocampal neurons. I used a standard curve of the recombinant Cplx1 protein for estimation of the protein concentrations. Linear regression analysis and percentage of transduced cells yielded estimates that endogenous Cplx1 is present at 12.25×10^{-5} pmol in a wild-type neuron, while Cplx1-WT and Cplx1-K69A/Y70A proteins are expressed at 1.55×10^{-5} pmol and 1.73×10^{-5} pmol respectively per transduced Cplx TKO neuron (Fig.32. and Table 20.).

32.A.



32.B.

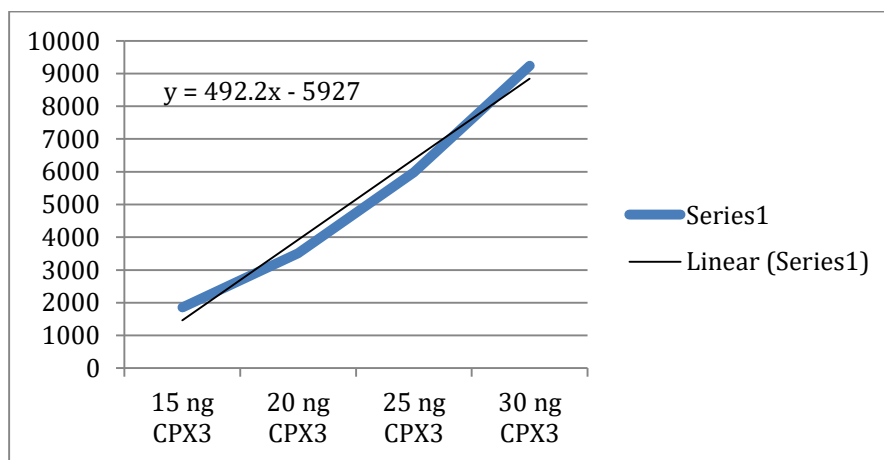


Figure 32.A.,B. Quantification of endogenous and lentiviral Cplx1 protein expression. (A) Western blot performed for the standard

curve of rCplx1 (30 ng, 25 ng, 20 ng, 15 ng, 10 ng, 5 ng). 5 µg of sample protein from wild type neuronal extract of total concentration 60 µg was used for the blot. Cplx TKO neuron cultures seeded at a density of 10⁶ cells per 6 cm petridish were infected separately with lentiviruses for Cplx1-WT and Cplx1-K69A/Y70A at DIV 2. The infected neurons were harvested at DIV 14 and total protein concentration was estimated. 10 µg of sample from total lentiviral protein harvest of 56 µg (Cplx1-WT) and 65 µg (Cplx1-K69A/Y70A) was used for the blot. **(B)** Regression analysis for standard curve and sample Cplx1 proteins. In comparison to the rCplx1 standard curve, 5 µg of total protein from wild type neurons contains 30.6 ng of Cplx1 protein, while 10 µg lentiviral protein from Cplx TKO + Cplx1-WT and Cplx TKO + Cplx1-K69A/Y70A contained 25 ng and 24 ng of the respective Cplx1 protein. Molecular weight of Cplx1 is 15.0 kDa. Calculations are shown in Table 20.

Table 20. Estimation of endogenous and lentiviral Cplx1 proteins

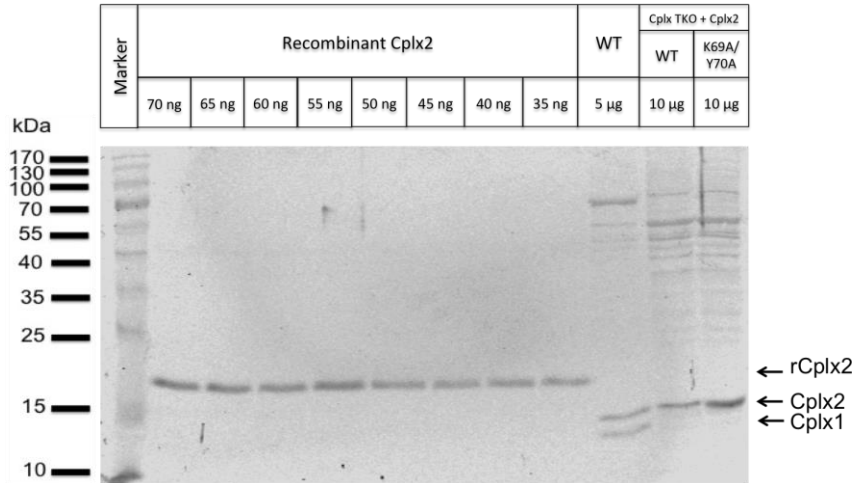
Cplx1 Protein (Mol. Wt. 15kDa)	Number of neurons		Cplx1 Content in Analyte (ng)	Total protein content in transduced neurons (pmol)
	Cultured	Transduced (EGFP Fluorescent)		
Cplx1-WT (Endogenous)	200,000	n.a.	30.6 ng in 5 µg of analyte (0.6% of total protein harvest)	24.5 pmol in 200,000 neurons
Cplx1-WT (Lentiviral)	1,000,000	600,000	25 ng in 10 µg of analyte (0.25% of total protein harvest)	9.3 pmol in 600,000 neurons
Cplx1- K69A/Y70A (Lentiviral)	1,000,000	600,000	24 ng in 10 µg analyte (0.24% of total protein harvest)	10.4 pmol in 600,000 neurons

3.2.3.2. Cplx2 protein estimation

Since Cplx2 is also prominently expressed in hippocampal neurons, I next calculated the protein concentrations of Cplx2-WT and Cplx2-K69A/Y70A in infected Cplx-TKO neurons in comparison to the endogenous levels of Cplx2 present in wild type hippocampal neurons. I used a standard curve of the recombinant Cplx2 protein for estimation of the protein

concentrations. Linear regression analysis and percentage of transduced cells yielded estimates that endogenous Cplx2 is present at 13×10^{-5} pmol in a wild-type neuron, while Cplx2-WT and Cplx2-K69A/Y70A proteins are expressed at 5.05×10^{-5} pmol and 15.03×10^{-5} pmol respectively per transduced Cplx TKO neuron (Fig.33. and Table 21.).

33.A.



33.B.

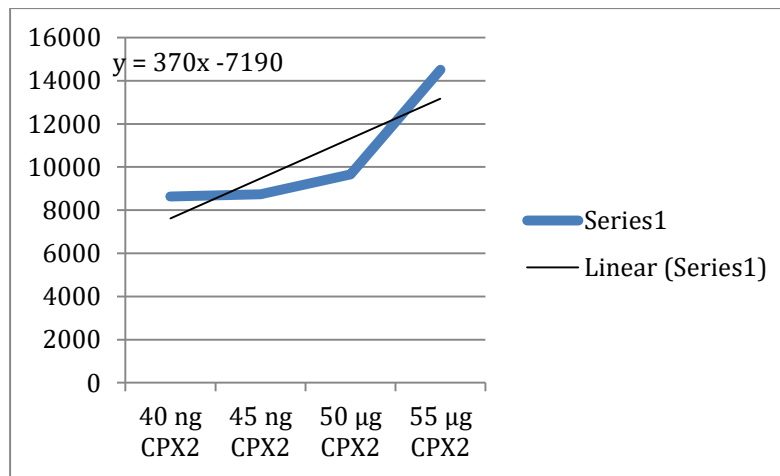


Figure 33.A.,B.

Quantification of endogenous and lentiviral Cplx2

protein expression. (A) Western blot performed for the standard curve of rCplx2 (70 ng, 65 ng, 60 ng, 55 ng, 50 ng, 45 ng, 40 ng, 35 ng). 5 µg of sample protein from wild type neuronal extract of total concentration 60 µg was used for the blot. Cplx TKO neuron cultures seeded at a density of 10^6 cells per 6 cm petridish were infected separately with lentiviruses for Cplx2-WT and Cplx2-K69A/Y70A at DIV 2. The infected neurons were harvested at DIV 14 and total protein concentration was estimated. 10 µg of sample from total lentiviral protein harvest of 115 µg (Cplx2-WT) and 188 µg (Cplx2-K69A/Y70A) was used for the blot. 10 µg of each of the infected samples was used for the blot. **(B)** Regression analysis for standard curve and sample Cplx2 proteins. In comparison to the rCplx2

standard curve, 5 µg of total protein from wild type neurons contains 33.4 ng of Cplx2 protein, while 10 µg total protein from Cplx TKO + Cplx2-WT and Cplx TKO + Cplx2-K69A/Y70A contained 39.6 ng and 72 ng of the respective Cplx2 protein. Molecular weight of Cplx1 is 15.3 kDa. Calculations are shown in Table 21.

Table 21. Estimation of endogenous and lentiviral Cplx2 proteins

Cplx2 Protein (Mol. Wt. 15kDa)	Number of neurons		Cplx2 content in Analyte (ng)	Total protein content in transduced neurons (pmol)
	Cultured	Transduced (EGFP Fluorescent)		
Cplx2-WT (Endogenous)	200,000	n.a.	33.4 ng in 5 µg Analyte (0.67% of total protein harvest)	26.0 pmol in 200,000 neurons
Cplx2-WT (Lentiviral)	1,000,000	600,000	39.6 ng in 10 µg Analyte (0.4% of total protein harvest)	30.3 pmol in 600,000 neurons
Cplx2- K69A/Y70A (Lentiviral)	1,000,000	600,000	72 ng in 10 µg Analyte (0.72% of total protein harvest)	90.2 pmol in 600,000 neurons

3.2.3.3. Cplx3 protein estimation

Cplx3 is faintly expressed in the hippocampus, but more distinctly expressed in the cortex. I next attempted to estimate the Cplx3 protein concentration in the cultured cortical neurons. However, there was no endogenous Cplx3 protein expression detectable (Fig.34.A). Therefore, I calculated the protein concentrations of Cplx3-WT infected Cplx-TKO neurons in comparison to the standard curve of the recombinant Cplx3 protein directly. Linear regression analysis and percentage of transduced cells yielded estimates that Cplx3-WT lentiviral protein is expressed at 0.875×10^{-5} pmol per transduced Cplx TKO neuron (Fig.34.B. and 34.C. and Table 22.). The lentiviral protein expression levels of Cplx3-K79A/Y80A and Cplx3-C155S mutants will be ascertained in future experiments.

34.A.

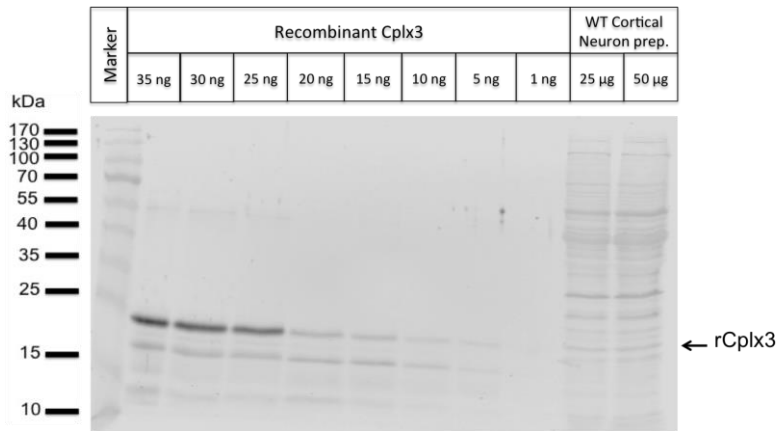
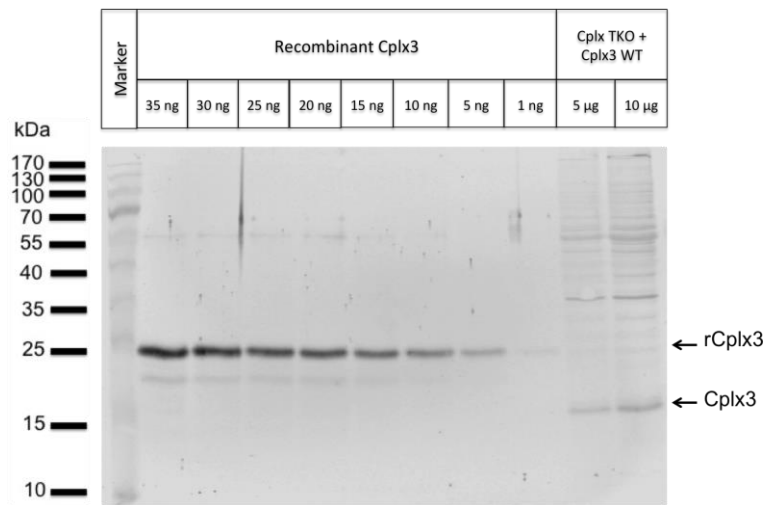


Figure 34.A.

Estimation of endogenous Cplx3 protein expression.

Western blot performed for the standard curve of rCplx3 (35 ng, 30 ng, 20 ng, 15 ng, 10 ng, 15 ng, 5 ng, and 1 ng). 25 μg and 50 μg of total protein from wild type cortical neuron lysate were also used for the blot. Cplx3 at its molecular weight of 17.6 kDa was undetectable.

34.B.



34.C.

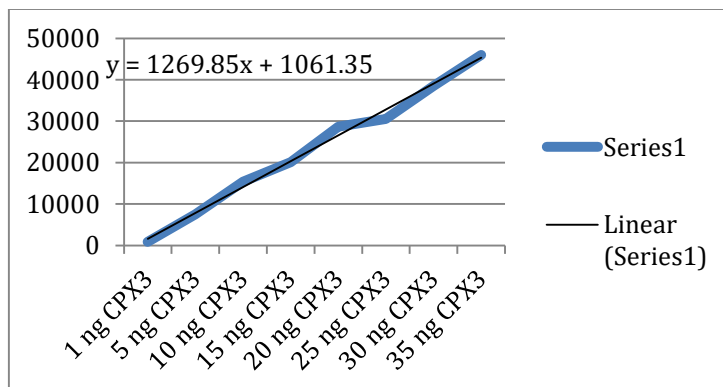


Figure 34.B,C.**Quantification of lentiviral Cplx3-WT protein expression.**

(B) Western blot performed for the standard curve of rCplx3 (35 ng, 30 ng, 20 ng, 15 ng, 10 ng, 5 ng, and 1 ng). Cplx TKO neuron cultures seeded at a density of 10^6 cells per 6 cm petridish were infected with lentivirus for Cplx3-WT at DIV 2. The infected neurons were harvested at DIV 14 and total protein concentration was estimated. 5 μ g and 10 μ g of sample from total lentiviral protein harvest of 200 μ g were used for the blot. **(C)** Regression analysis for standard curve and sample Cplx3 proteins. In comparison to the rCplx3 standard curve, 5 μ g total protein contained 2.5 ng of Cplx3 protein, while 10 μ g total protein contained 5.13 ng of the Cplx3-WT protein. Molecular weight of Cplx1 is 17.6 kDa. Calculations are shown in Table 22.

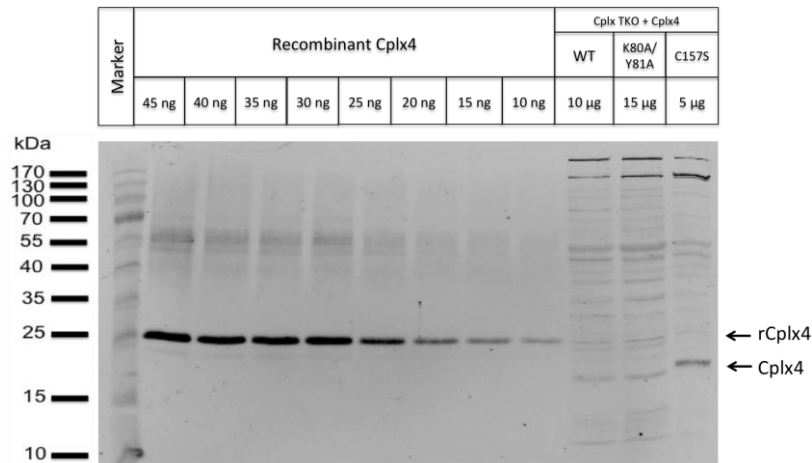
Table 22.**Estimation of lentiviral Cplx3-WT protein.**

Cplx3 Protein (Mol. Wt. 17.6kDa)	Number of neurons		Cplx3 content in Analyte (ng)	Total protein content in transduced neurons (pmol)
	Cultured	Transduced (EGFP Fluorescent)		
Cplx3-WT (Lentiviral)	1,000,000	650,000	2.5 ng in 5 μ g Analyte (0.05% of total protein harvest)	5.68 pmol in 650,000 neurons
Cplx3-WT (Lentiviral)	1,000,000	650,000	5.13 ng in 10 μ g Analyte (0.05% of total protein harvest)	5.83 pmol in 650,000 neurons

3.2.3.4. Cplx4 protein estimation

Since Cplx4 is not expressed in the brain, I calculated the protein expression levels of Cplx4-WT, Cplx4-K80A/Y81A and Cplx4-C157S infected Cplx-TKO neurons in comparison to the standard curve of the recombinant Cplx4 protein. Linear regression analysis and percentage of transduced cells yielded estimates that Cplx4-WT, Cplx4-K80A/Y81A and Cplx4-C157S are expressed at 0.876×10^{-5} pmol, 0.828×10^{-5} pmol, and 1.64×10^{-5} pmol per transduced Cplx TKO neuron, respectively. (Fig.35.A. and 35.B. and Table 23.).

35.A.



35.B.

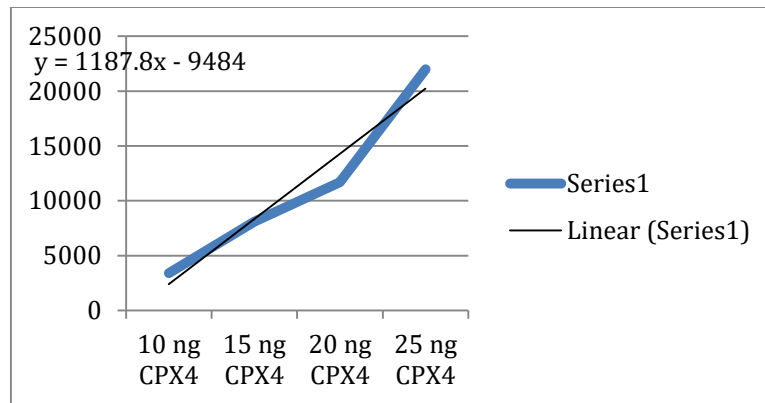


Figure 35.A.,B.

Quantification of lentiviral Cplx4 protein expression. (A) Western blot performed for the standard curve of rCplx4 (40 ng, 35 ng, 30 ng, 25 ng, 20 ng, 15 ng, 10 ng, 5 ng). Cplx TKO neuron cultures seeded at a density of 10^6 cells per 6 cm petridish were infected separately with lentiviruses for Cplx4-WT, Cplx4-K79A/Y80A, and Cplx4-C157S at DIV 2 - 10 µg, 15 µg and 5 µg of the respective proteins harvested at DIV 14 was used for the blot. **(B)** Regression analysis for standard curve and sample Cplx4 proteins. In comparison to the rCplx4 standard curve, 10 µg Cplx TKO + Cplx4-WT, 15 µg Cplx TKO + Cplx4-K80A/Y81A and 5 µg Cplx TKO + Cplx4-C157S contained 9.62 ng, 10.6 ng and 12.3 ng of the respective Cplx4 proteins. Molecular weight of Cplx1 is 17.6 kDa. Calculations are shown in Table 23.

Table 23. Estimation of lentiviral Cplx4 proteins.

Cplx4 Protein (Mol. Wt. 18.3kDa)	Number of neurons		Cplx4 content in Analyte (ng)	Total protein content in transduced neurons (pmol)
	Cultured	Transduced (EGFP Fluorescent)		
Cplx4-WT (Lentiviral)	1,000,000	600,000	9.62 ng in 10 μ g Analyte (0.09% of total protein harvest)	5.25 pmol in 600,000 neurons
Cplx4- K80A/Y81A (Lentiviral)	1,000,000	550,000	10.6 ng in 15 μ g Analyte (0.07% of total protein harvest)	4.55 pmol in 550,000 neurons
Cplx4-C157S (Lentiviral)	1,000,000	850,000	12.3 ng in 5 μ g Analyte (0.25% of total protein harvest)	14 pmol in 850,000 neurons

4. Discussion

4.1. Discussion - SNAP-29

4.1.1. SNAP-29 - localization and interactions with presynaptic SNAREs

The expression of SNAP-29 in the cortex and hippocampus of the mouse brain is clearly indicative of the fact that SNAP-29 is present in neurons (Fig.12. and 16.), although it is unknown if its localization is limited only to a subset of synapses.

The full length protein of SNAP-29 was found to share 17% sequence identity with SNAP-23 and SNAP-25, with the highest homology existing among the coiled coil domains at the N- and C-terminus (Steehmaier et al., 1998). A significant variation in the structure of the SNAP-29 protein is the complete absence of the conserved cysteine residue stretch that acts as a substrate for palmitoylation (Steehmaier et al., 1998). Palmitoylation is a post-translational modification that links C16-palmitate residues to the Cysteine residues via a covalent thioester bond and co-ordinates the protein sorting to membranes (Veit et al., 1996). Prior studies in mammalian cells demonstrated that newly synthesized wild type and non-palmitoylated mutant SNAP-23 protein could efficiently interact with Syntaxin *in-vivo* and associate to membranes (Vogel and Roche, 1999). Similarly, pulse-chase experiments revealed that newly synthesized wild type and non-palmitoylated mutant SNAP-25 is localized to Golgi via interactions with the transmembrane domain of Syntaxin-1A (Vogel et al., 2000). Mutations on the cysteine rich domain of SNAP-25 that prevent palmitoylation did not affect membrane association of SNAP-25 in the presence of Syntaxin, whereas non-palmitoylated mutant SNAP-25 was diffusely distributed in the cytosol in the absence of Syntaxin (Washbourne et al., 2001). Interaction with Syntaxins was found to be sufficient for membrane association of SNAP-23 and SNAP-25 but palmitoylation likely dictates the precise intracellular localization of the proteins (Greaves et al., 2010). The SNAP-47 protein, similar to SNAP-29 lacks the palmitoylation site, but co-purifies with synaptic vesicles in subcellular fractionation of mouse whole brain homogenate, forms ternary SNARE complex with Syntaxin-1A and Synaptobrevin-2 and aids SNARE-mediated liposome fusion (Holt et al., 2006).

A biochemical study performed by Su et al. (2001) on rat brain homogenates showed that Syntaxin-1A was co-immunoprecipitated by anti-SNAP-29 antibodies, and GST-fused SNAP-29 co-sedimented the native SNARE complex, alluding to a possible interaction between

SNAP-29 and the neuronal SNAREs. *In-vitro* binding assays and transfections in cultured mammalian cells revealed that GST-fused SNAP-29 interacts with numerous other Syntaxin paralogs such as Syntaxin-1A, -3, -4, -7, -13 and -17, which are present on plasma membrane, or intracellular organelles (Steggmaier et al., 1998; Hohenstein et al., 2001). Similarly, *Drosophila* SNAP-29 (also known as ubisnap) has been shown to interact with dSyntaxin-1 and dSyntaxin-16 in co-immunoprecipitation experiments of cultured Schneider cells derived from *Drosophila* embryos (Xu et al., 2014). A recent study concluded that SNAP-29 exhibits high affinity interaction with Syntaxin-17 *in-vitro* to form a binary t-SNARE complex that is stabilized by ATG14 – an autophagy specific regulator promoting fusion of proteoliposomes (Diao et al., 2015).

Immunocytochemical analysis of cultured hippocampal neurons previously showed extensive co-localization of SNAP-29 with the presynaptic marker Synaptophysin, and subcellular fractionation of rat brain synaptosomes revealed an enrichment of SNAP-29 in the synaptic vesicle and plasma membrane fractions (Su et al., 2001). In my study, the immunocytochemical experiment performed on cultured hippocampal neurons from WT mice showed a diffuse pattern of SNAP-29 expression in the soma, axons and dendrites, while the KO neurons exhibited a complete absence of SNAP-29 immunostaining (Fig.17.). Abundant SNAP-29 was previously found in actively myelinating oligodendrocytes, and Schwann cells with perinuclear enrichment on the endoplasmic reticulum (Schardt et al., 2009). Therefore, the presence of SNAP-29 on the axons is reasonable. However, the absence of an endogenous palmitoylation site in SNAP-29 and likely weak interactions with Syntaxins may contribute to the diffuse distribution of SNAP-29 in the neuronal soma. Also, co-localization of the presynaptic vesicle marker VGLUT-1 and SNAP-29 is not detectable at synapses of WT neurons. This result does not show an apparent preferential association of SNAP-29 to synaptic vesicles. However, confocal or STED imaging could give a better insight on the peripheral and subcellular localization of SNAP-29 at presynaptic terminals. Additionally, co-immunoprecipitation experiments and proteomic analysis could be performed to determine the interactions of neuronal SNAP-29 with other SNAREs, to confirm the proportion of the SNAP-29 protein associated to membranes as well as to organelles such as Golgi or endosomes, and assess if such subcellular targeting is indeed mediated by neuronal Syntaxins.

4.1.2. SNAP-29 - no key role in synaptic vesicle exocytosis

The proteins SNAP-25, SNAP-23 and SNAP-47 exert positive effect in synaptic vesicle fusion. Conversely, SNAP-29 has been shown to negatively modulate neurotransmitter release. Initial studies indicated that injection of a high concentration of exogenous SNAP-29 at cholinergic synapses of paired SCG neurons gradually reduced the EPSP amplitudes at frequencies of 0.05 Hz and 0.2 Hz (Su et al., 2001). Such activity dependent decline of release was attributed to inhibition of *cis*-SNARE disassembly post fusion, as SNAP-29 was found to compete with α -SNAP for SNARE binding, ultimately resulting in fewer SNAREs available for subsequent rounds of vesicle fusion (Su et al., 2001). A related study also ascribed the over-expressed SNAP-29 to inhibit release in an activity dependent manner. Over-expression of SNAP-29 in cultured hippocampal neuron pairs did not affect evoked post-synaptic currents or short-term plasticity but reduced the synaptic vesicle-refilling rate after stimulation at 0.1 Hz and 1 Hz (Pan et al., 2005). However, synaptic facilitation was observed upon siRNA mediated knockdown of endogenous SNAP-29 (Pan et al., 2005). Although the former study (Su et al., 2001) analyzed the effects of SNAP-29 over-expression, the contribution of endogenous SNAP-29 to synaptic release was neglected. A negative modulatory role for SNAP-29 was defined merely based on stimulation-frequency dependent effects, which cannot be considered as a sole parameter regulating synaptic release. The latter study (Pan et al., 2005) explored additional effects of diminished SNAP-29 expression on synaptic release, and concluded that down-regulation of SNAP-29 caused initial facilitation of the EPSC amplitudes, increased recovery rate after high-frequency stimulation, and consequently enhanced synaptic vesicle turnover. However, the slower synaptic depression or high initial facilitation are indicators of lower initial vesicular release probability at the synapse, and the effect of SNAP-29 knockdown on the number of release-ready vesicles, and the vesicular release probability were unaccounted for in the experiment.

The objectives of my study overrules the disadvantages of the previous studies for various reasons: 1) The present study deals with the measurement of synaptic output from an “autaptic” cultured neuron, which comprises of a homogenous population of synapses, whereas previous studies measured cumulative synaptic release from a varied population of synapses existing between multiple neurons. Synapses between different neurons have a high degree of variability in terms of vesicle pool and the release probability. Therefore, using a well-defined model such as autaptic neurons limits the discrepancies that arise due to synaptic variability. 2) The present study involves systematic analysis of various synaptic parameters such as single AP-evoked Ca^{2+} -dependent release at low-frequency stimulations,

Ca²⁺-independent release of the primed vesicle pool at the presynaptic terminal (measured by application of hypertonic sucrose solution), short-term synaptic plasticity under high-frequency stimulations, the release probability, the quantal release and its dependence on residual Ca²⁺. This type of analysis provides a comprehensive assessment of synaptic functionality. 3) The study utilizes both conditional and constitutive gene knockout animals. In this manner, non-specific off-target effects of knockdown approaches or proteins generated by incomplete knockdown are circumvented. The parallel use of conditional gene knockout circumvents compensatory processes that might arise in the course of constitutive gene knockout.

In my study, I found that conditional deletion of SNAP-29 from glutamatergic synapses did not significantly alter the AP-evoked Ca²⁺-triggered release, the readily releasable vesicle pool size, or vesicular release probability indicating that SNAP-29 does not contribute to vesicle priming or fusion at synapses. The synapses lacking SNAP-29 depressed to a similar extent as those containing SNAP-29 under high-frequency stimulations of 10 Hz and 40 Hz. This parameter also reflected the high yet unaltered vesicular release probability at the synapses devoid of SNAP-29. The quantal release measured after high-frequency stimulations showed a residual Ca²⁺-dependent increase of release events that was relatively similar at both WT and KO synapses. These results clearly indicate that SNAP-29 is not required for vesicle recovery after depletion. Thus, SNAP-29 does not play a role in modulating Ca²⁺-dependent and Ca²⁺-independent release, at glutamatergic synapses. Although the results from the conditional KO are convincing, effects of residual protein expression at these synapses could not be accounted for in this data set. Similarly, the role of SNAP-29 at GABAergic synapses, which are also abundant in the CNS, could not be studied in the conditional KO model used here. In the constitutive SNAP-29 KO, I found no alterations in the expression levels of the Syntaxin-1AB, Synaptobrevin-2, SNAP-25, SNAP-23 and SNAP-47 in SNAP-29 KO brains (Fig.16.). Therefore, compensatory effects in synaptic transmission due to up-regulation of other SNARE proteins are unlikely. Also, I found no significant differences in the various synaptic parameters tested, such as peak amplitudes of evoked post-synaptic currents, readily releasable primed vesicle pool size, vesicular release probability, or quantal release at glutamatergic and GABAergic synapses between the WT and KO. Both synapse types exhibited normal short-term synaptic depression indicative of high vesicular release probability.

The intact synaptic transmission at synapses devoid of SNAP-29 offers a few rational cues. The neuronal SNARE complex, which is essential for mediating vesicle fusion comprises

primarily of Syntaxin-1, Synaptobrevin-2 and SNAP-25. These proteins form the four-helical bundle essential for vesicle fusion (Fasshauer et al., 1998). The intrinsic stability of the four-helical bundle is partially due to high affinity interactions between the SNARE motifs of the three proteins. Many studies have shown that loss of one of the SNARE proteins severely impedes the vesicle fusion process at central synapses.

SNAP-25 deletion causes a dramatic decline in evoked transmitter release, size of the RRP, which is also indicated by the decreased number of membrane attached vesicles in hippocampal synapses (Bronk et al., 2007; Imig et al., 2014). A small reduction in spontaneous release of cultured hippocampal neurons of the SNAP-25 null mutants was observable, but all synaptic parameters could be restored upon lentiviral expression of SNAP-25a, SNAP-25b, and SNAP-23, albeit to variable degrees of significance (Delgado-Martinez et al., 2007). Considering the fact that the SNAP-25 null mutant neurons still express endogenous SNAP-29, the role of SNAP-29 in synaptic transmission might be minor, which agrees with my findings. One cannot presume that the expression of SNAP-29 in cultured neurons may be negligible because in my study, expression of SNAP-29 is evident in cultured hippocampal neurons (Fig.12.B.). Although SNAP-29 has been shown to interact with multiple Syntaxins in *in-vitro* assays and to also co-sediment the native neuronal SNARE complex (Su et al., 2001), the innate interaction between SNAP-29 and the neuronal SNAREs could be limited due to low-affinity binding of SNAP-29 and the SNAREs. Such weak affinity can be justified due to substantial variations in the sequence and structure of SNAP-29 compared with SNAP-25. Although the lentiviral expression of SNAP-23 in SNAP-25 null mutants predominantly caused asynchronous release, expression of SNAP-23 along with the presence of endogenous SNAP-25 did not alter the transmitter release kinetics, indicating a preferential use of SNAP-25 for maintenance of synchronous neurotransmission (Delgado-Martinez et al., 2007). Furthermore, no dramatic synaptic deficits or changes in release kinetics were observed in the absence of SNAP-29 in my study.

Thus, it can be concluded that the cognate neuronal SNARE proteins - Syntaxin-1 and Synaptobrevin-2 'preferentially' bind SNAP-25 to form the neuronal SNARE core complex and mediate subsequent release in neurons, while the binding of SNAP-29 to these SNAREs is likely minimal and therefore, SNAP-29 is not required for neurotransmitter release at glutamatergic and GABAergic synapses.

4.1.3. SNAP-29 - clinical implications due to loss of function

Human patients suffering from the CEDNIK syndrome - a disease characterized by neuropathy, ichthyosis, and palmoplantar keratoderma - were found to have a frameshift mutation at nucleotide G at SNAP-29 cDNA position 220 leading to premature termination of the coding sequence and a severely truncated protein product (Sprecher et al., 2005). A similar keratoderma phenotype was observed in the constitutive SNAP-29 KO mice, which is likely caused by abnormal lamellar granule maturation in the epidermis and secretion and retention of non-hydrolyzed glucosylceramide, resulting in decreased desquamation or separation of cells (Sprecher et al., 2005). The SNAP-29 KO mice were susceptible to perinatal lethality, which is an apparent clinical consequence of SNAP-29 deletion. CEDNIK syndrome patients exhibit severe psychomotor retardation or neuropathy; absence of tendon reflexes and macular atrophy were further substantiated by low amplitude responses in peripheral nerve conductance studies (Sprecher et al., 2005). Although deficits in synaptic transmission at the central synapses can be excluded as a plausible cause for perinatal lethality in SNAP-29 KO mice, they may suffer due to severe deficits in the functioning of the peripheral nervous system, which - based on the present study - are unlikely to involve synaptic deficits.

4.2. Discussion - Complexins

4.2.1. Mammalian Complexins improve the release efficacy of vesicles via binding to the neuronal SNARE complex

The Complexin family of proteins has distinctively evolved as neuron-specific regulators of the synaptic vesicle fusion machinery in higher eukaryotes with nervous systems (Brose, 2008). The small size and polar charge of Complexins makes them ideal candidates that mediate the cardinal process of transmitter release between neurons via a cascade of robust protein-protein interactions. In the literature, substantial evidence exists on the positive modulatory role of Complexins in synaptic vesicle fusion and release in mouse neurons (Reim et al., 2001, Reim et al., 2005; Xue et al., 2007, Xue et al., 2008). Many studies *in-vitro*, on invertebrate models, and in mice using different techniques have also revealed an inhibitory role of Complexins in vesicle fusion, confounding the preexisting notions.

In the present study, I have first attempted to comprehend the role of Complexins in mediating synchronous release of vesicles. Genetic loss of Cplx1 and Cplx2 in new-born mice (Cplx DKO) caused massive perturbations in synaptic neurotransmitter release that were apparent as reductions in amplitudes of evoked post-synaptic currents, vesicular release probability and apparent Ca^{2+} sensitivity of neurotransmitter release (Reim et al., 2001). Individual loss of Cplx3 had no effects on transmitter release at hippocampal glutamatergic and GABAergic synapses (Xue et al., 2008), and Cplx TKO neurons lacking Cplx1, Cplx2 and Cplx3 exhibited similar profound deficits in synaptic transmission as the Cplx DKO neurons, which I could corroborate as the preliminary findings in my study (Fig.24.). Cplx TKO neurons exhibited highly significant reductions in the Ca^{2+} -triggered EPSC amplitudes and the release probability of primed vesicles at their synapses, implying that Complexin facilitates release upon influx of Ca^{2+} . Previously, it was shown that loss of Complexins selectively reduced the synchronous phase of release but did not cause any alterations in the asynchronous release of vesicles (Reim et al., 2001). This finding raised doubts if the asynchronous release in neurons is indeed totally independent of Complexins.

The EPSC charge evoked by an action potential can be plotted as a cumulative integral that delineates the synchronous and asynchronous phases of release, both of which are dependent on Ca^{2+} , albeit with different affinity (Goda and Stevens, 1994). In my study, I found that Complexin loss leads to a decreased synchronous component of the EPSC, when compared with cells expressing endogenous Cplx1. However, the asynchronous component of release is

unaltered. Next, I investigated the cause for the presence of asynchronous release at similar levels in both Cplx CTRL and TKO neurons. For this purpose, I used the slow-Ca²⁺ chelating buffer EGTA-AM, which reduces asynchronous release but does not alter synchronous release in neurons. Prolonged exogenous application of EGTA-AM reduced the asynchronous component in Cplx CTRL neurons but not in the Cplx TKO neurons. Although EGTA-AM may still chelate the residual Ca²⁺ in the terminal and prevent release of the so called 'asynchronous pool' of vesicles in the Cplx TKO neurons, it is obvious that the vesicles that belong to the synchronous pool are likely 'desynchronized' due to the absence of Complexins. Thus, it can be inferred that vesicles from the synchronous pool in the Cplx CTRL neurons contributed to the asynchronous component of release in the Cplx TKO neurons.

An important factor that could affect the vesicle release process is the stability of the SNARE complex. The core complex formed by SNAP-25, Syntaxin-1 and Synaptobrevin-2 is a thermodynamically stable four helical bundle that brings the vesicles in close proximity to the presynaptic plasma membrane (Fasshauer et al., 1998). Loss of one of the SNARE components dramatically affects Ca²⁺-triggered exocytosis of synaptic vesicles. Individual deletions of the SNAP-25 and Synaptobrevin-2 proteins severely reduced amplitudes of the evoked EPSCs and the size of the RRP at the presynaptic active zone (Bronk et al., 2007; Deak et al., 2006). These findings imply that in the absence of SNARE components, the SNARE core complex required for maintenance of the primed pool of vesicles is disrupted leading to severe deficits in the number of primed vesicles competent for fusion and the magnitude of Ca²⁺-evoked transmitter release. The innately stable SNARE complex comprises of the four helices contributed by the SNARE components, connected by (leucine) zipper like layers with strong hydrophobic interactions between amino acids at the centre of the bundle (Pabst et al., 2000). It has been shown that Complexin binds in an anti-parallel orientation within the Syntaxin-Synaptobrevin groove of the SNARE complex, and this binding propagates the preassembled SNARE complex to a metastable state while reducing steric repulsions between the apposing membranes (Chen et al., 2002). Such an assembly is likely a prerequisite for greater release efficacy of the highly-fusogenic vesicles awaiting the action potential trigger and Ca²⁺ influx.

Major interactions were found between the central α -helical domain of Complexins and the Syntaxin-Synaptobrevin motifs exposed within the groove of the helical bundle. Of particular interest are the residues lysine (K) at position 69 and tyrosine (Y) at position 70 on the Cplx1 (also conserved at the same positions in Cplx2) central α -helix that interact via a salt bridge and a hydrogen bond, respectively with an aspartate residue (D) at position 218 of Syntaxin

(Chen et al., 2002). Disruption of this interaction due to alanine point mutations (K69A/Y70A) abolished Cplx1 binding to the SNARE complex in co-sedimentation assays (Xue et al., 2007). Also, SFV-mediated over-expression of Cplx1-K69A/Y70A in the Cplx DKO neurons did not rescue the deficits in release (Xue et al., 2007), while expression of a single allele of wild type Cplx1, could efficiently mediate transmitter release in response to increases in the cytosolic Ca²⁺ concentration. Another attractive candidate target on the Cplx3 and Cplx4 sequence is the 'CAAX' motif at the C-terminal end, which is required for farnesylation (attachment of a 15-Carbon moiety to the translated protein) and targeting to membranes *in-vivo* (Reim et al., 2005). Point mutation of cysteine to serine (Cplx3-C155S, Cplx4-C157S) completely eliminated membrane association of the proteins. Thus, the presence of multiple paralogs of mammalian Complexins is intriguing in terms of their requirement at central synapses. Furthermore, the conservation of the lysine-tyrosine amino acid duo among all known Cplx homologs and the unique requirement of the CAAX motif on Cplx3 and Cplx4 led to further speculation on the functional role of these residues, and the effects of stable long-term expression of the Complexin mutants in the Cplx TKO neurons.

In parallel to the present study, co-sedimentation assays were performed by my supervisor, Dr. K. Reim, who used with GST-fused full-length Complexin constructs and mouse brain homogenates to determine SNARE complex binding. Strong binding of Cplx1 and Cplx2 wild type constructs with the SNARE complex components Syntaxin-1, SNAP-25 and Synaptobrevin-2 was evident, while minimal binding of Cplx3-WT to the cognate SNAREs was still observable but hardly any binding was detectable in case of Cplx4 (Appendix 6.2.). It could be thus inferred that Complexins found in the brain have a higher binding affinity to the neuronal SNARE core components. However, alanine point mutations on the central α -helix of full-length Cplx1 (K69A/Y70A), Cplx2 (K69A/Y70A), Cplx3 (K79A/Y80A) and Cplx4 (K80A/Y81A) abolished the apparent SNARE complex binding of the respective constructs. Point mutation of the CAAX motif on Cplx3 (C155S) did not alter its binding to the SNARE complex. Hence, the mutants and the respective wild type constructs were expressed in the Cplx TKO neurons to obtain an insight on their functional role in transmitter release.

Reintroduction of the Complexin wild type paralogs - Cplx1, Cplx2, Cplx3 and Cplx4 - in the Cplx TKO neurons could rescue the deficit in AP-evoked release, vesicular release probability, synchronicity of release and short-term plasticity (Fig.26.E. and 26.F.). It is interesting to note that all Cplx paralogs can significantly rescue the peak amplitudes of EPSCs in the Cplx TKO neurons, but Cplx1 and Cplx2 seem to have a higher efficacy in restoring the synchronicity of

release in the TKO neurons when compared with Cplx3 and Cplx4 (Fig.26.B.). These facts corroborate the different affinities of the Complexin paralogs to the SNARE complex.

Similar to earlier findings, lentiviral expression of mutant Complexins devoid of a functional SNARE binding domain (Cplx1-K69A/Y70A, Cplx2-K69A/Y70A, Cplx3-K79A/Y80A and Cplx4-K80A/Y81A) in the Cplx TKO neurons could not rescue the Ca²⁺-evoked release, vesicular release probability, synchronicity of release and short-term plasticity. It is important to note that although endogenous Cplx3 can still bind the neuronal SNARE complex with lower affinity when compared with Cplx1 and Cplx2, lentiviral expression of wild type Cplx3 at levels far above the endogenous Cplx3 accentuates its rescue efficacy (Fig.29. and 34.A.). The presence of a functional farnesylation motif on the over-expressed wild type Cplx3 increases its local concentration once targeted to membranes (Reim et al., 2005), and this in turn, likely promotes the binding of Cplx3 to more SNARE complexes and efficiently supports vesicle fusion. This claim is also justified by the finding that the SNARE binding domain mutant Cplx3-K79A/Y80A, albeit possessing an intact farnesylation site, is unable to rescue the synaptic deficits in the TKO neurons. Comparably, the lack of a functional farnesylation site on Cplx3 (C155S), while not affecting the SNARE binding of Cplx3 due to the presence of its functional central α -helical domain (Appendix 6.2), is expected to abolish the increased local concentration of the proteins at the membranes, and the resultant cytosolic Cplx3 protein is expected to act less efficiently due to its low SNARE complex binding affinity. These predictions are met by my observation that Cplx3 (C155S) is much less efficacious in rescuing the synaptic defects in Cplx TKO neurons than wild type Cplx3 (Fig.29.). Similarly, wild type Cplx4 does not show an apparent binding to the neuronal SNARE complex, but it possesses the ability to partially rescue the synaptic deficits in the Cplx TKO neurons unlike its SNARE binding domain mutant Cplx4-K80A/Y81A or its farnesylation mutant Cplx4-C157S (Fig.30.). A plausible explanation for this result is that Cplx4 may still bind the neuronal SNARE complex with very low affinity, undetectable by standard biochemical methods. Analogous to Cplx3, farnesylation of the translated Cplx4 protein product targets it to the membranes (Reim et al., 2005), which would increase its local concentration and support binding to the SNARE complex in a more physiological environment within neurons.

In summation, the biochemical and physiological data clearly define that mammalian wild type Complexins play a significant positive role in facilitating and synchronizing Ca²⁺-triggered release. Farnesylation of Cplx3 and Cplx4 likely increases their local concentration at synapses and this bypasses their rather low SNARE complex binding affinity.

4.2.2. Mammalian Complexins act on a fusion-competent vesicle pool in glutamatergic autapses.

A recent ultrastructural study showed that the number of membrane tethered and membrane attached (docked) vesicles at the presynaptic active zone in hippocampal synapses of Cplx CTRL and Cplx TKO was unaltered (Imig et al., 2014). By the application of a hyperosmotic sucrose (500 mM) solution, the RRP of vesicles at the presynaptic terminal is completely depleted. The RRP is measured as the total charge of the transient synaptic current released during this Ca^{2+} -independent process (Rosenmund and Stevens, 1996). The RRP size was unaltered irrespective of whether and which Complexins were expressed. In correlation with the morphological data from EM studies and the functional data, it can be inferred that Complexins do not play an essential role in docking or priming of vesicles at the active zone. Xue et al. (2007) have shown that a significant reduction in the fraction of pool released and response onset latency was apparent at submaximal osmotic concentrations (250 mM Sucrose). This finding led to the conclusion that Complexin binding to the SNARE complex is required for lowering the energy required for fusion and increasing the propensity of vesicles to fuse, i.e. that Complexins act to increase the fusogenicity of vesicles.

Apart from exhibiting an increased spontaneous release rate, shRNA mediated knockdown of Complexins in cultured cortical neurons show an apparent reduction in RRP size, which has been attributed to a priming defect (Kaeser-Woo et al., 2012). One may argue that the increased spontaneous release or 'an unclamping effect' in the absence of Complexins may cause a consistent depletion of the RRP, although the spontaneous release rates in the absence of Complexins are unlikely to deplete the RRP. Further, the clamping and priming functions are separable in the Complexin knockdown neurons. It has been shown that introducing a Complexin 'poorclamp' mutant (K26E/L41K/E47K) in the knockdown neurons does in fact restore the pool size to wild type levels indicating that an RRP of vesicles can still be present in Complexin knockdown neurons if Complexin is otherwise functional (Yang et al., 2010). It is obvious that the low Ca^{2+} -evoked release at knockdown synapses implies an inherent defect in the vesicle fusogenicity in the absence of Complexins. It is likely that the highly fusogenic or 'superprimed' state of vesicles (Maximov et al., 2009) is unstable due to the acute loss of Complexins and thus the propensity of vesicles to fuse is decreased likely, causing a lower fraction of vesicles to be released even if a normal RRP is present. Another line of argument that could raise suspicions regarding the notion of changed RRP in the Complexin knockdown synapses concerns the methodology of application of the

hyperosmotic sucrose (500 mM) solution. Hypertonic sucrose unlike the intermediate concentration (250 mM), when applied to neurons using our fast perfusion system immediately floods the synaptic terminals to release all vesicles at the Cplx TKO synapses (Xue et al., 2008). However, the knockdown studies have invariably used a 'picospritzer' for sucrose application, which provides a point-source-like way of application, so that the target neurons likely receive a gradient of sucrose concentrations. In summary, I would argue based on my results and the arguments outlined above that Complexins are not involved in vesicle priming and RRP maintenance.

4.2.3. Mammalian Complexins do not 'clamp' vesicle fusion at glutamatergic synapses.

In the present study, the spontaneous release in the Cplx TKO neurons, measured by blocking action potentials, was reduced to a small extent. It is interesting to note that the frequency of spontaneous release (mEPSC) events is not significantly altered in Cplx TKO neurons expressing the Complexin SNARE binding domain mutants and farnesylation mutants when compared with neurons expressing the respective wild type Complexins, indicating that spontaneous vesicle fusion can occur independently of Complexin binding to the SNARE complex. This leads to the conclusion that a functional or functionally redundant Complexin does not necessarily have an effect on the spontaneous release in the neurons. In my study, I have shown that the preassembled SNARE complex in the presence of other SNARE co-factors but without Complexins does possess an intrinsic ability to catalyze fusion, albeit less synchronously. Thus, it is possible that the partially zippered SNARE complex, which is highly stable and protected at its central layers (Chen et al., 2002), is able to cause spontaneous fusion of vesicles in a probabilistic fashion, occurring on a prolonged time scale.

It is surprising to note the stark differences between spontaneous release observed in Complexin knockout neurons and knockdown neurons. Both autaptic and mass cultures of hippocampal neurons from Cplx TKO mice showed hardly any changes in spontaneous release. However, shRNA mediated Complexin knockdown caused a strong increase in spontaneous release in cultured cortical neurons. Lentiviral expression of Complexin carrying a '4M' (R48/R59/K69/Y70) alanine mutations, which abolishes SNARE complex binding in the knockdown neurons, behaved like an 'unclamping Complexin', exhibiting extremely high rates of spontaneous release, while point mutations on the Synaptobrevin-2 motif (Syb-2 3A) phenocopied the Complexin knockdown (Maximov et al., 2009). In this case, it was shown that Complexin binding to the SNARE complex is essential for its clamping function. High or

low extracellular Ca^{2+} does not cause the increase in mini-frequency seen upon Complexin perturbation (Yang et al., 2010), and it is unlikely that the neuron culture technique employed may cause such a dramatic phenotype, because mass cultured and autaptic hippocampal neurons of Cplx TKO mice exhibit similar phenotypes. Developmental compensation by the maturing synapses has been considered as a plausible cause of the lack of effects on spontaneous release in the constitutive Complexin knockout neurons (reviewed by Melia, 2007). On the other hand, it is possible that there may be off-target effects of the shRNA mediated knockdown in neurons, which leads to defects in the endogenous miRNA processing (Fineberg et al., 2009; Baek et al., 2014) and subsequent gene dysregulation. This might, in turn, cause an up-regulation or down-regulation of protein function and thus, incongruities in synaptic function.

4.2.4. Mode of Complexin function – Synaptotagmin interaction in transmitter release

My study sheds new light on the mode of action of Complexins along the molecular pathway governing synaptic vesicle exocytosis. All mammalian Complexins are facilitators of the synaptic vesicle fusion and act at a late-step of Ca^{2+} -dependent vesicle fusion. Primed vesicles release synchronously in the presence of Complexins. Although previous studies have shown that the N-terminus of Complexins is essential for facilitating release (Xue et al., 2010), in order to achieve synchronicity of release, the intact function of the central α -helical domain is essential in all Complexin paralogs. With the unique motif for post-translational farnesylation, the Cplx3 and Cplx4 are targeted to membranes and thus, are likely present at high local concentrations to bind SNARE complexes and catalyze efficient fusion.

With respect to Cplx3 and Cplx4, both the farnesylation motif and the SNARE binding motif are indispensable for their function. The Complexins likely operate in the synaptic vesicle fusion pathway by initially binding to the partially assembled SNARE complex, stabilizing it to a metastable state wherein the vesicle is highly fusogenic or superprimed, and aiding the complete zippering of the SNARE complex by reducing the energy barrier of membrane fusion. It is easy to envision that this action, coupled with the arrival of a Ca^{2+} trigger and Synaptotagmin binding to the SNAREs, causes the apposing membranes of the vesicle and the presynapse to fuse, resulting in neurotransmitter release.

In my study, I have attempted to contribute to the dissection of the molecular mechanisms of interaction of the primary Ca^{2+} -sensor Syt-1 and Complexin in the synaptic vesicle release

process. Syt-1 is anchored to the vesicle membrane and most studies imply that loss of Syt-1 almost completely eliminates synchronous vesicle fusion in neurons (Geppert et al., 1994; Nishiki and Augustine, 2004). In such a scenario, it is important to note that endogenous Complexins are unable to facilitate synchronous fusion in the absence of Syt-1. However, genetic deletion of Cplx1 and Cplx2 from Syt-1 KO animals reduced the mainly asynchronous transmitter release elicited in the Syt-1 KO neurons even further (Xue et al., 2010), showing that Complexins can indeed mediate some vesicle fusion independently of Syt-1. My data corroborate these findings in an interesting way. The total charge of EPSCs elicited in the absence of Complexins (Cplx TKO) is approximately 77% of the EPSC charge elicited by synchronous release in the presence of Complexins (Cplx CTRL) (Fig.25.A. and 25.B.). Correspondingly, the data I have acquired with exogenous application of EGTA-AM indicate that despite the presence of endogenous Syt-1 in the Cplx TKO neurons, the synchronous release of the vesicles within the 'synchronous pool' is impaired.

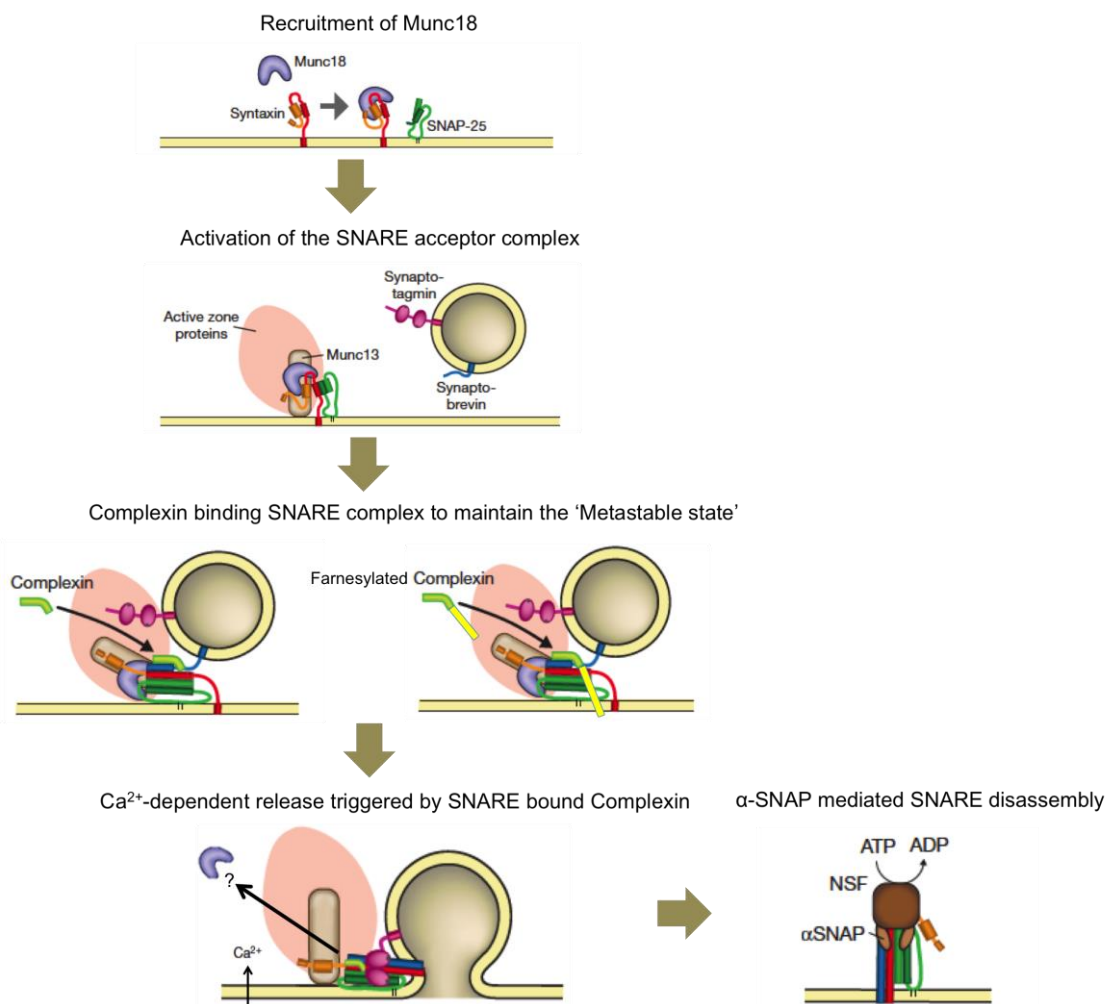


Figure 36. Complexin and molecular pathway of synaptic vesicle release. Munc18 binds to the closed conformation of Syntaxin-1 and the N-

peptide of Syntaxin-1A, after which various proteins, such as SNAP-25, Munc13, Syntaxin-1, Munc18, assemble to form the SNARE acceptor complex. As the synaptic vesicle approaches the active zone, it is docked to the membrane by the four-helical bundle formed by the SNARE core components. This process is supported by priming proteins, such as Munc13s, and CAPSs. Thereafter, Complexin binds to the preassembled SNARE complex with a high affinity via its central α -helical domain and maintains the SNARE complex in a 'metastable state' so that the vesicles are highly fusogenic (Superprimed). Upon arrival of a Ca^{2+} -trigger, the vesicles fuse by the co-operative action of Complexin and Synaptotagmin. Complexin binding to the SNARE complex improves the release efficacy. (Adapted and modified from Jahn and Fasshauer, 2012).

This observation is in nice correlation with the fact the Complexin and Syt-1 both cooperatively function in synchronizing vesicle release at synapses. Single vesicle content mixing assays have shown that cooperative action of Syt-1 and Ca^{2+} are the main thrust for fusion pore expansion, while Complexin is involved in pore formation and more robustly at the early stages of fusion-pore expansion (Lai et al., 2013). Also, ITC and TIRF microscopy based studies have shown that Cplx1 and a fragment of Syt-1 containing the C2AB domains can simultaneously bind to membrane-anchored SNARE complexes, and that full length Cplx1 binds more tightly to the membrane anchored SNARE complex and is not displaced by Syt-1 (Xu et al., 2013). Therefore, it can be interpreted that *in-vivo* Syt-1 is likely required for maintaining the speed of synchronous Ca^{2+} -dependent vesicle fusion, while Complexins are required to maintain the number of highly fusogenic vesicles via SNARE interaction, and thus improve the efficacy of synaptic vesicle release.

5. Summary and Perspectives

5.1. Summary and Perspectives - SNAP-29

SNAP-29 belongs to the SNAP-25 family of proteins and shares about 17% sequence identity with SNAP-25, the major neuronal SNARE protein. Early studies claimed that over-expression of SNAP-29 negatively modulates neurotransmission in SCG neurons by inhibiting SNARE disassembly post vesicle fusion, however, the role of endogenous SNAP-29 was neglected. In the present study, it is clear the conditional knockout of SNAP-29 from the forebrain glutamatergic neurons caused no obvious changes in synaptic parameters measured such as EPSC amplitudes, RRP size, vesicular release probability, and miniature release, when compared with wild-type littermate neurons. Similarly, constitutive knockout of SNAP-29 also caused no significant alterations in the synaptic parameters at both glutamatergic and GABAergic neurons, however, the new-born mice suffered from a keratoderma phenotype and were susceptible to perinatal lethality. Although synaptic deficits can be excluded as a possible cause for lethality, loss of the ubiquitously expressed SNAP-29 may have adverse effects on other secretory pathways.

Loss of SNAP-25 in neurons leads to dramatic deficits in synaptic parameters such evoked EPSC amplitudes, RRP size but the miniature spontaneous release was not severely affected. These results led to claims that endogenous SNAP-29 may play a role in mediating spontaneous fusion in the SNAP-25 null mutant neurons. However, loss of SNAP-29 does not cause any significant changes in spontaneous vesicle fusion, which may be compensated by the presence of endogenous SNAP-25. It would be interesting to test the SNAP-29 KO in the background of the SNAP-25 KO (SNAP-25/SNAP-29 DKO) to ascertain the effects of loss of both the proteins and to test the efficacy of transmitter release by individually reintroducing both paralogs.

5.2. Summary and Perspectives - Complexins

Complexins are small, highly charged proteins involved in the process of synaptic neurotransmitter release. Four mammalian Complexins paralogs Cplx1, Cplx2, Cplx3 and Cplx4 exist, of which Cplx1, Cplx2 and low levels of Cplx3 are expressed in the brain, while Cplx3 and Cplx4 are prominently expressed in the retina. Cplx1 and Cplx2 share 84% sequence identity while Cplx3 and Cplx4 share 58% sequence identity. All the paralogs have a conserved central α -helical domain that is essential for binding to the SNARE complex during the synaptic transmitter release process. Cplx3 and Cplx4 have a unique CAAX motif at their C-terminal end, which farnesylates the translated proteins and targets them to membranes. In the present study, genetic deletion of Cplx1, Cplx2 and Cplx3 (Cplx TKO) from the mouse brain impairs neurotransmitter release. Synaptic parameters such as evoked EPSC amplitudes, vesicular release probability, synchronous release and short-term plasticity are profoundly diminished in the Cplx TKO glutamatergic neurons. Lentiviral expression of wild type Cplx1, Cplx2, Cplx3 and Cplx4 in neurons can rescue the synaptic deficits and improve transmitter release significantly, but to variable extents. It is corroborated by their variable affinities to SNARE complex binding. Cplx1 and Cplx2 bind to the neuronal SNARE complex with high affinity, while Cplx3 binds with comparatively lower affinity and Cplx4 does not show any detectable binding to the neuronal SNARE complex. Point mutations on the central α -helical SNARE binding domain of Complexins abolished binding to the SNARE complex. None of the SNARE binding domain mutant Complexins could rescue the synaptic deficits in the Cplx TKO neurons. Point mutation on the CAAX motif of Cplx3 and Cplx4 was shown previously to abolish protein targeting to membranes and the farnesylation mutant Cplx3 and Cplx4 could also not rescue the synaptic deficits in the Cplx TKO neurons. Thus, it can be concluded that wild type Complexins can efficiently mediate synchronous neurotransmission in neurons. Intact functional central α -helix on Complexins is essential for binding to the SNARE complex. The farnesylation of Cplx3 and Cplx4 increases their local concentration at membranes and circumvents their low SNARE binding affinity, which facilitates transmitter release.

Complexins are essential for fast Ca^{2+} -triggered synchronous release in neurons, and their absence leads to a two-fold reduction in the apparent Ca^{2+} sensitivity of release. Exogenous application of tens of millimolar of Ca^{2+} could simply bypass this phenotype (Reim et al., 2001; Xue et al., 2008). However, extracellular Ca^{2+} in the range of tens of millimoles is not an optimal physiological measure to determine the efficacy and kinetics of evoked transmitter release, which occurs on a time scale of a few milliseconds sustained by very low

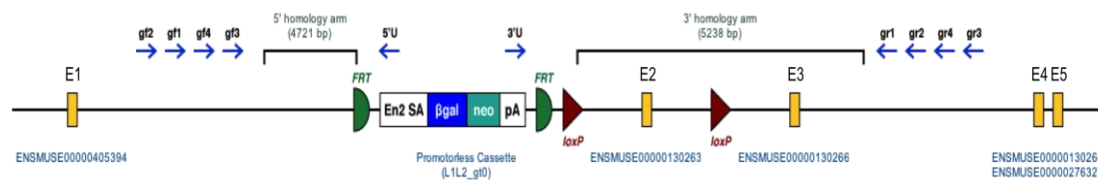
intraterminal Ca^{2+} concentrations. Experiments on uncaging- Ca^{2+} at the presynaptic terminals by UV-flash photolysis have shown that intracellular Ca^{2+} concentration in the range of a few hundred nanomolar is sufficient to trigger efficient transmitter release (Burgalossi et al., 2012). Therefore, it would be ideal to perform photolysis of caged- Ca^{2+} by UV-flash on Cplx-control and Cplx-TKO neurons to determine the exact amounts of Ca^{2+} diffusing into the terminal causing simultaneous release. Assessment of the kinetics of release will give a clear picture about the fusogenicity of primed vesicles at the synapse in the presence and absence of Complexins. This experiment will provide new insights on the molecular mechanisms underlying synaptic release mediated by the SNARE-complex bound Complexin in response to a transient physiological Ca^{2+} signal.

6. Appendix

6.1. Genetic deletion of SNAP-29 in mice

Exon 2 (E2) of the SNAP-29 gene was flanked by two LoxP sites on a target vector. Cre-mediated recombination to delete E2 was driven by crossing the floxed-mice with mice expressing cre-recombinase under the Nex promoter (Nex-cre mice, Goebbels et al., 2006), resulting in a conditional knockout of SNAP-29, or with mice expressing cre-recombinase under the adenovirus E1a promoter, resulting in a constitutive knockout of SNAP-29 (as shown below).

Targeted SNAP-29 allele:

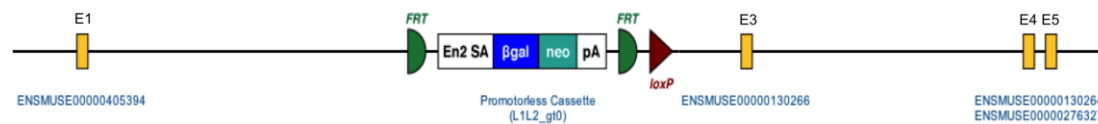


X



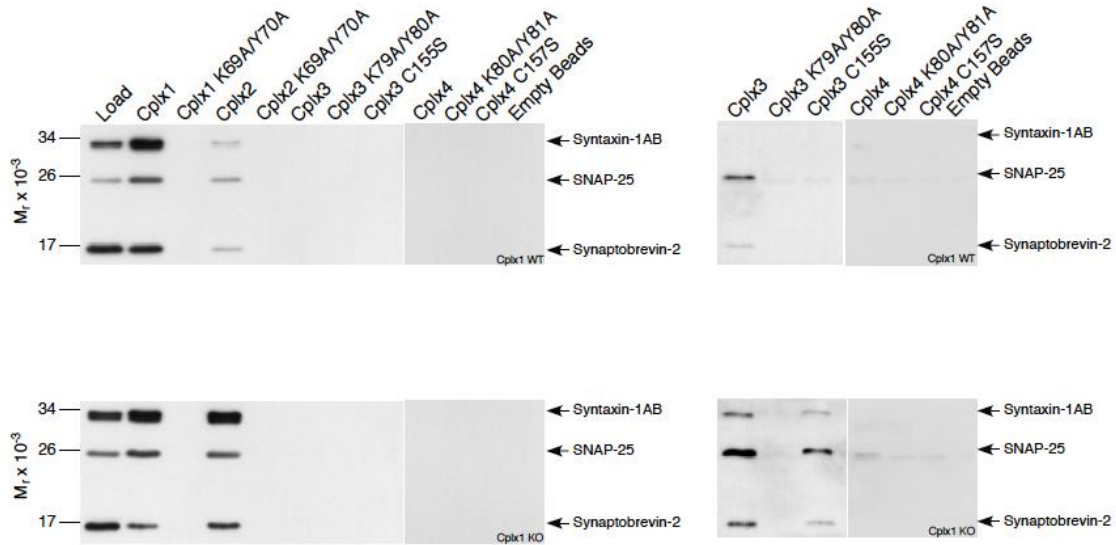
„Cre-recombinase“

Recombined SNAP-29 KO allele:



(Data from Georg Wieser, PhD student, MPIEM)

6.2. Co-sedimentation assay of GST-fused full length Complexins



(Data from Dr. Kerstin Reim)

Mouse brain homogenates from Cplx1 WT and Cplx1 KO animals were used for co-sedimentation assays to determine the binding affinities of various Complexins to the SNARE complex. Full-length constructs for Cplx1, Cplx2, Cplx3 and Cplx4 were used as wild type, carrying double point mutations on the lysine (K) and tyrosine (Y) residues in the respective SNARE binding domains. Point mutation of the Cysteine residue on the farnesylation domains (CAAX motif) of Cplx3 and Cplx4 was also used in the study. In the Cplx1 WT sample, SNARE binding of Cplx1-WT, Cplx2-WT and Cplx3-WT (at higher exposure times) is detectable. In the Cplx1 KO sample, binding of Cplx1-WT and Cplx2-WT to the cognate SNAREs is detectable at lower exposures, whereas binding of Cplx3-WT and Cplx3-C155S mutant (with an intact SNARE binding domain) is detectable at higher exposures. SNARE binding of Cplx4-WT is undetectable irrespective of the exposure times. Mutation of the SNARE binding domain on all Cplx paralogs abolishes SNARE binding.

7. Bibliography

- An, S.J., Grabner, C.P., and Zenisek, D. (2010). Real-time visualization of complexin during single exocytic events. *Nature neuroscience* *13*, 577-583.
- Arancillo, M., Min, S.W., Gerber, S., Munster-Wandowski, A., Wu, Y.J., Herman, M., Trimbuch, T., Rah, J.C., Ahnert-Hilger, G., Riedel, D., *et al.* (2013). Titration of Syntaxin1 in mammalian synapses reveals multiple roles in vesicle docking, priming, and release probability. *The Journal of neuroscience : the official journal of the Society for Neuroscience* *33*, 16698-16714.
- Archer, D.A., Graham, M.E., and Burgoyne, R.D. (2002). Complexin regulates the closure of the fusion pore during regulated vesicle exocytosis. *The Journal of biological chemistry* *277*, 18249-18252.
- Augustin, I., Betz, A., Herrmann, C., Jo, T., and Brose, N. (1999a). Differential expression of two novel Munc13 proteins in rat brain. *The Biochemical journal* *337*, 363-371.
- Augustin, I., Rosenmund, C., Sudhof, T.C., and Brose, N. (1999b). Munc13-1 is essential for fusion competence of glutamatergic synaptic vesicles. *Nature* *400*, 457-461.
- Basu, J., Shen, N., Dulubova, I., Lu, J., Guan, R., Guryev, O., Grishin, N.V., Rosenmund, C., and Rizo, J. (2005). A minimal domain responsible for Munc13 activity. *Nature structural & molecular biology* *12*, 1017-1018.
- Baek, S.T., Kerjan, G., Bielas, S.L., Lee, J.E., Fenstermaker, A.G., Novarino, G., and Gleeson, J.G. (2014). Off-target effect of doublecortin family shRNA on neuronal migration associated with endogenous microRNA dysregulation. *Neuron* *82*, 1255-1262.
- Bekkers, J.M., and Stevens, C.F. (1991). Excitatory and inhibitory autaptic currents in isolated hippocampal neurons maintained in cell culture. *Proceedings of the National Academy of Sciences of the United States of America* *88*, 7834-7838.
- Bennett, M.K., and Scheller, R.H. (1994). A molecular description of synaptic vesicle membrane trafficking. *Annual review of biochemistry* *63*, 63-100.
- Betz, A., Thakur, P., Junge, H.J., Ashery, U., Rhee, J.S., Scheuss, V., Rosenmund, C., Rettig, J., and Brose, N. (2001). Functional interaction of the active zone proteins Munc13-1 and RIM1 in synaptic vesicle priming. *Neuron* *30*, 183-196.
- Bowen, M.E., Weninger, K., Ernst, J., Chu, S., and Brunger, A.T. (2005). Single-molecule studies of synaptotagmin and complexin binding to the SNARE complex. *Biophysical journal* *89*, 690-702.
- Bracher, A., Kadlec, J., Betz, H., and Weissenhorn, W. (2002). X-ray structure of a neuronal complexin-SNARE complex from squid. *The Journal of biological chemistry* *277*, 26517-26523.

- Bronk, P., Deak, F., Wilson, M.C., Liu, X., Sudhof, T.C., and Kavalali, E.T. (2007). Differential effects of SNAP-25 deletion on Ca²⁺-dependent and Ca²⁺-independent neurotransmission. *Journal of neurophysiology* *98*, 794-806.
- Brose, N. (2008). For better or for worse: complexins regulate SNARE function and vesicle fusion. *Traffic* *9*, 1403-1413.
- Brose, N. (2009). Synaptogenic proteins and synaptic organizers: "many hands make light work". *Neuron* *61*, 650-652.
- Brose, N. (2013). Why we need more synaptogenic cell-adhesion proteins. *Proceedings of the National Academy of Sciences of the United States of America* *110*, 3717-3718.
- Brose, N., Hofmann, K., Hata, Y., and Sudhof, T.C. (1995). Mammalian homologues of *Caenorhabditis elegans* unc-13 gene define novel family of C2-domain proteins. *The Journal of biological chemistry* *270*, 25273-25280.
- Brose, N., Petrenko, A.G., Sudhof, T.C., and Jahn, R. (1992). Synaptotagmin: a calcium sensor on the synaptic vesicle surface. *Science* *256*, 1021-1025.
- Buhl, L.K., Jorquera, R.A., Akbergenova, Y., Huntwork-Rodriguez, S., Volfson, D., and Littleton, J.T. (2013). Differential regulation of evoked and spontaneous neurotransmitter release by C-terminal modifications of complexin. *Molecular and cellular neurosciences* *52*, 161-172.
- Burgalossi, A., Jung, S., Man, K.N., Nair, R., Jockusch, W.J., Wojcik, S.M., Brose, N., and Rhee, J.S. (2012). Analysis of neurotransmitter release mechanisms by photolysis of caged Ca²⁺(+) in an autaptic neuron culture system. *Nature protocols* *7*, 1351-1365.
- Cai, H., Reim, K., Varoqueaux, F., Tapechum, S., Hill, K., Sorensen, J.B., Brose, N., and Chow, R.H. (2008). Complexin II plays a positive role in Ca²⁺-triggered exocytosis by facilitating vesicle priming. *Proceedings of the National Academy of Sciences of the United States of America* *105*, 19538-19543.
- Cao, P., Yang, X., and Sudhof, T.C. (2013). Complexin activates exocytosis of distinct secretory vesicles controlled by different synaptotagmins. *The Journal of neuroscience : the official journal of the Society for Neuroscience* *33*, 1714-1727.
- Chen, X., Tomchick, D.R., Kovrigin, E., Arac, D., Machius, M., Sudhof, T.C., and Rizo, J. (2002). Three-dimensional structure of the complexin/SNARE complex. *Neuron* *33*, 397-409.
- Cho, R.W., Song, Y., and Littleton, J.T. (2010). Comparative analysis of *Drosophila* and mammalian complexins as fusion clamps and facilitators of neurotransmitter release. *Molecular and cellular neurosciences* *45*, 389-397.

- Craig, A.M., Banker, G., Chang, W., McGrath, M.E., and Serpinskaya, A.S. (1996). Clustering of gephyrin at GABAergic but not glutamatergic synapses in cultured rat hippocampal neurons. *The Journal of neuroscience : the official journal of the Society for Neuroscience* 16, 3166-3177.
- de Wit, H., Walter, A.M., Milosevic, I., Gulyas-Kovacs, A., Riedel, D., Sorensen, J.B., and Verhage, M. (2009). Synaptotagmin-1 docks secretory vesicles to syntaxin-1/SNAP-25 acceptor complexes. *Cell* 138, 935-946.
- Deak, F., Shin, O.H., Kavalali, E.T., and Sudhof, T.C. (2006). Structural determinants of synaptobrevin 2 function in synaptic vesicle fusion. *The Journal of neuroscience : the official journal of the Society for Neuroscience* 26, 6668-6676.
- Delgado-Martinez, I., Nehring, R.B., and Sorensen, J.B. (2007). Differential abilities of SNAP-25 homologs to support neuronal function. *The Journal of neuroscience : the official journal of the Society for Neuroscience* 27, 9380-9391.
- Diao, J., Cipriano, D.J., Zhao, M., Zhang, Y., Shah, S., Padolina, M.S., Pfuetzner, R.A., and Brunger, A.T. (2013). Complexin-1 enhances the on-rate of vesicle docking via simultaneous SNARE and membrane interactions. *Journal of the American Chemical Society* 135, 15274-15277.
- Diao, J., Liu, R., Rong, Y., Zhao, M., Zhang, J., Lai, Y., Zhou, Q., Wilz, L.M., Li, J., Vivona, S., *et al.* (2015). ATG14 promotes membrane tethering and fusion of autophagosomes to endolysosomes. *Nature*.
- Dittman, J.S., and Regehr, W.G. (1998). Calcium dependence and recovery kinetics of presynaptic depression at the climbing fiber to Purkinje cell synapse. *The Journal of neuroscience : the official journal of the Society for Neuroscience* 18, 6147-6162.
- Elias, G.M., Elias, L.A., Apostolides, P.F., Kriegstein, A.R., and Nicoll, R.A. (2008). Differential trafficking of AMPA and NMDA receptors by SAP102 and PSD-95 underlies synapse development. *Proceedings of the National Academy of Sciences of the United States of America* 105, 20953-20958.
- Elias, G.M., Funke, L., Stein, V., Grant, S.G., Brecht, D.S., and Nicoll, R.A. (2006). Synapse-specific and developmentally regulated targeting of AMPA receptors by a family of MAGUK scaffolding proteins. *Neuron* 52, 307-320.
- Fasshauer, D., Eliason, W.K., Brunger, A.T., and Jahn, R. (1998a). Identification of a minimal core of the synaptic SNARE complex sufficient for reversible assembly and disassembly. *Biochemistry* 37, 10354-10362.
- Fasshauer, D., Sutton, R.B., Brunger, A.T., and Jahn, R. (1998b). Conserved structural features of the synaptic fusion complex: SNARE proteins reclassified as Q- and R-SNAREs. *Proceedings of the National Academy of Sciences of the United States of America* 95, 15781-15786.

- Fernandez, I., Arac, D., Ubach, J., Gerber, S.H., Shin, O., Gao, Y., Anderson, R.G., Sudhof, T.C., and Rizo, J. (2001). Three-dimensional structure of the synaptotagmin 1 C2B-domain: synaptotagmin 1 as a phospholipid binding machine. *Neuron* *32*, 1057-1069.
- Fernandez-Chacon, R., Konigstorfer, A., Gerber, S.H., Garcia, J., Matos, M.F., Stevens, C.F., Brose, N., Rizo, J., Rosenmund, C., and Sudhof, T.C. (2001). Synaptotagmin I functions as a calcium regulator of release probability. *Nature* *410*, 41-49.
- Fineberg, S.K., Kosik, K.S., and Davidson, B.L. (2009). MicroRNAs potentiate neural development. *Neuron* *64*, 303-309.
- Frassoni, C., Inverardi, F., Coco, S., Ortino, B., Grumelli, C., Pozzi, D., Verderio, C., and Matteoli, M. (2005). Analysis of SNAP-25 immunoreactivity in hippocampal inhibitory neurons during development in culture and in situ. *Neuroscience* *131*, 813-823.
- Fuchs-Telem, D., Stewart, H., Rapaport, D., Nousbeck, J., Gat, A., Gini, M., Lugassy, Y., Emmert, S., Eckl, K., Hennies, H.C., *et al.* (2011). CEDNIK syndrome results from loss-of-function mutations in SNAP29. *The British journal of dermatology* *164*, 610-616.
- Gascon, S., Paez-Gomez, J.A., Diaz-Guerra, M., Scheiffele, P., and Scholl, F.G. (2008). Dual-promoter lentiviral vectors for constitutive and regulated gene expression in neurons. *Journal of neuroscience methods* *168*, 104-112.
- Geppert, M., Goda, Y., Hammer, R.E., Li, C., Rosahl, T.W., Stevens, C.F., and Sudhof, T.C. (1994). Synaptotagmin I: a major Ca²⁺ sensor for transmitter release at a central synapse. *Cell* *79*, 717-727.
- Gerber, S.H., Rah, J.C., Min, S.W., Liu, X., de Wit, H., Dulubova, I., Meyer, A.C., Rizo, J., Arancillo, M., Hammer, R.E., *et al.* (2008). Conformational switch of syntaxin-1 controls synaptic vesicle fusion. *Science* *321*, 1507-1510.
- Giraudo, C.G., Eng, W.S., Melia, T.J., and Rothman, J.E. (2006). A clamping mechanism involved in SNARE-dependent exocytosis. *Science* *313*, 676-680.
- Giraudo, C.G., Garcia-Diaz, A., Eng, W.S., Chen, Y., Hendrickson, W.A., Melia, T.J., and Rothman, J.E. (2009). Alternative zippering as an on-off switch for SNARE-mediated fusion. *Science* *323*, 512-516.
- Giraudo, C.G., Garcia-Diaz, A., Eng, W.S., Yamamoto, A., Melia, T.J., and Rothman, J.E. (2008). Distinct domains of complexins bind SNARE complexes and clamp fusion in vitro. *The Journal of biological chemistry* *283*, 21211-21219.
- Goda, Y., and Stevens, C.F. (1994). Two components of transmitter release at a central synapse. *Proceedings of the National Academy of Sciences of the United States of America* *91*, 12942-12946.

- Greaves, J., Gorleku, O.A., Salaun, C., and Chamberlain, L.H. (2010). Palmitoylation of the SNAP25 protein family: specificity and regulation by DHHC palmitoyl transferases. *The Journal of biological chemistry* *285*, 24629-24638.
- Guzman, R.E., Schwarz, Y.N., Rettig, J., and Bruns, D. (2010). SNARE force synchronizes synaptic vesicle fusion and controls the kinetics of quantal synaptic transmission. *The Journal of neuroscience : the official journal of the Society for Neuroscience* *30*, 10272-10281.
- Hammarlund, M., Palfreyman, M.T., Watanabe, S., Olsen, S., and Jorgensen, E.M. (2007). Open syntaxin docks synaptic vesicles. *PLoS biology* *5*, e198.
- Hanson, P.I., Heuser, J.E., and Jahn, R. (1997). Neurotransmitter release - four years of SNARE complexes. *Current opinion in neurobiology* *7*, 310-315.
- Haucke, V., Neher, E., and Sigrist, S.J. (2011). Protein scaffolds in the coupling of synaptic exocytosis and endocytosis. *Nature reviews Neuroscience* *12*, 127-138.
- Heine, M., Groc, L., Frischknecht, R., Beique, J.C., Lounis, B., Rumbaugh, G., Huganir, R.L., Cognet, L., and Choquet, D. (2008). Surface mobility of postsynaptic AMPARs tunes synaptic transmission. *Science* *320*, 201-205.
- Heuser, J.E., and Reese, T.S. (1973). Evidence for recycling of synaptic vesicle membrane during transmitter release at the frog neuromuscular junction. *The Journal of cell biology* *57*, 315-344.
- Hobson, R.J., Liu, Q., Watanabe, S., and Jorgensen, E.M. (2011). Complexin maintains vesicles in the primed state in *C. elegans*. *Current biology : CB* *21*, 106-113.
- Hohenstein, A.C., and Roche, P.A. (2001). SNAP-29 is a promiscuous syntaxin-binding SNARE. *Biochemical and biophysical research communications* *285*, 167-171.
- Holt, M., Varoqueaux, F., Wiederhold, K., Takamori, S., Urlaub, H., Fasshauer, D., and Jahn, R. (2006). Identification of SNAP-47, a novel Qbc-SNARE with ubiquitous expression. *The Journal of biological chemistry* *281*, 17076-17083.
- Huntwork, S., and Littleton, J.T. (2007). A complexin fusion clamp regulates spontaneous neurotransmitter release and synaptic growth. *Nature neuroscience* *10*, 1235-1237.
- Imig, C., Min, S.W., Krinner, S., Arancillo, M., Rosenmund, C., Sudhof, T.C., Rhee, J., Brose, N., and Cooper, B.H. (2014). The morphological and molecular nature of synaptic vesicle priming at presynaptic active zones. *Neuron* *84*, 416-431.
- Ishizuka, T., Saisu, H., Suzuki, T., Kirino, Y., and Abe, T. (1997). Molecular cloning of synaphins/complexins, cytosolic proteins involved in transmitter release, in the electric organ of an electric ray (*Narke japonica*). *Neuroscience letters* *232*, 107-110.

- Iyer, J., Wahlmark, C.J., Kuser-Ahnert, G.A., and Kawasaki, F. (2013). Molecular mechanisms of COMPLEXIN fusion clamp function in synaptic exocytosis revealed in a new *Drosophila* mutant. *Molecular and cellular neurosciences* 56, 244-254.
- Jahn, R., and Fasshauer, D. (2012). Molecular machines governing exocytosis of synaptic vesicles. *Nature* 490, 201-207.
- Jahn, R., and Scheller, R.H. (2006). SNAREs--engines for membrane fusion. *Nature reviews Molecular cell biology* 7, 631-643.
- Jaskolski, F., Coussen, F., Nagarajan, N., Normand, E., Rosenmund, C., and Mulle, C. (2004). Subunit composition and alternative splicing regulate membrane delivery of kainate receptors. *The Journal of neuroscience : the official journal of the Society for Neuroscience* 24, 2506-2515.
- Jockusch, W.J., Speidel, D., Sigler, A., Sorensen, J.B., Varoqueaux, F., Rhee, J.S., and Brose, N. (2007). CAPS-1 and CAPS-2 are essential synaptic vesicle priming proteins. *Cell* 131, 796-808.
- Junge, H.J., Rhee, J.S., Jahn, O., Varoqueaux, F., Spiess, J., Waxham, M.N., Rosenmund, C., and Brose, N. (2004). Calmodulin and Munc13 form a Ca²⁺ sensor/effector complex that controls short-term synaptic plasticity. *Cell* 118, 389-401.
- Jurado, S., Goswami, D., Zhang, Y., Molina, A.J., Sudhof, T.C., and Malenka, R.C. (2013). LTP requires a unique postsynaptic SNARE fusion machinery. *Neuron* 77, 542-558.
- Kaesler-Woo, Y.J., Yang, X., and Sudhof, T.C. (2012). C-terminal complexin sequence is selectively required for clamping and priming but not for Ca²⁺ triggering of synaptic exocytosis. *The Journal of neuroscience : the official journal of the Society for Neuroscience* 32, 2877-2885.
- Katz, B., and Miledi, R. (1963). A Study of Spontaneous Miniature Potentials in Spinal Motoneurons. *The Journal of physiology* 168, 389-422.
- Katz, B., and Miledi, R. (1967). Tetrodotoxin and neuromuscular transmission. *Proceedings of the Royal Society of London Series B, Biological sciences* 167, 8-22.
- Kim, E., and Sheng, M. (2004). PDZ domain proteins of synapses. *Nature reviews Neuroscience* 5, 771-781.
- Kirsch, J., Wolters, I., Triller, A., and Betz, H. (1993). Gephyrin antisense oligonucleotides prevent glycine receptor clustering in spinal neurons. *Nature* 366, 745-748.
- Klenchin, V.A., and Martin, T.F. (2000). Priming in exocytosis: attaining fusion-competence after vesicle docking. *Biochimie* 82, 399-407.

- Krishnakumar, S.S., Radoff, D.T., Kummel, D., Giraudo, C.G., Li, F., Khandan, L., Baguley, S.W., Coleman, J., Reinisch, K.M., Pincet, F., *et al.* (2011). A conformational switch in complexin is required for synaptotagmin to trigger synaptic fusion. *Nature structural & molecular biology* 18, 934-940.
- Krueger, D.D., Tuffy, L.P., Papadopoulos, T., and Brose, N. (2012). The role of neurexins and neuroligins in the formation, maturation, and function of vertebrate synapses. *Current opinion in neurobiology* 22, 412-422.
- Kummel, D., Krishnakumar, S.S., Radoff, D.T., Li, F., Giraudo, C.G., Pincet, F., Rothman, J.E., and Reinisch, K.M. (2011). Complexin cross-links prefusion SNAREs into a zigzag array. *Nature structural & molecular biology* 18, 927-933.
- Laemmli, U.K. (1970). Cleavage of structural proteins during the assembly of the head of bacteriophage T4. *Nature* 227, 680-685.
- Li, F., Pincet, F., Perez, E., Giraudo, C.G., Taresté, D., and Rothman, J.E. (2011). Complexin activates and clamps SNAREpins by a common mechanism involving an intermediate energetic state. *Nature structural & molecular biology* 18, 941-946.
- Lin, M.Y., Rohan, J.G., Cai, H., Reim, K., Ko, C.P., and Chow, R.H. (2013). Complexin facilitates exocytosis and synchronizes vesicle release in two secretory model systems. *The Journal of physiology* 591, 2463-2473.
- Liu, J., Guo, T., Wei, Y., Liu, M., and Sui, S.F. (2006). Complexin is able to bind to SNARE core complexes in different assembled states with distinct affinity. *Biochemical and biophysical research communications* 347, 413-419.
- Liu, Y., Schirra, C., Stevens, D.R., Matti, U., Speidel, D., Hof, D., Bruns, D., Brose, N., and Rettig, J. (2008). CAPS facilitates filling of the rapidly releasable pool of large dense-core vesicles. *The Journal of neuroscience : the official journal of the Society for Neuroscience* 28, 5594-5601.
- Lu, B., Song, S., and Shin, Y.K. (2010). Accessory alpha-helix of complexin I can displace VAMP2 locally in the complexin-SNARE quaternary complex. *Journal of molecular biology* 396, 602-609.
- Ma, C., Li, W., Xu, Y., and Rizo, J. (2011). Munc13 mediates the transition from the closed syntaxin-Munc18 complex to the SNARE complex. *Nature structural & molecular biology* 18, 542-549.
- Malsam, J., Parisotto, D., Bharat, T.A., Scheutzow, A., Krause, J.M., Briggs, J.A., and Sollner, T.H. (2012). Complexin arrests a pool of docked vesicles for fast Ca²⁺-dependent release. *The EMBO journal* 31, 3270-3281.

- Malsam, J., Seiler, F., Schollmeier, Y., Rusu, P., Krause, J.M., and Sollner, T.H. (2009). The carboxy-terminal domain of complexin I stimulates liposome fusion. *Proceedings of the National Academy of Sciences of the United States of America* *106*, 2001-2006.
- Martin, J.A., Hu, Z., Fenz, K.M., Fernandez, J., and Dittman, J.S. (2011). Complexin has opposite effects on two modes of synaptic vesicle fusion. *Current biology : CB* *21*, 97-105.
- Marz, K.E., and Hanson, P.I. (2002). Sealed with a twist: complexin and the synaptic SNARE complex. *Trends in neurosciences* *25*, 381-383.
- Maximov, A., Tang, J., Yang, X., Pang, Z.P., and Sudhof, T.C. (2009). Complexin controls the force transfer from SNARE complexes to membranes in fusion. *Science* *323*, 516-521.
- McMahon, H.T., Missler, M., Li, C., and Sudhof, T.C. (1995). Complexins: cytosolic proteins that regulate SNAP receptor function. *Cell* *83*, 111-119.
- Melia, T.J., Jr. (2007). Putting the clamps on membrane fusion: how complexin sets the stage for calcium-mediated exocytosis. *FEBS letters* *581*, 2131-2139.
- Naldini, L., Blomer, U., Gallay, P., Ory, D., Mulligan, R., Gage, F.H., Verma, I.M., and Trono, D. (1996). In vivo gene delivery and stable transduction of nondividing cells by a lentiviral vector. *Science* *272*, 263-267.
- Pabst, S., Hazzard, J.W., Antonin, W., Sudhof, T.C., Jahn, R., Rizo, J., and Fasshauer, D. (2000). Selective interaction of complexin with the neuronal SNARE complex. Determination of the binding regions. *The Journal of biological chemistry* *275*, 19808-19818.
- Pabst, S., Margittai, M., Vainius, D., Langen, R., Jahn, R., and Fasshauer, D. (2002). Rapid and selective binding to the synaptic SNARE complex suggests a modulatory role of complexins in neuroexocytosis. *The Journal of biological chemistry* *277*, 7838-7848.
- Pan, P.Y., Cai, Q., Lin, L., Lu, P.H., Duan, S., and Sheng, Z.H. (2005). SNAP-29-mediated modulation of synaptic transmission in cultured hippocampal neurons. *The Journal of biological chemistry* *280*, 25769-25779.
- Radoff, D.T., Dong, Y., Snead, D., Bai, J., Eliezer, D., and Dittman, J.S. (2014). The accessory helix of complexin functions by stabilizing central helix secondary structure. *eLife* *3*.
- Rapaport, D., Lugassy, Y., Sprecher, E., and Horowitz, M. (2010). Loss of SNAP29 impairs endocytic recycling and cell motility. *PloS one* *5*, e9759.
- Ravichandran, V., Chawla, A., and Roche, P.A. (1996). Identification of a novel syntaxin- and synaptobrevin/VAMP-binding protein, SNAP-23, expressed in non-neuronal tissues. *The Journal of biological chemistry* *271*, 13300-13303.

- Reim, K., Mansour, M., Varoqueaux, F., McMahon, H.T., Sudhof, T.C., Brose, N., and Rosenmund, C. (2001). Complexins regulate a late step in Ca²⁺-dependent neurotransmitter release. *Cell* *104*, 71-81.
- Reim, K., Wegmeyer, H., Brandstatter, J.H., Xue, M., Rosenmund, C., Dresbach, T., Hofmann, K., and Brose, N. (2005). Structurally and functionally unique complexins at retinal ribbon synapses. *The Journal of cell biology* *169*, 669-680.
- Rhee, J.S., Betz, A., Pyott, S., Reim, K., Varoqueaux, F., Augustin, I., Hesse, D., Sudhof, T.C., Takahashi, M., Rosenmund, C., *et al.* (2002). Beta phorbol ester- and diacylglycerol-induced augmentation of transmitter release is mediated by Munc13s and not by PKCs. *Cell* *108*, 121-133.
- Rosenmund, C., Sigler, A., Augustin, I., Reim, K., Brose, N., and Rhee, J.S. (2002). Differential control of vesicle priming and short-term plasticity by Munc13 isoforms. *Neuron* *33*, 411-424.
- Rosenmund, C., and Stevens, C.F. (1996). Definition of the readily releasable pool of vesicles at hippocampal synapses. *Neuron* *16*, 1197-1207.
- Sabatini, B.L., and Regehr, W.G. (1996). Timing of neurotransmission at fast synapses in the mammalian brain. *Nature* *384*, 170-172.
- Sato, M., Saegusa, K., Sato, K., Hara, T., Harada, A., and Sato, K. (2011). *Caenorhabditis elegans* SNAP-29 is required for organellar integrity of the endomembrane system and general exocytosis in intestinal epithelial cells. *Molecular biology of the cell* *22*, 2579-2587.
- Schardt, A., Brinkmann, B.G., Mitkovski, M., Sereda, M.W., Werner, H.B., and Nave, K.A. (2009). The SNARE protein SNAP-29 interacts with the GTPase Rab3A: Implications for membrane trafficking in myelinating glia. *Journal of neuroscience research* *87*, 3465-3479.
- Schaub, J.R., Lu, X., Doneske, B., Shin, Y.K., and McNew, J.A. (2006). Hemifusion arrest by complexin is relieved by Ca²⁺-synaptotagmin I. *Nature structural & molecular biology* *13*, 748-750.
- Scheuss, V., Schneggenburger, R., and Neher, E. (2002). Separation of presynaptic and postsynaptic contributions to depression by covariance analysis of successive EPSCs at the calyx of held synapse. *The Journal of neuroscience : the official journal of the Society for Neuroscience* *22*, 728-739.
- Schneggenburger, R., Lopez-Barneo, J., and Konnerth, A. (1992). Excitatory and inhibitory synaptic currents and receptors in rat medial septal neurones. *The Journal of physiology* *445*, 261-276.

- Schoch, S., Deak, F., Konigstorfer, A., Mozhayeva, M., Sara, Y., Sudhof, T.C., and Kavalali, E.T. (2001). SNARE function analyzed in synaptobrevin/VAMP knockout mice. *Science* 294, 1117-1122.
- Seiler, F., Malsam, J., Krause, J.M., and Sollner, T.H. (2009). A role of complexin-lipid interactions in membrane fusion. *FEBS letters* 583, 2343-2348.
- Shin, O.H., Lu, J., Rhee, J.S., Tomchick, D.R., Pang, Z.P., Wojcik, S.M., Camacho-Perez, M., Brose, N., Machius, M., Rizo, J., *et al.* (2010). Munc13 C2B domain is an activity-dependent Ca²⁺ regulator of synaptic exocytosis. *Nature structural & molecular biology* 17, 280-288.
- Siksou, L., Varoqueaux, F., Pascual, O., Triller, A., Brose, N., and Marty, S. (2009). A common molecular basis for membrane docking and functional priming of synaptic vesicles. *The European journal of neuroscience* 30, 49-56.
- Sollner, T., Bennett, M.K., Whiteheart, S.W., Scheller, R.H., and Rothman, J.E. (1993a). A protein assembly-disassembly pathway in vitro that may correspond to sequential steps of synaptic vesicle docking, activation, and fusion. *Cell* 75, 409-418.
- Sollner, T., Whiteheart, S.W., Brunner, M., Erdjument-Bromage, H., Geromanos, S., Tempst, P., and Rothman, J.E. (1993b). SNAP receptors implicated in vesicle targeting and fusion. *Nature* 362, 318-324.
- Sorensen, J.B., Nagy, G., Varoqueaux, F., Nehring, R.B., Brose, N., Wilson, M.C., and Neher, E. (2003). Differential control of the releasable vesicle pools by SNAP-25 splice variants and SNAP-23. *Cell* 114, 75-86.
- Speidel, D., Varoqueaux, F., Enk, C., Nojiri, M., Grishanin, R.N., Martin, T.F., Hofmann, K., Brose, N., and Reim, K. (2003). A family of Ca²⁺-dependent activator proteins for secretion: comparative analysis of structure, expression, localization, and function. *The Journal of biological chemistry* 278, 52802-52809.
- Sprecher, E., Ishida-Yamamoto, A., Mizrahi-Koren, M., Rapaport, D., Goldsher, D., Indelman, M., Topaz, O., Chefetz, I., Keren, H., O'Brien T, J., *et al.* (2005). A mutation in SNAP29, coding for a SNARE protein involved in intracellular trafficking, causes a novel neurocutaneous syndrome characterized by cerebral dysgenesis, neuropathy, ichthyosis, and palmoplantar keratoderma. *American journal of human genetics* 77, 242-251.
- Steggmaier, M., Yang, B., Yoo, J.S., Huang, B., Shen, M., Yu, S., Luo, Y., and Scheller, R.H. (1998). Three novel proteins of the syntaxin/SNAP-25 family. *The Journal of biological chemistry* 273, 34171-34179.
- Stevens, C.F., and Tsujimoto, T. (1995). Estimates for the pool size of releasable quanta at a single central synapse and for the time required to refill the pool. *Proceedings of the National Academy of Sciences of the United States of America* 92, 846-849.

- Stevens, C.F., and Wesseling, J.F. (1999). Augmentation is a potentiation of the exocytotic process. *Neuron* 22, 139-146.
- Strenzke, N., Chanda, S., Kopp-Scheinflug, C., Khimich, D., Reim, K., Bulankina, A.V., Neef, A., Wolf, F., Brose, N., Xu-Friedman, M.A., *et al.* (2009). Complexin-I is required for high-fidelity transmission at the endbulb of Held auditory synapse. *The Journal of neuroscience : the official journal of the Society for Neuroscience* 29, 7991-8004.
- Su, Q., Mochida, S., Tian, J.H., Mehta, R., and Sheng, Z.H. (2001). SNAP-29: a general SNARE protein that inhibits SNARE disassembly and is implicated in synaptic transmission. *Proceedings of the National Academy of Sciences of the United States of America* 98, 14038-14043.
- Sudhof, T.C. (2004). The synaptic vesicle cycle. *Annual review of neuroscience* 27, 509-547.
- Sudhof, T.C. (2012). The presynaptic active zone. *Neuron* 75, 11-25.
- Suh, Y.H., Terashima, A., Petralia, R.S., Wenthold, R.J., Isaac, J.T., Roche, K.W., and Roche, P.A. (2010). A neuronal role for SNAP-23 in postsynaptic glutamate receptor trafficking. *Nature neuroscience* 13, 338-343.
- Sutton, R.B., Fasshauer, D., Jahn, R., and Brunger, A.T. (1998). Crystal structure of a SNARE complex involved in synaptic exocytosis at 2.4 Å resolution. *Nature* 395, 347-353.
- Tafoya, L.C., Marnett, M., Miyashita, T., Guzowski, J.F., Valenzuela, C.F., and Wilson, M.C. (2006). Expression and function of SNAP-25 as a universal SNARE component in GABAergic neurons. *The Journal of neuroscience : the official journal of the Society for Neuroscience* 26, 7826-7838.
- Tang, J., Maximov, A., Shin, O.H., Dai, H., Rizo, J., and Sudhof, T.C. (2006). A complexin/syntaxin 1 switch controls fast synaptic vesicle exocytosis. *Cell* 126, 1175-1187.
- Thomson, A.M. (2000). Facilitation, augmentation and potentiation at central synapses. *Trends in neurosciences* 23, 305-312.
- Tokumaru, H., Shimizu-Okabe, C., and Abe, T. (2008). Direct interaction of SNARE complex binding protein syntaxin/complexin with calcium sensor syntaxin 1. *Brain cell biology* 36, 173-189.
- Trimbach, T., Xu, J., Flaherty, D., Tomchick, D.R., Rizo, J., and Rosenmund, C. (2014). Re-examining how complexin inhibits neurotransmitter release. *eLife* 3, e02391.
- Towbin, H., Staehelin, T., and Gordon, J. (1979). Electrophoretic transfer of proteins from polyacrylamide gels to nitrocellulose sheets: procedure and some applications. *Proceedings of the National Academy of Sciences of the United States of America* 76, 4350-4354.

- Ubach, J., Lao, Y., Fernandez, I., Arac, D., Sudhof, T.C., and Rizo, J. (2001). The C2B domain of synaptotagmin I is a Ca²⁺-binding module. *Biochemistry* 40, 5854-5860.
- Varoqueaux, F., Sigler, A., Rhee, J.S., Brose, N., Enk, C., Reim, K., and Rosenmund, C. (2002). Total arrest of spontaneous and evoked synaptic transmission but normal synaptogenesis in the absence of Munc13-mediated vesicle priming. *Proceedings of the National Academy of Sciences of the United States of America* 99, 9037-9042.
- Voets, T., Toonen, R.F., Brian, E.C., de Wit, H., Moser, T., Rettig, J., Sudhof, T.C., Neher, E., and Verhage, M. (2001). Munc18-1 promotes large dense-core vesicle docking. *Neuron* 31, 581-591.
- Washbourne, P., Cansino, V., Mathews, J.R., Graham, M., Burgoyne, R.D., and Wilson, M.C. (2001). Cysteine residues of SNAP-25 are required for SNARE disassembly and exocytosis, but not for membrane targeting. *The Biochemical journal* 357, 625-634.
- Wesolowski, J., Caldwell, V., and Paumet, F. (2012). A novel function for SNAP29 (synaptosomal-associated protein of 29 kDa) in mast cell phagocytosis. *PloS one* 7, e49886.
- Wilcox, K.S., Buchhalter, J., and Dichter, M.A. (1994). Properties of inhibitory and excitatory synapses between hippocampal neurons in very low density cultures. *Synapse* 18, 128-151.
- Wojcik, S.M., Katsurabayashi, S., Guillemin, I., Friauf, E., Rosenmund, C., Brose, N., and Rhee, J.S. (2006). A shared vesicular carrier allows synaptic corelease of GABA and glycine. *Neuron* 50, 575-587.
- Wojcik, S.M., Rhee, J.S., Herzog, E., Sigler, A., Jahn, R., Takamori, S., Brose, N., and Rosenmund, C. (2004). An essential role for vesicular glutamate transporter 1 (VGLUT1) in postnatal development and control of quantal size. *Proceedings of the National Academy of Sciences of the United States of America* 101, 7158-7163.
- Wong, S.H., Xu, Y., Zhang, T., Griffiths, G., Lowe, S.L., Subramaniam, V.N., Seow, K.T., and Hong, W. (1999). GS32, a novel Golgi SNARE of 32 kDa, interacts preferentially with syntaxin 6. *Molecular biology of the cell* 10, 119-134.
- Wragg, R.T., Snead, D., Dong, Y., Ramlall, T.F., Menon, I., Bai, J., Eliezer, D., and Dittman, J.S. (2013). Synaptic vesicles position complexin to block spontaneous fusion. *Neuron* 77, 323-334.
- Xu, H., Mohtashami, M., Stewart, B., Boulianne, G., and Trimble, W.S. (2014). Drosophila SNAP-29 is an essential SNARE that binds multiple proteins involved in membrane traffic. *PloS one* 9, e91471.

- Xu, J., Brewer, K.D., Perez-Castillejos, R., and Rizo, J. (2013). Subtle Interplay between synaptotagmin and complexin binding to the SNARE complex. *Journal of molecular biology* *425*, 3461-3475.
- Xue, M., Craig, T.K., Xu, J., Chao, H.T., Rizo, J., and Rosenmund, C. (2010). Binding of the complexin N terminus to the SNARE complex potentiates synaptic-vesicle fusogenicity. *Nature structural & molecular biology* *17*, 568-575.
- Xue, M., Lin, Y.Q., Pan, H., Reim, K., Deng, H., Bellen, H.J., and Rosenmund, C. (2009). Tilting the balance between facilitatory and inhibitory functions of mammalian and *Drosophila* Complexins orchestrates synaptic vesicle exocytosis. *Neuron* *64*, 367-380.
- Xue, M., Reim, K., Chen, X., Chao, H.T., Deng, H., Rizo, J., Brose, N., and Rosenmund, C. (2007). Distinct domains of complexin I differentially regulate neurotransmitter release. *Nature structural & molecular biology* *14*, 949-958.
- Xue, M., Stradomska, A., Chen, H., Brose, N., Zhang, W., Rosenmund, C., and Reim, K. (2008). Complexins facilitate neurotransmitter release at excitatory and inhibitory synapses in mammalian central nervous system. *Proceedings of the National Academy of Sciences of the United States of America* *105*, 7875-7880.
- Veit, M., Sollner, T.H., and Rothman, J.E. (1996). Multiple palmitoylation of synaptotagmin and the t-SNARE SNAP-25. *FEBS letters* *385*, 119-123.
- Vogel, K., and Roche, P.A. (1999). SNAP-23 and SNAP-25 are palmitoylated in vivo. *Biochemical and biophysical research communications* *258*, 407-410.
- Vogel, K., Cabaniols, J.P., and Roche, P.A. (2000). Targeting of SNAP-25 to membranes is mediated by its association with the target SNARE syntaxin. *The Journal of biological chemistry* *275*, 2959-2965.
- Yang, X., Cao, P., and Sudhof, T.C. (2013). Deconstructing complexin function in activating and clamping Ca²⁺-triggered exocytosis by comparing knockout and knockdown phenotypes. *Proceedings of the National Academy of Sciences of the United States of America* *110*, 20777-20782.
- Yang, X., Kaeser-Woo, Y.J., Pang, Z.P., Xu, W., and Sudhof, T.C. (2010). Complexin clamps asynchronous release by blocking a secondary Ca²⁺ sensor via its accessory alpha helix. *Neuron* *68*, 907-920.
- Yoon, T.Y., Lu, X., Diao, J., Lee, S.M., Ha, T., and Shin, Y.K. (2008). Complexin and Ca²⁺ stimulate SNARE-mediated membrane fusion. *Nature structural & molecular biology* *15*, 707-713.
- Zhang, X., Rizo, J., and Sudhof, T.C. (1998). Mechanism of phospholipid binding by the C2A-domain of synaptotagmin I. *Biochemistry* *37*, 12395-12403.

Zucker, R.S. (1989). Short-term synaptic plasticity. *Annual review of neuroscience* 12, 13-31.

Zucker, R.S., and Regehr, W.G. (2002). Short-term synaptic plasticity. *Annual review of physiology* 64, 355-405.

8. Curriculum Vitae

Name: Nandhini Sivakumar
Nationality: Indian
Date of Birth: 9th July 1987
Place of Birth: Anantapur, India
Email: sivakumar@em.mpg.de
Address: Department of Molecular Neurobiology
Max-Planck-Institute of Experimental Medicine
37075, Göttingen, Germany.

Education and Research Projects

Bachelor of Technology degree in Biotechnology (July 2004 - May 2008)
SRM University, Kattankulathur - 603203, India.

Bachelor's Thesis: "Antilarval and antimicrobial activities of *Phyllanthus nodiflora*
and *Plumbago zeylanica*."

Master of Science degree in Molecular Genetics (September 2008 - January 2010)
University of Leicester, Leicester LE1 7RH, United Kingdom.

Master's Thesis: "Validating candidate therapeutic targets for Huntington's
disease in mammalian cells."

Doctoral degree in Sensory and Motor Neuroscience (March 2011 - May 2015)
Georg-August-Universität Göttingen, Göttingen - 37073, Germany.
Doctoral Research at the Department of Molecular Neurobiology,
Max-Planck-Institute of Experimental Medicine, Göttingen 37075, Germany.

Doctoral Thesis: "Synergistic SNARE modulators of Neurotransmission -
Complexins and SNAP-29."

Publication

Funfschilling, U., Jockusch, W.J., Sivakumar, N., Mobius, W., Corthals, K., Li, S., Quintes, S., Kim, Y., Schaap, I.A., Rhee, J.S., *et al.* (2012). Critical time window of neuronal cholesterol synthesis during neurite outgrowth. *The Journal of neuroscience : the official journal of the Society for Neuroscience* 32, 7632-7645.

Scholarship and Funding

Open Master's Scholarship for Master of Science, University of Leicester, UK.

Doctoral Research - SFB889 Cellular Mechanisms of Sensory Processing of the German Research Foundation (Deutsche Forschungsgemeinschaft, DFG) and Max-Planck-Society, Germany.

Teaching Experience

Lab Rotation Supervisor for: Dennis Nestvogel
(International MSc/PhD Neuroscience Program, 2012).

GGNB Methods Course - Nerve cell culture and patch clamp recordings from nerve cells, 2013